

DISSERTATION

DNA STRAND BREAK ASSOCIATED BYSTANDER EFFECT (DSB-ABE) IS
LINKED TO GENE MUTATIONS IN NAÏVE CELLS AND INDICATES THE
INVOLVEMENT OF A MAPK PATHWAY

Submitted by

Nasir Jalal

Department of Cell and Molecular Biology

In partial fulfillment of the requirements

For the Degree of Doctor of Philosophy

Colorado State University

Fort Collins, Colorado

Summer 2012

Doctoral Committee:

Advisor: Howard L. Liber

Co- Advisor: Susan M. Bailey

Jac Nickoloff

James Bamberg

ABSTRACT

DNA STRAND BREAK ASSOCIATED BYSTANDER EFFECT (DSB-ABE) IS LINKED TO GENE MUTATIONS IN NAÏVE CELLS AND INDICATES THE INVOLVEMENT OF A MAPK PATHWAY.

The goal of this project was to investigate whether radiation independent DNA damage, specifically a single induced DNA double strand break (DSB) can produce bystander signal, which is capable of inducing genomic instability in non-targeted cells. Previously uncharacterized E18 (modified TK6 cells) with a unique I-Sce1 insert in intron 2 of the thymidine kinase (*TK1*) gene were allowed to generate a bystander signal following electroporation of the rare cutting restriction enzyme I-Sce1 carried by a plasmid to induce DNA damage at the I-Sce1 site. Mutation assays were carried out to measure mutation fraction (MF) in directly targeted cells and using medium transfer, in non-targeted cells as a measure of bystander signal production. Transfection of the plasmid carrying *I-Sce1* gene resulted in production of sufficient bystander signal into the medium to increase the bystander MF, when conditioned medium was applied from directly targeted to naïve E18 cells. The DSB-ABE exhibited temporal kinetics over a 10 hour duration. The relative direct and bystander MF increase due to the electroporation of three rare cutting restriction enzymes namely Not1 an 8 base cutter, Sfi1 a 13 base cutter (technically 8 because of the 5 non-specific bases in sequence) and I-Sce1 an 18 base cutter, showed that DSB-ABE does not show a dose-response. The bystander signal

inhibition using superoxide dismutase (an enzyme that degrades reactive oxygen species) and PD 98059 (MEK1/2 inhibitor) indicated that the bystander signal activated the MAPK pathway in naïve cells. Higher levels of bystander mutation fraction were attempted through chemical inhibition of the three known enzymes of DNA repair (ATM, ATR and DNA PK) in directly targeted cells. Results reveal that inhibition of repair of I-Sce1 induced damage was not linked to bystander response. Further, sufficient bystander signal was produced by a presumably single I-Sce1 induced DNA break. The bystander signal produced, exhibited a dose-response in naïve cells and there was suggestion for the involvement of MAPK pathway.

TABLE OF CONTENTS

Chapter 1: Introduction and background.....	1
Study goals.....	44
Hypothesis.....	45
Aims.....	47
Chapter 2: Materials and Methods.....	49
Chapter 3: Results.....	59
Chapter 4: Discussion and Conclusion.....	125
References:.....	136
Appendices:.....	150
List of abbreviations.....	158

LIST OF TABLES

Table number (chapter number)	Page
Table 3.01 (Chapter 3) Statistical analysis of comparison of Direct and Bystander MF due to transfection of three I-Sce1 plasmids into E18 cells.....	78
Table 3.02 (Chapter 3) Statistical analysis of Direct and Bystander MF due to electroporation of restriction enzymes into E18 cells.....	83
Table 3.03 (Chapter 3) Statistical analysis of time course experiments.....	92
Table 3.04 (Chapter 3) Statistical analysis of bystander signal inhibition using SOD and PD98059.....	109
Table 4.01 (Chapter 4) Percentage contribution of I-Sce1 induced deletions in cell model used by Honma et al. (2003).....	126
Table 4.02 (Chapter 4) Average of averages of direct MF induced by I-Sce1 from all experiments.....	129
Table ST.201 (Appendix 2) Statistical analysis of mutation effects of lipofecting restriction enzymes into E18 cells.....	156

LIST OF FIGURES

Figure number	Page
Chapter 1:	
Figure 1.1 (Chapter 1) Bystander effect.....	1
Figure 1.2 (Chapter 1) Mechanism of radiation induced bystander effect (RIBE) redrawn from Hei, 2008.....	17
Chapter 2:	
Figure 2.1 (Chapter 2) Map of the vector pAdTrack CMV I-Sce1.....	50
Chapter 3:	
Figure 3.1 (Chapter 3) Detection of I-Sce1 site in E18 cells.....	60
Figure 3.2 (Chapter 3) Digestion of I-Sce1 site with restriction enzyme.....	61
Figure 3.3 (Chapter 3) Location of I-Sce1 site in <i>TK1</i> gene.....	64
Figure 3.4 (Chapter 3) Schematic for I-Sce1 induced LOH	65
Figure 3.5 (Chapter 3) GFP fluorescence in transfected E18 cells.....	68
Figure 3.6 (Chapter 3) Transfection efficiency due to electroporation.....	69

Figure 3.7 (Chapter 3) Direct and bystander MF with electroporation buffer and phosphate buffered saline (PBS).....	71
Figure 3.8 (Chapter 3) Bystander signal generation at 5, 10 and 15 hours.....	73
Figure 3.9 (Chapter 3) Comparison of direct and bystander MF of three I-Sce1 plasmids.....	75
Figure 3.10(Chapter 3) Direct and bystander MF due to electroporation of restriction enzymes into E18 cells.....	82
Figure 3.11 (Chapter 3) Experimental design of the time course experiment...	86
Figure 3.12 (Chapter 3)Results of direct and bystander MF at 0,2,3,4,5 and 10 hours.....	88
Figure 3.13 (Chapter 3) Temporal response of direct and bystander MF induced by I-Sce1 vector alone.....	90
Figure 3.14 (Chapter 3) Overall observed MF ‘D’ in the time Course experiments.....	96
Figure 3.15 (Chapter 3) Standardized mutation fraction caused by increasing dose of ionizing radiation.....	99

Figure 3.16 (Chapter 3) Effect of inhibition of DNA PK on direct and bystander mutagenesis.....	101
Figure 3.17 (Chapter 3) Effect of inhibition of three DNA repair enzymes on direct and bystander mutagenesis.....	105
Figure 3.18 (Chapter 3) Bystander signal inhibition using SOD and PD98059..	108
Figure 3.19 (Chapter 3) Direct and bystander MF in E18 and control cell line TK6.....	112
Figure 3.20 (Chapter 3) Proposed model for DSB-ABE	123
Appendices (supplementary data):	
Figure S 1.1 (Appendix 1) Transfection efficiency due to electroporation.....	152
Figure S 1.2 (Appendix 1) Direct and bystander MF in Lipofected E18 cells.....	153
Figure S 2.1 (Appendix 1) Mutation effects on E18 cells of lipofecting restriction enzymes.....	156

Chapter 1: Introduction

This dissertation is part of a larger NASA project aimed at addressing radiation carcinogenesis Gap cancer 3, which is: how can models of cancer risk be utilized to reduce the uncertainties in radiation quality effects from solar particle events (SPEs) and galactic cosmic rays (GCRs).

Radiation-induced bystander effect (RIBE) is a condition in which cells that have not been directly targeted by ionizing radiation (IR) exhibit symptoms of exposure such as chromosomal instability, telomere aberrations, cell death and micronucleation (Prise et al., 2003) Fig.1.1.

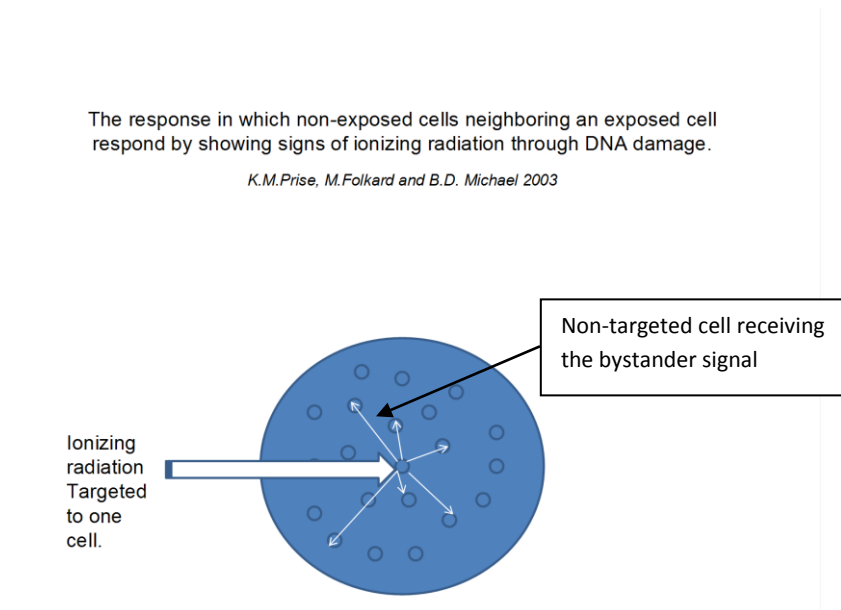


Fig. 1.1

The effects of radiation on a cell are many and random. There are **direct** as well as **indirect effects** the latter of which are referred to as bystander effects or BSE. Mutagens

other than ionizing radiation may also produce BSE. **Direct effects are those that result from interaction of IR with all cell components while indirect effects result via a mediator, e.g., factors released into the medium surrounding exposed cells, which then signal to naïve cells and cause DNA damage.** Examples of direct effects of radiation include genomic instability, chromosomal rearrangements, delayed mutation, DNA nucleotide repeat instability, cellular transformation and cell death. It is postulated that the same effects can be observed in naïve cells which are exposed to bystander signal from targeted cells. It is still unknown what form or forms of damage to targeted cells actually leads to the generation of bystander signal. The hypothesis that this project investigates is that DNA damage also increases the mutation rate in directly targeted and non-targeted naïve cells. This is not to say that only DNA damage could cause BSE or is required in any way to initiate a BSE. Besides specific DNA damage, ionizing radiation can cause damage to other cell components and may therefore up regulate BSE. This DNA damage could cause base damage, single strand breaks, double strand breaks or even the production of reactive oxygen and nitrogen species due to the ionizing effect.

DNA damage response and repair of endogenous and exogenous sources of damage represent important defenses to prevent tumorigenesis. Hence better understanding of the link between DNA damage and bystander mutagenesis will provide us with new strategies for cancer treatment.

Background:

Nagasawa and Little, (1992) first demonstrated that targeting an α -particle microbeam to a few cells caused the neighboring non-targeted cells to show radiation induced sister chromatid exchanges (SCE), the field of bystander mutagenesis has become a topic of much debate and research. Evidence shows that as well as direct DNA damage dependent effects, the radiation treated cells produce signals that are hereby referred to as 'bystander signals' that can affect the neighboring non-irradiated cells. This phenomenon has been called 'bystander effect' (Mothersill and Seymour 2000).

Radiation-induced bystander effect is a condition in which cells that have not been directly hit by ionizing radiation, exhibit symptoms of exposure such as chromosomal instability, telomere aberrations, cell death and micronucleation. The effects of radiation on a cell are many and random. Ever since the discovery of bystander effect (Nagasawa and Little 1992) it has been associated with variable doses of targeted nuclear radiation until Shao, et.al., (2004) presented data for a non-nuclear (cytoplasmic) target of the phenomenon. It was argued (Shao et al., 2004; Prise et al., 2006) that DNA damage is not essential for bystander signaling and that cytoplasmic targets could also produce the bystander effect. It has been re-affirmed that bystander signaling is independent of DNA damage and DNA repair capacity of the irradiated cells (Kashino et al., 2007). This relatively new field of research is therefore at a critical stage and it is important to determine whether DNA damage due to targeted nuclear radiation is the only source of bystander signaling or not. Attention was therefore turned to a non-radioactive approach to induce DNA damage and investigate whether restriction enzymes could also produce sufficient bystander signal to induce mutations in naïve cells.

The effects of radiation induced bystander signal on naïve cells are many and have been studied in detail. Using either precision microbeams or low-dose internal radiation β -particles in mammalian cells investigators were able to establish end-points in naïve mammalian cells, which are discussed in further detail in the literature review section. Direct evidence of bystander effect in humans does not exist, as yet, and there are few data available for in-vivo systems (Blyth et al., 2010). In one such study tritiated thymidine labeled lymphocytes were transferred into the spleen of unirradiated control group of mice but no change in apoptotic or proliferative capacity of spleen cells was observed. This does not in any way rule out the existence of bystander effects in mammals generally and humans specifically; it just suggests that more research is required to understand the phenomenon and to evaluate the existence of bystander signaling in mammals and humans.

1.01. Radiation induced bystander effect (RIBE) and its implications for cancer treatment:

Bystander end-points have been observed at low doses of ionizing radiation <0.5 Gy (Seymour and Mothersill 2004) which support the linear no threshold hypothesis, according to which there is no minimum safe dose of radiation for humans and even small doses can cause cumulative biological effects. All types of radiation exposure are regulated according to this hypothesis and take into account radiation quality factors. Direct evidence for bystander effects in humans does not exist (Blyth et al., 2010) but 3D artificial human tissue irradiations with helium ion (Sedelnikova et al., 2007) have demonstrated bystander effects suggesting that they may very well exist in humans

following radiation exposure. The γ -H₂AX focal formation, an indicator of DNA damage (Hu et al., 2006) was not as immediate and pronounced as in cultured cells. The γ -H₂AX foci normally appeared 30 to 40 minutes after irradiation of cultured cells but in geometric human tissues the foci formed 12-48 hours later and gradually decreased over a one week period (Sedelnikova et al., 2007). Whole body nematode worm irradiations provide evidence that supports the existence of bystander effects (Bertucci et al., 2009). The expression of a GFP chimera of a body stress gene hsp-4 (heat shock protein-4) was measured in regions of the body that did not receive gamma exposure.

Another approach for investigating bystander effects used the implantation of cancer tissues in naïve mice. DNA damage in proliferative tissues distant from the implanted cancerous tissues suggested that bystander effects operate in-vivo. The BSE could have a detrimental impact on naïve cells making up proliferative tissues such as the gastrointestinal crypts and skin (Redon et al., 2010). An inflammation cytokine CCL2/MCP-1 was implicated in the process of this distant tissue DNA damage caused by cancer implants.

Most radiation induced bystander effects are studied with regards to dose dependence, signal potency, signaling range, radiation source dependence, timing and cell type dependence (Blyth and Sykes 2011). Bystander effects are classified into three groups, namely (1) bystander effect, (2) abscopal effects and (3) cohort effect. Class 1 signifies radiation induced signal mediated effects in unirradiated cells, within the irradiated volume. Class 2 signifies radiation induced effects in unirradiated tissues outside an irradiated volume, whereas class 3 signifies radiation induced, signal mediated effects within the irradiated volume and between irradiated cells.

It is presently assumed that while using radiation for cancer treatment, the benefit outweighs risk, but this trade off needs to be looked at more closely. As radiotherapy targets the tumor cells, it may inadvertently cause the targeted cells to release bystander signals into the tissue fluid which could then affect the non-targeted cells to induce tumorigenic transformations. This concept is further discussed in section 2.05.

1.02. Oxidative stress for bystander signal generation:

Oxidative stress is mainly caused by increased levels of reactive oxygen species (ROS) in the environment of a cell. Oxygen derived free radicals can be generated by endogenous metabolism or exogenous sources such as ionizing radiation, UV exposure, redox cycling drugs, and carcinogenic compounds (Halliwell and Gutteridge 2006). Inflammation also leads to reactive oxygen and nitrogen species production, which are a hallmark of cancer hence, an important aspect of critical tumor progression (Colotta et al., 2009).

ROS have been described as the energy landscape of a cell, to maintain normal homeostasis. Increased levels of ROS can cause DNA damage, as well as a whole range of cellular responses such as apoptosis, senescence, cell cycle arrest and even possibly cancer (Lehnert, 2002). Increased levels of ROS can be generated in response to exposure of a cell to low levels of ionizing radiation (IR) but they can also be helpful for a cell to avert the toxic effects of exposure (known as an adaptive response of a cell which makes the cell resistant to radiation upon subsequent exposures). It has also been argued that the long-term ROS effects can be damaging whereas the short-term effects of ROS may be protective. In the long term these increased ROS levels may cause proliferation of cells that is accompanied by accumulation of mutations (Lehnert, 2002). ROS have been

shown to form oxidative DNA adducts such as 8-hydroxguanine which in turn can lead to base modifications and transversions such as GC to TA; therefore the oxidative state (ROS) of a cell has been implicated as a possible bystander signal that leads to the activation of stress response pathways, induction of proto-oncogenes e.g., c-fos, c-jun and c-myc, and modified DNA base products that lead to DNA strand breaks, which ultimately are linked to an array of mutations, cell transformation and metastasis (Christen et al., 1999; Wiseman et al., 1996).

Other stress-response studies carried out in non-targeted cells have shown that growth-related bystander response was observed in cells that received supernatants from α -particle irradiated cultures (Iyer and Lehnert, 2000). Such a response led to the upregulation of reactive oxygen species (ROS) in the bystander naïve cells and it was mediated by the redox-potential activated TGF- β 1 cytokine. These observations also showed that such a bystander response was associated with decreased levels of p-53 and p-21waf1. In this project, to eliminate ROS (that could have been generated by electroporation) as a possible candidate of bystander signal it was degraded with superoxide dismutase (SOD), discussed later in the literature review.

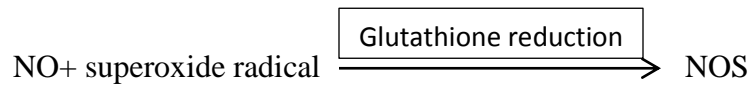
1.03 Involvement of cellular environment in bystander signal generation:

Activation or inactivation of signaling pathways involving tyrosine kinase, transcription factors, oxidation of cellular thiols and calcium homeostasis depends on the concentration of biological oxidants and thus the redox potential (Allen et al., 2000; Gabbita et al., 2000). It was, hence, argued that the redox potential of the signaling pathways is an important factor to consider in bystander signaling.

In studies involving the use of low-dose ionizing radiation with β -particles, the antioxidant dimethylsulphoxide (DMSO) reduced the lethal effects in bystander cells produced by growing them with ^3H -thymidine-labeled cells (Bishayee et al., 2001). It was argued in this research that because of the very short range β -particles emitted by tritiated thymidine they can traverse a distance of (1 micron) and not cause cross-irradiation. Maximal protection of cells from bystander effect was observed in the presence of DMSO and lindane, by inhibiting both reactive oxygen species (ROS) and Gap junction intercellular communication (GJIC). Oxidative metabolism of γ -radiation targeted cells has also been investigated by some researchers (Lyng et al., 2000 and 2006; Mothersill et al., 2000). The use of antioxidants such as L-lactate and L-deprenyl (Mothersill et al., 2000) or drugs that inhibit collapse of mitochondrial membrane potential (Lyng et al., 2000; 2006) resulted in inhibition of the cytotoxic effects of conditioned medium on bystander cells upon transfer from irradiated cultures. Chemical inhibition of bystander signal with antioxidants signifies that this signal could be ROS based, while drugs that collapse mitochondrial membrane potential indicate the involvement of calcium ion signaling or components of apoptotic signaling as possible candidates of bystander signal.

1.04: Nitrogen oxygen species (NOS) and bystander signal:

A small and highly diffusible molecule, nitric oxide is commonly used by the human body as a biological signal and regulator but generates a metabolic by-product called nitrogen oxygen species (NOS) upon reaction with superoxide radicals. (Rubanyi et al., 1991)



Matsumoto, et. al., (2001) showed that inducible nitric oxide, produced by cells targeted with X-radiation, mediated the accumulation of p-53 and hsp72 protein in wild type glioblastoma cells, when conditioned medium was transferred from X-irradiated glioblastoma cells expressing mutant p-53. They also showed that this accumulation of proteins could be inhibited when medium was treated with NOS scavengers or a nitric oxide synthase inhibitor. According to Ohba et al. (1998) the oxidative stress mediators also play a role in the Abscopal effects, when cytotoxic effects were observed at distant sites from solid tumors such as hepatocellular carcinomas that were targeted by radiation. It was again argued that such Abscopal effects were mediated by redox-potential sensitive cytokines. Despite extensive efforts, it is still not known which specific factors or signaling mechanisms lead to the generation of a bystander signal.

1.05. Nuclear DNA damage for bystander effect----to be or not to be?

A recent controversy has surfaced (Prise et al., 2006) relating to the topic of whether or not nuclear DNA damage is essential for the bystander effect and, if so, how could it impact the current radiotherapy intervention for cancer patients.

Most particle radiotherapy focuses the depth deposition of dose to the actively dividing cells of a tumor mass. Calculations for dose depth deposition are based on the stopping power of radioactive particles in water as governed by the Bragg's peak principle (Bragg and Kleeman, 1903). This model is reasonably accurate and the measured stopping of

ions in compounds deviates less than 20%. The depth-dose deposition is measured mainly by calculating the stopping power of electrons/photons/protons emitted by the particle beam. Since most of these measurements are done in water (Siikonen et al., 2011), assuming that human body is 90% water, the exact dose deposition traversing through the living tissue is rarely achieved. Siikonen et al. (2011) have discussed ways to reduce the error but still radiotherapies inadvertently damage healthy cells surrounding the tumor mass. A software program called SRIM (Stopping and range of ions in matter) was developed by Ziegler, (2003) and constantly upgraded with up to 25,000 stopping values added until now. The software corrections made to the experimental calculation of stopping power of ions in compounds have been reported with the maximum accuracy of 89% in case of Helium ions, compared to their last SRIM program of 1998. This suggests that there is an 11% chance of error. So the 20% error from Bragg's rule combined with 11% from SRIM, suggests that radiotherapies and radiation exposure can still cause damage to DNA of healthy cells besides targeting the tumor mass (Trikalinos et al., 2009).

It has also been argued that the direct DNA damage from targeted ionizing radiation can result in the production of oxidative stress which could be responsible for the generation of bystander signals (Prise et al., 1999; Milligan et al., 2000 and 2001). These groups have tried to evaluate the yield of single and double strand breaks resulting from low and high LET (linear energy transfer) radiation exposures. In experiments using irradiated plasmid DNA, in the presence and absence of endonuclease III enzyme (which recognizes base modification and introduces a DNA break for base excision) they measured total single and double strand break damage incurred by radiation. The authors argue that ionizing radiation induced DNA damage is predominantly produced by

radiation mediated OH- radicals, an indication that oxidative stress is involved. Prise et al. (1999) estimated that low LET γ -radiation could produce a double strand break (DSB) yield of up to 6.3×10^{-8} Gy/base pair. High LET radiation could cause an additional 9% DSBs and use of endo III enzyme could further raise the yield by 2.5%. Addition of endo III did not affect the background levels of single or double strand break yield in the control group. Milligan et al. (2000) confirmed the findings of Prise et al. (1999) and both groups agreed on the involvement of clustered DNA damage being caused by OH-radicals. They used scavengers to reduce additional damage from these free radicals. Both teams also acknowledged that high LET radiations cause more DNA damage compared to low LET. Löbrich et al. (1994) used rare cutting restriction enzymes to get small enough fragments of DNA that could be separated by pulse field gel electrophoresis (PFGE). PFGE was then used to compare fragments of DNA that resulted from varying doses of targeted ionizing radiation. Almost 40 DSBs were produced in one P3 human epithelial teratoma cell by 1 Gy of X-rays and the induction of DSBs had a linear relationship with dose.

If free radicals are a by-product of radiation induced DNA damage, then recent findings of free radicals and reactive oxygen species as being possible candidates of bystander signal could be explained logically (Wiseman et al., 1996; Christen et al., 1999; Lehnert 2002;). This logical outcome was also discussed by Ward, (2002). The rationale for implicating DNA DSBs as responsible for the biological effects of radiation is that these effects are not caused by auto-oxidation. The traditional biological effects are dependent on multiple radicals reacting on opposite strands of the DNA (Ward, 1981). It has been argued that radiolytically generated OH- radicals form a radical with deoxyribose but due to steric considerations it is unlikely that this radical can cause a break on the adjoining

strand of DNA; hence single strand breaks are more logical in this scenario. It has also been argued that if these radicals act on opposite strands then a double strand break can potentially be caused (Ward, 1981).

Ward, (2002) also reasoned that DSBs induced by high LET radiation are an “attractive candidate” for investigating the production of bystander signal. However he questioned the ability of one DSB being able to generate the bystander signal. Ward, (2002) also proposed three sources of bystander signal generation from radiation targeting:

- 1) A hydrated electron
- 2) The ability of low energy electrons to induce single or double strand breaks and
- 3) Radiation induced damage caused at sites that are otherwise inaccessible for species that cause auto-oxidative damage.

The ability of radiation targeted human keratinocytes to produce bystander signal that could cause apoptosis in non-targeted naïve cells was tested by Lyng et al. (2000). Medium transfer from irradiated to unirradiated cells caused the appearance of characteristic early apoptotic end-points in naïve cells. The group reported no dose response for bystander signal generation by cells that were directly targeted by 0.5 to 5 Gy of radiation using a Cobalt 60 source.

Another school of thought argues that for bystander signal production, nuclear DNA damage is not essential. To test this hypothesis of bystander signaling Shao et al. (2004) used precision microbeams to specifically target the cytoplasm of radioresistant T98G glioma cells (grown either singly or in co-culture with normal human fibroblasts AG01522) with charged Helium ions ($^3\text{He}^{2+}$). Even when one helium ion specifically

traversed through the cytoplasm of one glioma cell, bystander responses were induced in the neighboring non-targeted glioma or fibroblast cells. Having used micronucleation as the end-point for bystander response in naïve cells, the team measured a 36% increase of micronuclei in glioma cells versus 78% increase in normal fibroblasts. The team also demonstrated that the bystander response could be inhibited if cell populations were treated with 2-(4-carboxyphenyl)-4,4,5,5-tetramethyl-imidazoline-1-oxyl-3-oxide or filipin, which are both scavengers of nitric oxide hence suggesting the involvement of reactive nitrogen species as possible candidates of bystander signal. The team concluded that direct DNA damage is not essential for bystander signaling and that the whole cell should be considered a sensor for radiation damage. The system used by Shao et al. (2004) raises some questions, for example, the fact that p53 mutant glioma cells were only traversed by helium ions to generate bystander signal and not normal human fibroblasts. The group used Nile red stained cells to avoid hitting the nuclei and set coordinates with 2 micron precision, to target one helium ion to traverse the cytoplasm. If the cytoplasm was indeed targeted, we cannot rule out mitochondrial DNA as a target, hence becoming the source of extranuclear DNA damage for bystander signal production. Further investigation is therefore required to test if DNA damage is the source of bystander signal production.

The third aspect of this paradigm is whether DNA repair has a role to play in bystander signaling. DNA damage induced bystander signal production may not be affected by DNA repair, since repair could take hours, while bystander signal production has been shown to be immediate, reaching its maximum within one hour of radiation exposure. In fact DNA double strand breaks were found as soon as 2 minutes after irradiation

exposure in one experiment (Hu et al., 2006) while bystander effect in terms of $\gamma\text{H}_2\text{AX}$ foci could be detected almost 30 minutes after medium transfer to naïve cells.

It was demonstrated by Kashino et al. (2007) that activation of bystander signal in DNA repair deficient *xrs5* cells is independent of DNA repair capacity. However the investigators irradiated Chinese hamster ovarian (CHO) cells and separated the conditioned bystander signal containing medium to later apply to repair deficient *xrs5* cells. They reported no increase in micronuclei in the naïve bystander repair deficient cells and reasoned that activation of bystander signal is independent of the DNA repair capacity of irradiated cells. The investigation sheds some light into the fact that DNA damage and its repair capacity are independent of each other. This also suggests that bystander signal generation could precede the repair process.

For bystander signal experiments involving medium transfer it is important to maintain experimental conditions, cell type and even the cell cycle phase as reasoned by Hei et al. (2008) who argued that extranuclear and extracellular events also contribute to the overall low dose radiation induced bystander effects. Kashino et al. (2007) demonstrated that radiation induced bystander signals can be free radical based, and could be suppressed with DMSO. However this signal can vary under variable conditions and can activate different signal transduction pathways in the naïve cells (Dent et al., 2003). The implications of radiation-induced bystander signaling vis-à-vis cancer therapy have been discussed in detail by Prise and O'Sullivan (2009). The authors have reasoned that based on current understanding, the role of radiation induced bystander response has to be in context of our knowledge of how cells communicate with each other. They have further

reasoned that molecular pathways and targets outside the directly exposed fields could give a cumulative response to the radiation therapy.

This aspect is important for my project because until now only ionizing radiation and chemically induced DNA damage had been linked to bystander signaling, but my data demonstrates that radiation independent DNA damage (double strand breaks (DSBs) to be specific) also leads to the production of bystander mutagenesis. This has implications for cancer therapy since drugs such as alkylating agents function by disrupting the structure of DNA and creating DSBs (Lieberman et al., 1971). Since most of these drugs are not targeted to the tumor mass they are certain to have non-cancer cell targets, that receive DNA damage, and thus possibly set up a cascade of bystander signaling events.

1.06. Nature of bystander signal:

TGF- α , TGF- β , TNF- α cytokines and reactive oxygen species (ROS):

The nature of bystander signal can vary according to the experimental model, treatment conditions, culture conditions and even the phase of cell cycle (Hei et al., 2008). Following is an account of some of the possible candidates of radiation induced bystander signal (RIBE). Since these have been widely implicated in RIBE, these signals may have a role to play in radiation independent bystander effects.

Although radiation exposure may trigger one pathway in a specific cell type, it does not mean that the same pathway would be triggered in a different cell type (Dent et al., 2003). Radiation can trigger multiple pathways in a cell. Mitogen-activated protein kinase (MAPK) pathway signaling has been associated with growth factor mediated regulation of such diverse cellular functions as proliferation, differentiation, senescence

and apoptosis. Release of factors such as tumor growth factor (TGF- α), tumor necrosis factor (TNF- α) and reactive oxygen species (ROS) from irradiated cells activate mitogen activated protein kinase (MAPK), extracellular signal regulated kinase (ERK1/2), MEK1/2 and cyclo-oxygenase (COX-2) pathways in the naïve cells that received conditioned medium. Tumor growth factor- β (TGF- β) release from irradiated cells activates reduced nicotinamide adenine dinucleotide phosphate NAD(P)H oxidase and has been reported to cause the formation of γ -H₂AX foci in naïve cells that receive conditioned medium. TGF- β causes suppression of proliferation and differentiation in lymphocytes, cytolytic T-cells, natural killer cells and macrophages, thus preventing immune surveillance of a growing tumor mass (Pardali and Moustakas, 2007). An IR dose dependent release of TGF- α in DU145 xenografts was measured by Hagan et al., (2004) who demonstrated that this factor acts as a bystander signal stimulating the growth of naïve cells. The role of TGF- α in prostate cancer was also highlighted by Hagan et al. (2004) in palliative cancer therapy, which puts into picture the fact that if bystander signaling is a result of radiotherapy in cancer patients, then it is all the more important to know its nature and dynamics. Once irradiated the xenografts produce TGF- α through the first wave of ERK1/2 activation in directly targeted cells, while the same cytokine in medium when applied to naïve cells activated the second wave of ERK1/2 signaling cascade. The data presented herein indicates that this signaling cascade may also be involved in DNA strand break-associated bystander effect (DSB-ABE).

Calcium Signaling:

Apoptosis is a major end-point of bystander induced cells, while ROS was found involved in decreased mitochondrial membrane potential and increased intracellular Ca^{+2} levels (Lyng et al., 2006). Chelation of calcium and blockage of voltage dependent Ca^{+2} channels suppressed apoptosis induction in bystander cells. Hei et al. (2008) suggested a unifying model to explain the possible pathways involved in RIBE Fig 1.2

Cytoplasmic radiation targeting can also produce a BSS thus showing nuclear DNA damage is not required (Shao et al., 2004; Prise et al., 2006; Kashino et al., 2007). However it is still possible that DNA damage, arising from mitochondrial DNA or intracellular calcium signaling could serve the same function in bystander effect.

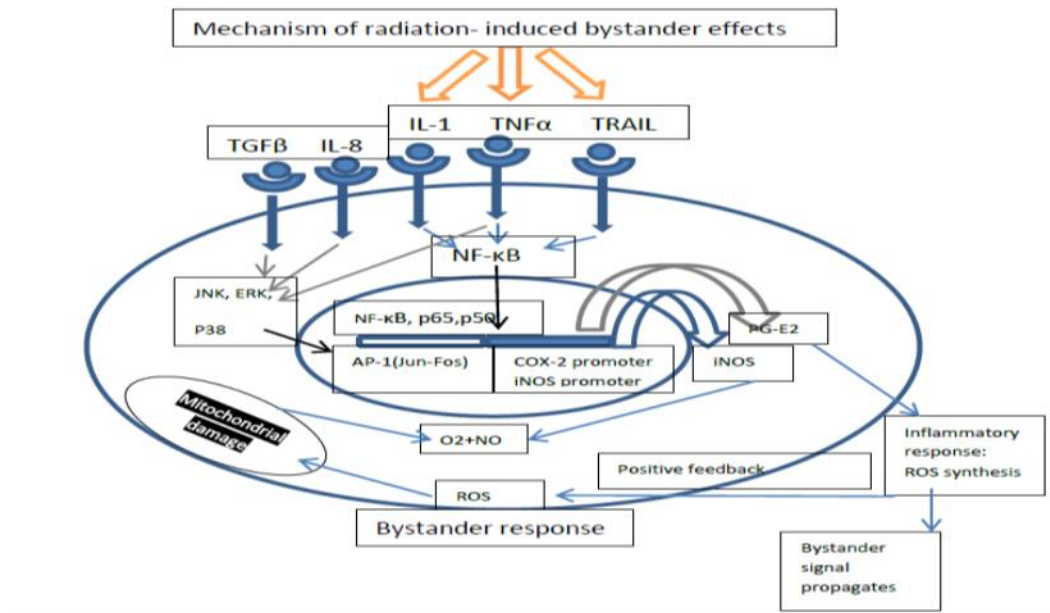


Figure 1.2 Redrawn from Tom K. Hei's research article (2008).

1.07. Various end points of radiation induced bystander effects (RIBE) in mammalian cells:

Although a wide variety of bystander end-points have been studied and often discussed en bloc for showing evidence to the existence of bystander effects, they should not be mistaken for a singular/generic bystander effect (Blyth and Sykes, 2011). Many biological systems have been shown to produce bystander effect under different set of conditions and thus a variety of bystander signals have been reported. The evidence does not in any way suggest that bystander end points are generic but just gives a summary of many that have been observed in various systems upon exposure to different set of chemicals, irradiations, or environmental stresses. Two different cell types may trigger different bystander signaling pathways upon the same kind of radiation exposure (Dent et al., 2003).

Using either precision microbeams or low-dose internal radiation β -particles in mammalian cells various investigators were able to measure bystander effect by using these end-points of bystander signaling in a variety of naïve mammalian cells:

- a. Genetic (Seymour et al., 1986).
- b. Epigenetic (Seymour et al., 1986).
- c. Lethal mutations and altered gene expression (O'Reilly et al., 1994).
- d. Activation of signal transduction pathways (Dent et al., 2003; Hagan et al., 2004).
- e. γ -H₂AX foci formation (Hei et al., 2008).
- f. Delayed Apoptosis (Lyng et al., 2000; Prise et al., 2005).

- g. Sister chromatid exchanges (SCE) (Nagasawa and Little, 1992).
- h. Micronucleation (Jamali et al., 1996; Azzam et al., 2002).
- i. Neoplastic transformation in non-targeted cells (O'Reilly et al., 1994).

One of the earliest investigations into RIBE showed that irradiation of targeted cells results in surviving colonies or clones that demonstrated delayed lethal mutations, which could be measured in terms of plating efficiencies (Seymour et al., 1986). In a separate investigation number of lethal mutations and delayed genetic mutations at the *hprt* locus among the progeny of cells from CHO (Chinese hamster ovary cells) and BALB/3T3 mice was measured. Reduced cloning efficiency was measured for up to 30 population doublings after X-ray exposure and delayed mutations at the *hprt* locus were recorded after 6-7 population doublings (Little et al., 1990).

The explanation into how delayed mutations were inherited remains unclear. The two possible explanations could be:

1. Unrepaired DNA damage is passed on to the daughter cells for many generations until the damage becomes a heritable mutation.
2. Radiation exposure leads to a process that causes persistent elevation in background spontaneous mutations.

Delayed effect of a fractionated dose of radiation on bystander cells was also investigated in -vitro (Mothersill and Seymour, 2002) and the results have been shown to be important for human patients receiving fractionated doses for radiotherapy. Although RIBE has been undoubtedly associated with low dose radiation exposures, higher doses used for radiotherapy may also exhibit bystander effects. HPV-G cells were given two doses of γ -

rays separated by 2 hours of recovery and conditioned medium removed from directly targeted cells was applied to naïve bystander cells. Survival of naïve HPV-G cells was low when conditioned medium was transferred from cells that were given a fractionated dose, compared to cells that were given one whole dose. This trend was surprisingly constant for over 1000 fold-range of doses from 0.005 Gy to 5.0 Gy (Mothersill and Seymour, 2002). And although most radiotherapy is carried out using fractionated doses, the team concludes that the bystander effects of these radiotherapy doses must be further investigated. This important research has implication for an adaptive response of cells, where an initial priming dose imparts some radioresistance against a second much larger dose. Whether the first dose was lower than the second or higher or the same, the same bystander effect was observed on the survival of naïve cells, upon conditioned medium transfer.

The adaptive response (where cells become resistant to the effect of radiation after first exposure) was investigated using the same cell line (HPV-G) and with separated conditioned medium as a priming dose to be applied to naïve cells (Maguire et al., 2007). Conditioned medium from cells irradiated at a higher dose was used as a challenge dose for naïve cells. Several end-points of RIBE that included reactive oxygen species ROS, apoptosis, calcium influx, loss of mitochondrial membrane potential, and calcium influx were examined. ROS were found to be involved in apoptosis while calcium influx varied in magnitude across the exposed cell population. No change in mitochondrial membrane potential was recorded for 0.5 Gy conditioned medium used as primer and separated by a 24 hours challenging dose of 5.0 Gy conditioned medium. This study concluded that HPV-G cells did show an adaptive response.

This account underlines the extent of complexity that this phenomenon can demonstrate using the same cell line but looking at different end-points of bystander signaling.

1.08: Spatial and temporal response of radiation induced bystander effects (RIBE):

Very few experiments have been designed that measure the spatio-temporal kinetics of bystander signaling (Hu et al., 2006; Staudacher et al., 2010; Zhang et al., 2009). Choosing an optimal time for release of bystander signal into the surrounding medium is critical to ensure consistent measurement of a chosen end-point in the naïve cells. The peak time observed in some of these experiments (Hu et al., 2006) was 30 minutes after irradiation and used γ H₂AX foci as the end-point. But DNA DSBs due to irradiation could be observed as soon as 2 minutes after exposure. The average level of double strand break (DSB) formation at 30 minutes after irradiating AG1522 normal human diploid fibroblasts was 3 fold in directly targeted and 2 fold in naïve cells, compared to the control. The level of DSB remained steady for up to 6 hours and then declined. The study also reported that medium containing the bystander signal could be transferred to anywhere in the petri plate (specially designed, having mylar sheathing and aluminum shielding) to induce DSB in naïve (unirradiated cells). The percentage of DSB induced in naïve cells did not seem to depend on radiation dose delivered to the targeted cells. The team also demonstrated the existence of temporal kinetics of bystander signal at least at very early stages of post-irradiation and depended on the proximity of the naïve cells to the cells producing the signal. The team also showed that dimethylsulfoxide (DMSO) and lindane significantly inhibited the number of induced DSB in naïve cells, suggesting the involvement of ROS and gap junctional intercellular communication for bystander signal.

Zhang et al., (2009) worked with a cell line (WTK1) and reported that maximum mutations at thymidine kinase locus were recorded 1 hour after bystander signal containing conditioned medium was applied to naïve cells. It was also demonstrated that the directly targeted cells needed at least 1 hour to generate sufficient bystander signal and that it diminished in 12-24 hours. The E18 system shows that DNA strand break associated bystander effect (DSB-ABE) causes the production of bystander signal almost immediately (10 minutes) after breaks are induced and that the maximum mutations at thymidine kinase locus can be recorded at 5 hours. The signal does appear to diminish at 10-15 hours.

It is likely that radiolytically generated reactive oxygen species (ROS) are too unstable to travel to naïve bystander cells and act as a potent bystander signal since they decay in nano seconds and diffuse over a distance of few nanometers (Ward 1981; Hamada et al., 2007). In another unique investigation (Schettino et al., 2003) a single cell was targeted with low dose radiation and clusters of DNA damage were observed in naïve cells, as a function of bystander effect and data showed that bystander effect was independent of the dose of radiation exposure. They were also able to establish a spatial response by observing transfer of bystander signal up to 3 mm away from the targeted cell and suggested a chain reaction that is set up by the one targeted cell to series of naïve cells. In a temporal and spatial kinetics investigation Hu et al. (2006) demonstrated that bystander signal could travel as far as 7.5 mm away from the radiation targeted region and that bystander end-points could be observed only 2 minutes after exposure of directly targeted cells and transfer of conditioned medium to naïve cells. They also demonstrated that the bystander effect remained stable for up to 6 hours after exposure but they argued that a

time-dependent double strand break response in bystander cells could be observed based on the distance of naïve cells from directly targeted cells.

Lyng et al. (2000) used a p-53 null immortalized human keratinocyte cell line to measure the increase in reactive oxygen species (ROS) in the medium of irradiated cells as a means to measure bystander effect. They found out that increase in ROS continued for about 6 hours after the medium was transferred from targeted cells to naïve ones.

Zhang et al. (2009) also investigated some of the temporal aspects of bystander effect while working with a p-53 mutant lymphoblast cell line WTK1. The teams conducted kinetic studies and found out that it required up to 1 hour to generate sufficient signal to induce maximum level of mutations at the TK locus in the naïve cells that received conditioned medium from cells targeted by ionizing radiation.

1.09: Saturation effect of radiation induced bystander signal:

It has been argued in most medium transfer experiments that if the bystander signal is soluble in medium then its dilution should decrease the effect on any end-point under consideration. Some experiments have been done to prove that point.

In an experimental model cell system WTK1 (Zhang et al., 2009) it was shown that a four fold dilution of the conditioned medium (containing bystander signal) was required to render the medium ineffective for its bystander property; in contrast a 20 fold decrease in irradiated cell number (used to generate a bystander signal) was required to achieve the same dilution effect. The team also reported an adaptive response of cells which imparts a radiation resistant property to the targeted cells if primed with a low IR dose. Other

interesting data suggested that low levels of bystander signal exposure imparted an adaptive property to naïve cells also.

Some investigators have investigated the effect of radiation dose on naïve bystander cells as a source of bystander signal reduction. Ponnaiya et al. (1997; 2004 and 2011) who worked with radiation induced bystander effect (RIBE) has shown convincing data that a definite radiation exposure dose response could not be observed in naïve cells. The end points observed in these studies included micronuclei formation and chromosomal aberrations in bystander cells and their progeny.

1.10: TK6, the parent cell line of E18 and its genomic details:

The mutation assay for thymidine kinase locus of TK6 cell line was first developed by Liber and Thilly, (1982) and the locus characterized later by Grosovsky et al. (1993). This human lymphoblastoid cell line comes from the spleen of a donor and has a doubling time of 12-16 hours (Liber and Thilly, 1982). The 13.5 kb human TK1 gene is located on chromosome 17q23.2, oriented from telomere to centromere (Honma et al., 2003) and it is an autosomal gene that codes for a salvage pathway enzyme for nucleotide synthesis. TK6 is a heterozygous TK^{+/-} cell line with frame-shift mutation in exons 4 and 7 of the inactive allele while a 9 base pair deletion in exon 1 of the active allele was introduced in a cell line (TX528) derived from TK6. The targeting vectors used to construct E18 contained genomic DNA only through exon 3 thus they cannot correct the exon 4 or 7 frameshifts and would restore the same alleles as in the active parental TK6. Since the cells used in this present study were unsynchronized therefore almost 50% were expected to be in G1 phase (Little et al., 1995) the genetic outcome of double strand

breaks was due to the chromosomal double strand breaks. Most DNA double strand breaks in G1 phase are repaired by end joining (EJ) while any left over damage is repaired by homologous recombination (HR) in the post-DNA replication phases of S and G2 (Honma et al., 2003). It has also been argued that EJ can operate throughout the cell cycle. For this reason it is safe to postulate that most of the I-Sce1 induced DNA double strand breaks are repaired by end-joining which causes small to large scale deletions, resulting in loss of heterozygosity (LOH) and thus allowing the mutation assay to isolate mutants from cell population.

1.11: E18 Cell model system and I-Sce1 as a tool for double strand break analysis:

I-Sce1 endonuclease is a mitochondrial intron-encoded endonuclease of *Saccharomyces cerevisiae* which has a very low probability of cutting the DNA even within large genomes.

The first demonstration of using I-Sce1 as a tool to study genetic recombination in the mitochondria of yeast cells was done by Nakagawa et al. (1992). Since then investigators have been inserting I-Sce1 restriction site into specially designed cell models for site-directed mutagenesis. The objective for this insertion has been to use it as a powerful tool of gene targeting to specifically induce double strand breaks using I-Sce1 restriction enzyme and studying the fate of this site directed DNA damage (Cohen-Tannoudji et al., 1998). In separate investigations it was demonstrated that double strand breaks can be initiated by the expression of I-Sce1 enzyme at pre-determined location in a mammalian genome (Choulika et al., 1995; Bellaiche et al., 1999). The cell model system used in this project was a modified lymphoblast cell line derived from TK6 that has an I-Sce1 insert

in intron 2 of the thymidine kinase gene (refer to materials and method section for details). Expression of I-Sce1 endonuclease should induce only one double strand break at a specific site in the TK1 gene given its 18 base restriction sequence. The probability of this sequence occurring twice in the human genome, other than the sequence inserted, is very low and it was recently shown that only five off-target (non-specific) sites for I-Sce1 exist in the human genome (Petek et al., 2010). This system can potentially mimic the radiation dependent double strand break DNA damage that has previously been linked to bystander mutations in naïve cells. And using this system to induce one DNA double strand break at the I-Sce1 site, it should be possible to answer the question of whether DNA damage is actually involved in the process of bystander signaling or not. If so how many breaks are required to generate a sufficient bystander signal to be measured in terms of increased mutation fraction in naïve bystander cells.

A similar cell line using I-Sce1 insert in intron 4 of TK1 gene was constructed by Honma et al. (2003) to identify the relative contribution of DNA repair using the two dominant DNA repair pathways of non homologous end-joining (NHEJ) and homologous recombination (HR). The I-Sce1 cell line developed by Honma et al. (2003) was also derived from TK6 cells but the I-Sce1 insert was in intron 4, only 75 bp upstream of exon 5 in the active TK1 allele (whereas I-Sce1 insert in E18 is 640 bp upstream of exon 3). Honma et al. (2003) reported that 70 percent of all cells targeted for I-Sce1 induced double strand breaks were repaired by end-joining which was also accompanied by deletions ranging from 100-4000 base pairs. In 23 out of 34 mutants analyzed for hemizyosity, the deletion size was more than 876 bp while 3 out of 34 mutants had deletions of over 7.8 kilobases (kb). Molecular analysis of the remaining 30% cells showed that repair caused complex DNA rearrangements like sister chromatid exchanges

(SCEs). It has been acknowledged by other investigators (Honma et al., 2003) that the relative contribution of (end-joining to homologous recombination) EJ:HR of double strand break repair may vary in mammalian cell lines, but EJ is the predominant mechanism (Takata et al., 1998; Essers et al., 2000). As is logical and also affirmed by Honma et al. (2003) the I-Sce1 system cannot recover every genetic consequence and is biased in favor of large sized deletions that include the nearest exon resulting in loss of heterozygosity (LOH); smaller deletions however that do not affect the TK function remain undetected because they will not be isolated as TFT resistant mutants. Honma's assay was developed to detect the fate of I-Sce1 induced double strand breaks, however they did not report the use of a control vector, therefore the system and their assay was biased in the use of only one targeting vector i.e., pCMV3xnlS I-Sce1 and not comparing the effect of transfecting this vector with a control non I-Sce1 containing vector.

1.12 p-53 regulation of DNA damage checkpoints:

The p-53 protein has been shown to play a pivotal role in DNA damage repair pathways, including double strand breaks, single strand breaks, base excision and mismatch repairs (Vousden and Lane, 2007). Following DNA damage, p-53 is phosphorylated and stabilized by its dissociation from MDM2, and going through post-translational modifications it binds to DNA at target gene promoters that contain p-53 response elements (Riley et al., 2008). In addition to the classical belief of p-53 being the guardian of genome a more collective aspect has been presented (Efeyan and Serrano, 2007) arguing two definite roles as (a) guardian of genome and (b) policeman of oncogenes. The former role is activated by DNA damage stress signaling through ATM/ATR and

chk1/2 kinases while the latter role depends on the p-53 stabilizing protein ARF. Given a cell that undergoes DNA damage and given the cell type, the presence of p-53 will determine entry of a cell into S-phase and its subsequent exit. The crucial observation that p-53 was either mutated or inactivated in almost 50% of human cancers (Efeyan and Serrano, 2007) led to a logical conclusion that if the cell does not have a cell cycle checkpoint, then it must be vulnerable to an override of p-53 independent checkpoints (Vogelstein and Kinzler, 1992). These logical conclusions were confirmed in two research papers (Powell et al., 1995; Russell et al., 1995) that demonstrated the use of caffeine to induce sensitization of p-53 deficient rat fibroblasts or human lung adenocarcinoma cells respectively to DNA damaging agents like ionizing radiation. The p-53 independent checkpoints were argued to be operating at the G2-M transition mediated by the ATM/ATR-chk1/2-cdc25c-cyclinB/cdc2 pathway.

1.13: Variable levels of p-53 can regulate apoptosis or cell cycle arrest:

Ceballos et al. (2005) have reasoned that higher p-53 levels in human leukemia K562 cells can induce apoptosis while lower levels promote cells cycle arrest. These cells harbor a temperature sensitive allele of p-53 and the gene array analyses were compared with cells carrying wild type p-53. The team successfully demonstrated that c-Myc activation can impair p-53 mediated apoptosis by downregulating many down stream targets genes of p-53 in leukemia cells that lack ADP ribosylation factor (ARF). On the other hand the cells expressing wild type p-53 encoded chaperones HSP105, HSP 90 and HSP 27 that impart protection against programmed cell death. This research was important as to how apoptosis could be affected by p-53 levels in a cell. The team also

looked at cancer cell lines derived from various tissues to validate their results and generalize the role of p-53. Two tumor cell lines that were developed from Non-Hodgkin's lymphoma were shown by immunoprecipitation to have mutant type p-53 (Chang et al., 1994) and it was reasoned that p-53 mutation could indicate disease progression. However (ARF) was shown to be mutated or repressed by promoter methylation in many lymphomas and tumors in general (Krug et al., 2002).

Ceballos et al., (2005) have also shown that p-53 mediated cell cycle arrest is promoted by p-21 which inhibits cyclin dependent kinase (CDK). p-21 on the other hand is inhibited by a c-Myc/Miz1 heterodimer complex and that this complex is required for c-Myc mediated repression of many genes besides p-21. A c-Myc/Max complex on the contrary upregulates certain genes upon binding with specific DNA sequences called (E-boxes).

1.14 p-53 status of TK6/E18 cell line:

While working with WTK1 and TK6 (Xia, et.al in 1995) reported that both cell lines were derived from a single donor but vary in their p-53 status. They determined that WTK1 and TK6 both lymphoblast cell lines contain an equal level of p-53 mRNA and that irradiation leads to increased levels of p-53 but to a greater extent in TK6. TK6 contains the wild type p-53 while WTK1 contains the mutated form (due to a homozygous mutation in codon 237 of exon 7 of p-53 gene). They reported that due to this mutated p-53 WTK1 cells were more radio-resistant than TK6 which exhibited elevated p-53 levels (up to 4.4 fold higher). TK6 cell line showed immediate apoptosis

following irradiation exposure while WTK1 divided at least once before apoptosing.

1.15. Restriction enzymes Not 1, Sfi1 and I-Sce1:

Not 1 is an 8 base cutter with recognition sequence GC[^]GGCCGC but being methylation dependent it cuts less frequently. This sequence occurs 3000 to 5000 times in the human genome (Zabarovsky et al., 1994) the broad range corresponds to the methylation dependence. Sfi1 is a 13 base cutter with a recognition sequence of GGCCN[^]NNNNGGCC (Nolin and Dobkin, 1991). This sequence occurs 20,000 times in the human genome (Myers, 1999) and interestingly makes 4 DNA breaks instead of the usual 2 (Wentzell et al., 1995). Since Sfi1 is a tetrameric protein unlike the other restriction enzymes therefore it recognizes two restriction sites on adjacent DNA strands and then make 4 cuts simultaneously. Sfi1 works like an 8 base cutter, due to its non-specific restriction sequence recognition but it cuts more frequently than Not1 because it is a tetrameric protein and methylation independent. I-Sce1 is an 18 base cutter (TAGGGATAA[^]CAGGGTAAT) and cuts once at the I-Sce1 site within the TK gene (refer to figure 3.10). Five sequences similar to the wild type I-Sce1 endonuclease cleavage site have been identified in the human HT-1080 cells located on chromosomes 1, 9, 11, 16 and 17. Two additional sites on chromosomes 1 and 16 were blocked by DCM methylation of the CCAGG sequence, bringing the total number possible off-target cleavage site of I-Sce1 to seven (Petek, et.al., 2010). A more recent estimate of the human genome, based on chromosomes 21 and 22 shows that there could be as many as

15,000-20,000 Not1 sites, of which 6000-9000 are unmethylated in any given cell. (Kutsenko et al., 2002).

1.16. DNA damage and repair in radiation targeted cells:

The cells that are directly targeted by radiation produce a bystander signal. It is assumed that this induced DNA damage may be involved in the production of a bystander signal (Prise et al., 1999). Zhang et al. (2008) showed that through RNA interference, the factors that regulate DNA repair could be inhibited and that p-53 status of lymphoblasts (WTK1 p-53 mutant, TK6 p-53 wild, NH32 p-53 null) did not affect either the production or reception of radiation induced bystander signaling. They also demonstrated that inhibition of DNA PK (one of the major enzymes involved in non homologous end-joining repair) caused the mutation fraction of directly irradiated cells to increase in WTK1 cells but decrease in TK6 and NH32 cells. However DNA PK inhibition led to increased mutation fraction in bystander cells, regardless of the p53 status of a cell line. This suggests that the reception of bystander signal by naïve cells is independent of p-53 status but the production of signal may have some p-53 involvement. Honma et al. (2003) have also concluded through targeted DNA double strand breaks at an I-Sce1 site that non homologous end-joining (NHEJ) efficiently repairs most of the induced double strand breaks in DNA. If however there is a misrepair of DNA double strand breaks; it becomes expressed as a mutation and sometimes large deletions cause mutations that could be lethal.

Later studies conducted on the dose and time responses of lethal mutations and chromosomal instability due to ionizing radiation (Mothersill et al., 2000) showed that

there was an absence of lethal mutations in the descendants of HPV-G keratinocytes that received a low dose (0.5 Gy) of γ rays, compared to cells that were given higher doses (1-3 Gy). The team also showed that when descendants of cells that were exposed to (0.5Gy) α -particles were allowed to form colonies, their colony forming ability was reduced by 80%. The team did not rule out a relationship between lethal mutations and low LET radiations but argued that this relationship could be more complex.

1.17. DNA damage and repair dynamics in bystander induced cells:

Reports of DNA damage in bystander induced cells have been appearing in literature for some time now, but most of these studies are based on an indirect measure of the bystander effect like the phosphorylated H₂AX foci formation. Sokolov et al. (2007) reported the accumulation of DNA double strand breaks in bystander cells by measuring γ -H₂AX focus formation. In addition the team also reports of having effected double strand breaks in naïve bystander cells by transferring conditioned medium from cancer cells. Another study (Burdak-Rothkamm et al., 2007) indicated that the additional occurrence of 1.3-2 foci on an average could account for the DNA double strand breaks in bystander induced normal human astrocytes and T98 glioma cells. The team also reasoned that since DMSO, Filipin and anti-TGF β -1 could inhibit the induction of γ -H₂AX, therefore membrane bound signaling could be involved.

Bystander induced cells showed induction of AP endonuclease 1 (APE1), proliferating cell nuclear antigen (PCNA) and replication protein A (RPA). These factors point towards the participation of Base excision repair (BER) for repairing the single strand breaks in bystander induced cells (Hamada et al., 2007). The team therefore reasoned that

BER inhibition should amplify the bystander induction. The authors have also discussed that bystander induced γ -H₂AX foci formation involves ATR but not ATM or DNA PK, this would also indirectly confirm findings of Zhang et al. (2008) who reported an increased mutation fraction in naïve bystander cells, when conditioned medium was transferred from DNA PK inhibited cells. It has been argued by Hamada et al. (2007) that bystander induced cells generally show an up regulation of p-53 and p-21 but a down regulation of CDC2, cyclin B1 and Rad 51. However these claims could vary depending on the model and the treatment given to a system being investigated for bystander dynamics.

A team recently reported to have found no evidence of bystander induction in human fibroblasts by using carbon and uranium heavy ions to target single cells. They used γ -H₂AX foci, sister chromatid exchanges and micronucleation as end-points (Fournier et al., 2009). The team did argue that culture condition or other factors may have caused this behavior but they mentioned that the results of investigation did not exceed the experimental error values. Hence they concluded that the bystander effects are either lacking or less pronounced.

1.18. DNA repair enzymes and effect of inhibition on bystander mutagenesis:

In the event of DNA damage many damage sensor enzymes are activated that trigger the repair process. Of known involvement are Ataxia telangiectasia mutated (ATM), ATM and RAD 3 related (ATR) and DNA dependent protein kinase (DNA PK). In the bystander induced cells, the inhibition of DNA PK and ATM was reported to have no influence on the number of γ -H₂AX foci, but a mutation of ATR could abrogate this

induction (Burdak-Rothkamm et al., 2007). It was interesting to note that chemical inhibitors were compared to mutated form of ATR for a study; however this was due to the fact that a commercially available ATR inhibitor does not exist. This investigation also reported that bystander focus formation was restricted to the S-phase of cell cycle. The foci were reported to persist in bystander cells for up to 72 hours but 20 hours post-irradiation, showed the maximum induction.

It is again important to mention that these end-points could vary with the experimental model, culture conditions and treatment conditions. This is a matter of controversy in the field of radiation induced bystander effect (RIBE), however with regard to γ -H₂AX focal formation, there is a clear understanding that they can appear in bystander induced cells as soon as 2 minutes after ionizing radiation exposure and can persist (at significantly elevated levels) for up to 6 hours (Hu et al., 2006).

The kinase enzymes of DNA repair can be specifically inhibited using small molecules like CGK 733 for ATM at low concentrations (600nM) or ATM/ATR in tandem at high concentrations (10uM) and NU7026 (5uM) for DNAPK (Crescenzi et al., 2008). ATM and DNAPK have been shown to be inhibited but one specific inhibitor for ATR has not yet been found. One compound NVP-BEZ235 (Toledo et al., 2011) is still being tested for its efficacy.

1.19 Electroporation of small molecules and plasmids into host cells:

Electroporation is a highly efficient way of transforming cells. Small molecules and vectors can be easily and efficiently transported into host cells via electrically induced

pores in the membrane (Jaroszeski et al., 2000; Marty et al., 2006; Mir et al., 2005). A pulse duration of 20-40 ms is required to for efficient electrodiffusive transport of electrically charged DNA in the presence of at least 1 mM Ca^{2+} . Studies done in yeast cells have shown that electrodiffusion of free DNA in the medium is 7×10^4 times more efficient than simple diffusion. The primary field effect of membrane electroporation causes a cascade of events for transport of DNA into the host cells which includes pore formation, pore enlargement and transport of large molecules across the membrane (Neumann et al., 2000). It has also been determined that production of heat and free radicals during electroporation can be successfully inhibited using super oxide dismutase (SOD) and catalase (Benov et al., 1994). Lipid peroxidation and hemolysis in red blood cells can also be induced during electroporation, depending on pulse field strength and duration. Although this research was done using 2-7.5 KV of voltage and exponential decay, most contemporary electroporations are done at much lower voltages and square waves (Jordan et al., 2008).

1.20: Electroporation induced DNA damage in mammalian cells:

Evidence exists to show that electroporation can cause DNA damage in the host mammalian cells (Meaking et al., 1995). The number of DNA breaks was shown to increase with either the applied voltage or an increase in capacitance. DNA damage increased markedly at field strengths of over 400 V/cm but that could be counteracted by lowering the capacitance from 1160 uF to 690 uF. At a voltage of 900 V/cm an associated temperature increase of about 7°C was observed. Based on this data it is safe to assume that in restriction enzyme experiments structural loss of the protein may not be

an issue. However the team concluded that electropermeabilization unlike radiation induced DNA damage, may be small.

Naked DNA in aqueous solution was also tested for effects of electroporation and shown to cause nicks (Goldberg and Rubinsky 2010). This suggests that although electroporation may be an efficient way of transforming mammalian cells but this transformation comes at the cost of limited DNA damage and possibly the production of some free radicals. In my experiments these factors were considered and data normalized to subtract the DNA damaging effects of electroporation.

1.21: Electroporation versus Lipofection:

In a study using neuronal cells the relative transfection efficiency of two delivery systems was established. Lipofection proved to be more toxic than electroporation and also did not give higher transfection efficiency. These cells were grown to a density of 1×10^6 cells/mL and washed in ice cold PBS. The cells were resuspended at 2.5×10^6 cells and electroporated in a 250uL reaction. The investigators suggested putting the cells back on ice for 15 minutes after shocking before being added to growth medium. The same parameters were used for my experiments except that incubation on ice did not prove beneficial and also could not be implemented (in some experiments) where bystander signal production immediately after electroporation had to be investigated. Transfection efficiency with electroporation was as high as $100\% \pm 8.2$, while with lipofection it was approximately 40%. (Li et al., 1997). In a separate optimization for electroporation investigation (Jordanet et al., 2008) square waves were found to be more stable vis-à-vis

voltage when compared to exponential decay and a 250 Volt square wave produced the best results for transfection.

1.22: Superoxide dismutase (SOD) degrades superoxide radicals:

Super oxide dismutases (SOD) are a class of metalloenzymes that are present in all oxygen using organisms and function by imparting protection against the oxidative damage of high concentrations of superoxide radical anion (\bar{O}_2) (Moscone & Miscini, 1988).

The redox activity of SOD has been reasoned by (Davis et al., 2004) as the primary cellular defense against oxidative damage by simply reducing super oxides (\bar{O}_2) to oxygen (O_2) and hydrogen peroxide (H_2O_2). Overexpression of SOD has been demonstrated to have anti-proliferative and anti-tumor effects in-vitro and in-vivo. Highly toxic by-products of cellular metabolism like reactive oxygen species (ROS) and hydrogen peroxide were successfully degraded in α -particle (0-10cGy) bystander induced human diploid fibroblasts using 300 units/mL of super oxide dismutase (SOD) (Azzam et al., 2002). They showed that SOD and catalase, acting on reactive oxygen species based bystander signals, could significantly reduce the number of micronuclei in radiation-induced bystander cells and they also down-regulated p-53 and p-21. SOD is inactivated (but not inhibited) by large concentrations of hydrogen peroxide (~15mM) but it may even be protected to some extent by the catalase enzyme (Bray et al., 1974).

During acute inflammatory responses the elevated levels of pro-inflammatory cytokines enhance the deleterious effects of ROS (Davis et al., 2004). If the nature of DNA strand

break induced bystander signal is ROS then degrading of these super oxides with superoxide dismutase (SOD) and catalase should lower the bystander MF.

1.23: Bystander effects are not unique to ionizing radiation:

As already mentioned, bystander signals can vary either by type of cells, treatment conditions or even the phase of cell cycle following is an account of some treatments other than radiation that can also produce a bystander effect. Bystander effects have also been demonstrated through the use of chemotherapeutic drugs (Asur et al., 2010) and photodynamic stress agents (Dahle et al., 2001). Some chemotherapeutic agents that are known to cause the production of bystander effects are:

- a) Mitomycin C (Rugo et al., 2005)
- b) Phleomycin (Demidem et al., 2006)
- c) Paclitaxel (Alexandre et al., 2003)

It is known that in attached cells the bystander signal is transmitted through gap junctions and in suspension cells this happens via soluble factors released into the medium (Lyng et al., 2006) and that bystander signals could be detected in the medium for up to 24 hours after radiation exposure.

1.24: Bystander induced activation of MAPK targets:

Evidence exists in the literature (Hei et al., 2006; 2008) to suggest that radiation induced bystander signals can activate some downstream MAPK targets such as p90RSK which is

a member of ETS oncogene family (ELK1), activating transcription factor 2 (ATF2) and cyclooxygenase (COX2). Some investigators have also implicated small signaling molecules, used in the animal kingdom, released in response to environmental stress to be involved in bystander signaling. Some of these bystander signaling amines have been reported to include 5-Hydroxytryptamine (5-HT, serotonin), L-DOPA, glycine or nicotine, following ionizing radiation exposure (Poon et al., 2007). MAPK pathway activation has also been observed in bystander cells by Azzam et al. (2002) and involvement of oxidative metabolism alleged as being a possible bystander signal. Super oxide dismutase (SOD) and catalase were shown to significantly inhibit the number of micronuclei formed, and decreased activation of downstream stress targets like p-21 and p-53 in naïve AG 1522 cells. It was suggested that reactive oxygen species derived from flavin containing oxidase enzyme (presumably NADP [H] oxidase) were the main source of upregulation of oxidative stress proteins p-21 and p-53. Other proteins believed to be activated as a response to stress included, NF κ B, Raf-1, ERK1/2, c-Jun, p-38 MAP kinase. At least ERK1/2 and p38 again indicate towards the involvement of a MAPK pathway.

1.25: Inhibition of Mitogen activated protein kinase (MAPK) pathway and bystander signaling:

Angelika et al. (1998) have demonstrated that a small organic compound called PD 98059 can be used to inhibit cyclo-oxygenase 1 and 2 along with the inhibition of thromboxane synthase. At a concentration of 20 μ M, PD 98059 was shown to be highly efficient to inhibit thrombin-induced activation of p42mapk and p38mapk . The nature of

DNA strand break induced bystander signal can therefore also be tested by using PD 98059 (Cell signaling Cat # 9900S) if MAPK pathway is involved. Azzam et al. (2002) also demonstrated that several downstream signaling proteins of the MAPK pathway were activated in naïve cells that were exposed to conditioned bystander signal containing medium. Within 1 minute of exposure to 5cGy radiation, Raf-1, ERK ½, JNK and p38 were notably phosphorylated (activated). It was also argued that since many downstream proteins of the MAPK pathway are activated by reactive oxygen species (ROS) therefore the team was successful in partially inhibiting ERK1/2 and JNK with 30 minute SOD and catalase inhibition.

1.26: MAPK activation initiated by small GTP- binding proteins:

G-protein coupled receptors (GPCR) are identified as one of the most common membrane proteins involved in transmission of signals from extracellular environments to the cytoplasm (Gutkind, 2006). MAPK proliferative pathways have been reported to show activation upon mitogenic stimulation through a GPCR dependent manner. Extracellular signal regulated kinase (ERK) is a downstream signaling protein whose enzymatic activity increases upon mitogenic stimulation and impeding its function leads to loss of cellular proliferation. It has also been reasoned that constitutive activation of proteins upstream of MAPK can lead to a transformed phenotype and constitutive activation of MAPK itself can lead to tumorigenesis in mammalian cells (Mansour et al., 1994).

It was reported that MAPK activation is initiated by small GTP-binding proteins, including RAS. These activations however are short-lived and must be converted to long-

lasting forms to participate in this activation cascade as reported by Wilkinson and Millar, (2000). Mansour et al. (1994) have also proposed that prolonged activation of MAPK kinase, kinase, can lead to activation of oncogenic proteins like Ras, Raf, Src and Mos. Constitutively active MAPK mutants were designed that had 400 times the normal expression in wild type cells, which when expressed in HEK293 and NIH 3T3 cells showed many hallmarks of tumorigenic effect like cell rounding, high saturation density, loss of contact inhibition, and unorganized growth pattern.

1.27: Raf and MEK plays a role in cancer progression and phosphorylates c-Myc:

There is also substantial evidence that validates the role of Raf and MEK in cancer progression and promotion of cancer growth (Shields et al., 2000). Thus MEK1/2 are prime candidates for inhibition in a DNA strand break induced bystander effect that can otherwise promote cancer progression during radiotherapy and DNA targeting chemotherapy. MAPK pathway has been successfully inhibited using small molecules like PD98059 (McCubrey, et. al., 2007) and U0126 (Liang et al., 2011). There is some debate about the specificity of these inhibitors since they are phosphor inositide 3 kinase specific and there are other important kinase enzymes that may also be affected or inhibited. A p-38 inhibitor PD98059 was used to investigate the role of MAPK pathway in DSB-ABE. McCubrey et al. (2007) have identified c-Myc as one of the downstream signaling proteins of the MAPK pathway. According to them ERKs enter the nucleus to directly phosphorylate many transcription factors including Ets-1, c-jun and c-Myc.

1.28: ERK1/2 and p38 kinases phosphorylate p-53 at Serine 15:

In the MAPK cascade the downstream kinases ERK1/2 and p38 have been shown (She et al., 2000) to phosphorylate p-53 at serine 15 in response to ultraviolet radiation exposure of mouse epidermal cell lines (JB6). ERKs and p38 were reported to form a complex with p-53 after UV(B) irradiation of these cells and that abrogation of the function of ERKs and p38 with PD98059 or SB202190 resulted in abrogation of the p-53 phosphorylation.

If DSB-ABE follows the same route, then that might suggest a link between bystander signaling that leads to increased mutation fraction in naïve cells. As already mentioned oxidative stress and reactive oxygen species (ROS) can also lead to the downstream activation of p-21 and p-53 (Azzam et al., 2002) therefore the nature of bystander signal may involve the MAPK pathway and ROS.

1.29: The possible MAPK/c-Myc/p-53 link for DNA damage associated bystander effect:

DNA damage sensor proteins are phosphatidyl inositol 3 kinase (PI3K) enzymes that set up a cascade of events leading to DNA repair or cell cycle arrest or apoptosis. The extent of DNA damage determines the fate of a cell. If the DNA damage is heavy and repair done at the cost of large deletions, then the mutant may be set on a track to programmed death or apoptosis. Apoptotic signaling due to DNA damage has been explained in many systems but most systems have been reported to use a p-53 mediated pathway.

One of the downstream signaling proteins of MAPK pathway is c-Myc (McCubrey et al., 2007) which plays a vital role in growth control, differentiation and apoptosis. Overexpression of c-Myc sensitizes cells to undergo programmed cell death (Hoffman

and Liebermann 2008). The decision to undergo cell death and its regulation, however, is dependent on a specific cell type and its physiological status. Hoffman et al. (2008) have also identified that this apoptosis is p-53 mediated in cells that bear massive DNA damage (Ceballos et al., 2005).

Study Goals

My first study goal was to investigate if bystander effect is generated by DNA damage and if so to find out what is the minimum number of breaks required. The other goal of the project was to investigate whether DNA damage is also one of the end-points of bystander effect in naïve cells.

This project was designed to study possible bystander effects from radiation independent DNA damage and to examine this phenomenon a special cell model was required. This cell model was derived from a TK6 cell line developed in Dr. Howard Liber's lab in which intron 2 of the human *TK1* gene has had a sequence targeted by the I-Sce1 restriction endonuclease inserted at a unique BsrGI site at position 1090 of the *TK1* gene (Lippert et al., 1998). These cells had not been further characterized. Here, this modified TK6 cell line called E18 was first characterized and then used for the investigations. I-Sce1 endonuclease is a mitochondrial intron-encoded endonuclease of *Saccharomyces cerevisiae* that has a very low probability of cutting the DNA even within large genomes because it recognizes an 18 base restriction sequence. It was demonstrated that double strand breaks can be initiated by I-Sce1 at a pre-determined location in a mammalian genome using the I-Sce1 system (Honma et al., 2003). E18 cells are thymidine kinase heterozygotes (tk+/-), and therefore mutations at this locus (tk+/- → tk-/-) can be easily quantified by selecting cells in the pyrimidine analog trifluorothymidine (TFT). E18 cells also contain a single unique I-Sce1 site built into the active allele. Therefore, if I-SceI enzyme is expressed in the cell, a single double strand break will be introduced within the target gene locus. It is already known that this can lead to a significant increase in gene mutation frequency in the targeted cells that express I-SceI (Honma et

al., 2003) but it is not known whether this sort of damage is sufficient to elicit a significant level of bystander signal that can be transferred to naïve non-targeted cells.

There are various distinct methods to introduce restriction enzymes or vectors into cells. The plasmid vector pAdTrackCMV I-SceI was obtained from Dr. Jac Nickoloff's lab at Colorado State University. This expression vector not only contains I-SceI, but also expresses GFP, so that transfection/expression frequencies in percentage can be monitored by green fluorescence.

A second approach was used in which various restriction enzyme-induced breaks were generated to limit the damage in the targeted cell to DSBs. A positive bystander effect was measured as an increase in gene mutations, at the thymidine kinase locus.

The nature of DNA strand break induced bystander signal is another area for investigation. To explore the nature of bystander signal some chemical inhibitors/enzymes were used to either inhibit the generation of DNA strand break associated bystander signal or its reception by the naïve cells.

Hypothesis statement:

Turning focus from radiation induced bystander effects (RIBE) to DNA strand break associated bystander effects (DSB-ABE) it is important to understand the hypothesis and how it was tested.

My hypothesis is that a single DSB, induced independently of IR, can produce a bystander signal and effect in naïve cells.

To elaborate on the hypothesis; if radiation of nuclear DNA causes random DNA strand breaks that lead to the release of bystander signal then radiation independent DSBs should also produce the same effect. Direct as well as bystander mutation fractions were measured, which are hereby referred to as Direct MF or Bystander MF, as the indirect measure of bystander mutagenesis (BM). Direct effects are those caused by the direct exposure of cells to a mutagen or in this project the restriction enzymes while indirect effects are a by-product of the direct exposure, possibly released into the medium of exposed cells, which when transferred to naïve cells causes DNA damage (Seymour et al., 1986; Nagasawa et al., 1992; Hei et al., 2008). Some of the direct effects of radiation include genomic instability, chromosomal rearrangements, delayed mutation, DNA nucleotide repeat instability, cellular transformations and cell death. It is postulated that the same effects can be observed in naïve cells which are exposed to bystander signal from targeted cells. It is still unknown what form or forms of damage to targeted cells actually leads to the generation of a range of bystander signals. One of the hypotheses is that DNA damage can also increase the mutation rate and that is what was investigated in this research. This is not to say that only DNA damage could cause bystander effect (BSE) or is required in any way to initiate a BSE. Besides specific DNA damage, ionizing radiation can cause stochastic genome-wide damage and therefore tends to up regulate BSE. The DNA damage could be base damage, single strand breaks, double strand breaks or the stress could result in production of reactive oxygen and nitrogen species due to the ionizing effect or radiation-independent induced DNA damage.

Electroporation was used as the delivery system of choice due to its high transfection efficiency and low cell mortality. Electroporation has recently been used for electrochemotherapy and gene delivery (Jaroszinski, et. al., 2000) but my investigations

have revealed that electroporation not only causes additive DNA damage but also results in the production of bystander signals that would increase mutations in the non-targeted cells in-vivo, thereby putting the patient at an increased risk of secondary tumors arising from electrochemotherapeutic practices.

DNA damage response to endogenous and exogenous sources of damage is an important defense mechanism of a cell to prevent it from becoming tumorigenic. Hence understanding the link between DNA damage and bystander mutagenesis will provide us with new strategies to combat secondary cancers. To test this hypothesis following aims were pursued.

Aim 1: To determine if radiation independent double strand breaks produce bystander signals.

Specific aims for aim 1:

A: To characterize the *TK1* locus of E18 lymphoblast model cell line.

B: To specify an optimal delivery system for transfecting host cells.

C: To optimize parameters of delivery system of choice.

D: To measure bystander mutagenesis (BM) generated by double strand breaks (DSBs) in terms of increased mutation fraction in naïve cells.

Aim 2: To measure if a single double strand break (dsb) in a fraction of cells could produce a measurable bystander signal to increase mutation fraction in naïve cells.

Specific aims for aim 2:

A: To compare the relative effect on induced bystander mutation fraction (BSMF) by transfecting I-Sce1 plasmid versus I-Sce1 enzyme.

B: To measure DNA damage dose effect on bystander signal generation in terms of increased BSMF.

C: To establish temporal kinetics and measure the “BSE induced by I-Sce1 alone” as differentiated from “total induced BSE (from electroporation and I-Sce1).”

Aim 3: To investigate the nature of bystander signaling process through chemical inhibition.

Specific aims for aim 3:

A: To measure the effect of inhibiting DNA damage repair processes on bystander signal production.

B: To inhibit various known pathways of bystander signaling to determine the nature of DNA strand break induced bystander signal.

Chapter 2: Materials and methods

Cell culture:

E18 lymphoblastoid cells are a TK6 derivative suspension cell line with an I-Sce1 restriction site (18 base restriction sequence) engineered in intron 2 of the active thymidine kinase (*tk1*) allele on 17q23.2-25.3 (Fig.2.1). If I-Sce1 enzyme is transfected into these cells, only one double strand break should be generated, however about five additional off-target sites have been recently identified in the human genome (Petek et.al., 2010).

Lymphoblasts were maintained in suspension and grown in T-75 flasks containing RPMI 1640 medium supplemented with 10% Horse serum and 5% Penicillin, streptomycin (PenStrep). The cells were passaged for 3-4 days in a non-antibiotic supplemented medium to avoid any additional stress on the culture to undergo electroporation. They were grown to a density of 1×10^6 cells/mL (incubated at 37°C and 5% CO₂) but never allowed to go past that density to prevent contact inhibition.

Plasmids:

The experimental pAdTrackCMV I-Sce1 used in this research was acquired from Dr. Jac Nickoloff's laboratory at Colorado State University while the control plasmid pAdTrack CMV was purchased from Addgene Inc., (cat# 16405 mammalian plasmid). They were both grown in *E.Coli* DH5 α cells, cultured in Kanamycin supplemented LB broth respectively and sub-cultured in LB agarose plates also supplemented with Kanamycin for 16 hours. Plasmid DNA was extracted with Qiagen's miniprep spin kit (Cat # 27104). Plasmids pQCXIH I-Sce1 and pIRES-Hyg3 I-Sce1 were the courtesy of Dr. John P.

Murnane (Department of Radiation Oncology, University of California, San Francisco, USA).

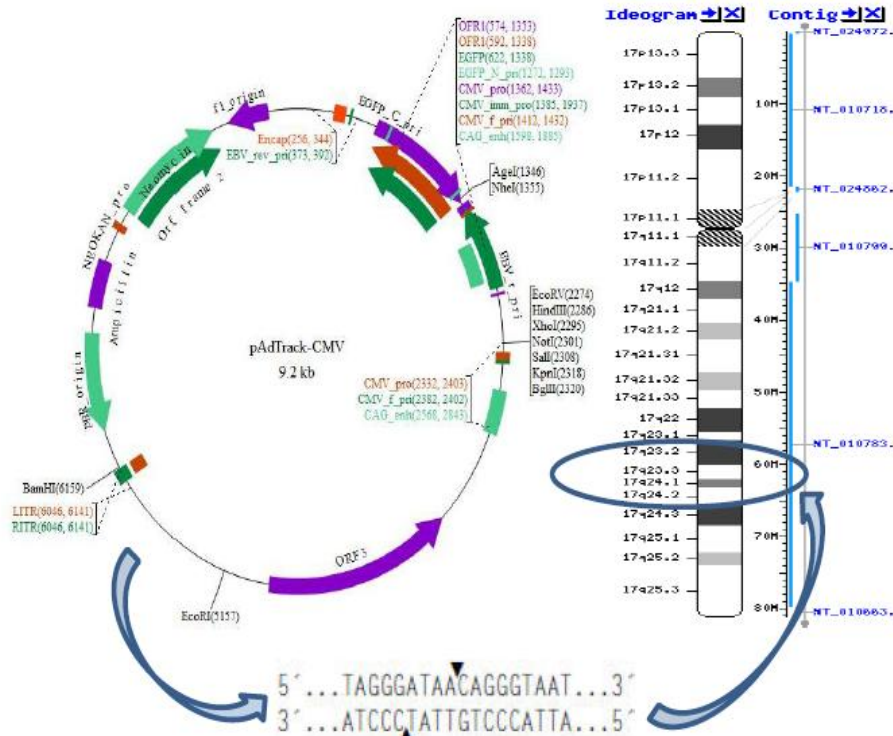


Figure 2.1 (a) pAdTrack CMV vector map which carries the I-Sce1 gene.

Figure 2.1 (b) Map of chromosome 17 showing where the I-Sce1 restriction enzyme causes a DNA DSB.

Primers:

For the amplification of 223 bp region of intron 2 of *TK1* gene of E18 cells the primers used were: forward >5' TCA AGT GAT CAA CGC ACC TC 3' and reverse < 5' CCT GCC CCA ACA TTC TTT TA 3'. While the 700 bp region of *TK1* gene containing the I-Sce1 site was amplified using these primers: forward > 5'-CGC CTC CAC CCA GCT AAT-3', reverse < 5' AGT GGG GAA GGC AGA AGC-3'.

Polymerase chain reaction:

A Roche expand high fidelity PCR kit (cat # 11732641001) was used to prepare 25uL reactions as per vendor specifications to be run for gel electrophoresis. Thermocycler was set as stage 1 (1 cycle: 95°C, 2 minutes). Stage 2 (30 cycles: 94°C for 30 seconds, 60°C for 30 seconds and 72°C for 1 minute). Stage 3 (1 cycle: 72°C for 5 minutes and 4°C hold)

DNA estimation:

All DNA was extracted using the Qiagen miniprep kits (Cat # 27104) and stored at -20°C and DNA concentrations were determined with nano drop and recorded in ng/uL.

Digestion of amplified DNA with enzymes:

pTKUAS Vector concentration used for digestion was 80ng/uL, TK6 PCR product was 21.4 ng/uL and E18 PCR product was 25 ng/uL. These DNA samples were incubated with or without 2 units of I-Sce1 enzyme at 37 °C for 16 hours to get complete digestion or 8 hours to get partial digestion products. The undigested or digested products were analyzed with gel electrophoresis.

Gel electrophoresis: A 2% agarose gel was prepared by dissolving 1 gm of ultra pure lab grade agarose in 50 mL of 1x TBE buffer and supplemented with 0.004% ethidium bromide. The gel was run at 250 volts in a gel electrophoresis chamber, also filled with

1xTBE buffer, for 40 minutes. The gels were pictured using the Trans UV illuminator attached to the Kodak Imaging software at 3.5 second exposure. 12uL samples of each test category were loaded in each well.

Electroporation parameters for lymphoblastoid cells (optimized for the specific cell line being used in this project): The cells were pelleted by spinning at 1K rpm for 5 minutes and resuspended in electroporation buffer to get a total density of 5×10^6 c/250 uL (or 20×10^6 c/mL) of electroporation buffer to prepare the stock for reaction mixture. Measured 10-25ug of total plasmid DNA extracted from the *E Coli* DH5a cells (DNA extraction was performed using Plasmid Miniprep kit from Promega). Added 10-25ug of total Plasmid DNA per electroporation reaction to a 1.5mL tube and then added the 250uL of cells resuspended in electroporation buffer. Following settings were used for the BioRad Gene Pulser (as specified by the Vendor):

Parameters for electroporation in a BioRad gene pulser

Cell density 5×10^6 c/250 uL or 20×10^6 c/mL	Voltage: 250 V
Volume for reaction mixture: 250 uL	Field strength: 0.625 kV/cm
DNA concentration 10-25 ug/pulse/reaction	Capacitor: 960 uF
Cuvette gap: 4 mm	Time constant: 60 msec

Immediately after electroporation the cells were immersed into warm/fresh RPMI medium (supplemented with 10% Horse serum and 5% Penstrep) and incubated at 37°C for 5 hours to get 50-70% electroporation efficiency. Cell viability in post-electroporation conditions was approximately 95-97%.

Recipe for the Electroporation buffer (For 1L buffer):

Sodium chloride (NaCl) 8 g, disodium hydrogen phosphate ($\text{Na}_2\text{HPO}_4 \cdot 7\text{H}_2\text{O}$) 2.16 g, potassium chloride (KCl) 0.2 g, monobasic potassium phosphate (KH_2PO_4) 0.2 g, dissolved in 800 ml ddH₂O, adjusted the pH to 7.3, added double distilled water to get a final volume of 1000 ml.

PBS used in place of electroporation buffer:

A 250 uL reaction mixture for transfection, using a working solution of 1X phosphate buffered saline (PBS) was used for electroporation in place of electroporation buffer, for comparison. Other conditions were kept exactly the same as used for electroporation buffer.

Lipofection: (as per vendor protocol):

Transfection reagent marketed by Mirus® and specifically called the Mirus TranIT 2020 reagent was used for testing transfection efficiency and comparing the results with transfection efficiency of electroporation. Grew cells to 4×10^6 cells/mL and incubated 2.5 mL of culture medium/well for 18-24 hours in a 6 well plate. (plated 10×10^5 c/well therefore 2.5 mL of 4×10^6 cells/mL had the required cell number)

TransIt 2020: DNA complex was prepared by warming and vortexing the Mirus TransIt reagent before use. Added 250 uL of OptiMEM reduced serum medium in a sterile 1mL polystyrene tube and mixed with 2.5 ug of plasmid DNA and pipeted (titrated) gently to

mix completely. Then added 7.5 uL of TransIT reagent and incubated the stock at room temperature for 15-30 mins. Later added 43 uL/reaction of this TransIT: DNA stock mix to the 1 mL Eppendorf tube containing the cells for transfection. Incubated these transfected cells for up to 72 hours and harvested to establish the transfection efficiency by counting the green fluorescing cells.

Transfection efficiency:

Transfection efficiency was established by using the GFP marker gene of pAdTrackCMV I-Sce1 plasmid. At 5, 10 or 15 hours after electroporation or lipofection the cells were fixed in Methanol: Acetic acid (3:1) and counterstained with DAPI and those with green fluorescence were counted at 100X. Five random fields of view were scored for each slide and following formula used for determining the percentage of green fluorescing cells.

Percentage transfection(TE%) =

$$\frac{\text{average of total number of green cells in 5 random fields of view}}{\text{average of total number of cells per view}} \times 100$$

Microscopy:

Microscopy was performed at the department of ERHS facility at Colorado State University, and cells were analyzed at 100 X in oil immersion while photography was done using the Nikon camera attached to the microscope. The MetaVue software managed imaging system, exposure and photography.

Irradiation (γ -rays):

Cell cultures for irradiation were grown to a density of 1×10^5 cells/mL in T-75 flasks and irradiated at 0.0, 0.25, 0.50, 0.75 and 1.0 Gy with γ -source irradiator (G. L. Shepherd Mark-I/68A SS-056 at Colorado State University's facility). The flasks containing cell culture were put on a turn table for a uniform exposure to the γ -ray source Cesium 137. After exposure the cells were allowed a recovery period of 3 hours in an incubator set at 37 °C.

Restriction Enzymes:

2.5 μ L of enzyme reaction mix containing 25 units of each enzyme, buffer and BSA were suspended in a 250 μ L electroporation mix that contained E18 cells at a density of 20×10^6 cells/mL. The enzymes Not1 (cat # R3189), Sfi1 (cat # R0123S) and I-Sce1 (cat # R0694S) were obtained from New England Biolabs. The Mock electroporation was done using the non-digesting protein substitute albumin, while the absolute control for electroporation had E18 cells only. The specific controls for each enzyme were not electroporated but were mixed with the same units of enzyme.

Chemical inhibitors:

ATM/ATR inhibitor CGK 733: A 10 mM stock was prepared in DMSO and used at a concentration of 600 nM to inhibit ATM and at a concentration of 10 μ M to inhibit ATM/ATR together. The inhibitor was added to directly targeted cells and allowed an incubation period of 16 hours before transferring the conditioned medium from direct to naïve bystander cells. The Directly targeted cells with the inhibitor were centrifuged at

1000 RPM for 5 minutes and the conditioned medium (supernatant) carefully removed from pelleted cells. The pelleted cells were later resuspended in fresh RPMI medium supplemented with horse serum and penstrep and incubated another 72 hours to allow mutant expression.

DNA PK inhibitor NU7026: A dose of 1 uL/mL from a 10 uM stock of NU7026 (SIGMA CAS 154447-35-5, Lot# 098K46282) prepared in DMSO was used for inhibition. In a 50 mL RPMI culture medium of directly targeted cells; 50 uL of NU7026 stock solution was added. Cells were allowed a 16 hour inhibition period immediately after they were electroporated with the plasmid. At the end of inhibition period the medium containing bystander signal was transferred to naïve bystander cells and incubated another 72 hours for mutants to express themselves.

ROS degradation by super oxide dismutase (SOD): SOD was purchased from MP biomedical (cat # 190117, Lot # 9463J). The enzyme was prepared according to vendor specifications at 5 mg/mL in 0.05 M monobasic potassium phosphate (KH_2PO_4) and 0.1 mM Ethylenediamine tetra-acetic acid (EDTA) and used at 10 uL/mL.

MEK1/2 inhibitor (PD98059): This inhibitor was purchased from Cell Signaling (Cat# 9900S, Lot# 0013) and prepared according to vendor specifications. 1.5 mg of powder was dissolved in 280 uL of DMSO for a 20 mM stock and made 50 uL aliquots to be stored at -20°C . The 50 uL (20 mM) stock was diluted in 150 uL of phosphate buffered saline (PBS) to get a working solution at 5 mM. This inhibitor, according to the vendor is MEK1 inhibitor but other investigators have shown it to inhibit cyclo-oxygenase -2 (COX-2) also (reference literature review 1.14).

Mutation Assay:

E18 human lymphoblasts are thymidine kinase heterozygotes (tk+/-), and therefore mutations at this locus (tk+/- → tk-/-) can be easily quantified by selecting cells in the pyrimidine analog trifluorothymidine (TFT 4 ug/mL). E18 cells also contain a single unique I-Sce1 site built into the active allele that can be targeted by an extremely rare 18 base cutter restriction enzyme I-Sce1 nuclease.

In order to reduce the background MF prior to experiment, 1×10^5 cells/mL were treated for 48 hours with CHAT (complete RPMI 1640 medium with 10^{-5} M deoxycytidine, 2×10^{-4} M hypoxanthine, 2×10^{-7} M aminopterin and 1.75×10^{-5} M thymidine), followed by 24 hour growth in THC (CHAT without aminopterin); cell were used within five days of this treatment.

For directly targeted cells were incubated at 37°C and 5% CO₂ for **5 hours after electroporation to generate a bystander signal** and the conditioned medium was separated from direct cells by centrifugation at 1000 RPM to be transferred to 1×10^5 cells/mL naïve cells which were in turn incubated for **72 hours to allow for mutant expression**. Following 72 hour incubation after transfection the cells were plated in 96 well plates at 20,000 cells per well in the presence of 4 ug/mL TFT (trifluorothymidine) to isolate mutants (mutant fraction MF) and at 1 cell per well to determine the plating efficiency (PE). 12 days after plating the PE plates were counted for wells with colonies while MF plates were re-fed with 25 uL/well of 4 ug/mL TFT. At 20 days post-plating the MF plates are counted for wells with colonies. Mutant fractions are determined using the general formula for Poisson distribution. Mutant fractions were determined using the general formula for Poisson distribution:

PE was calculated as:
$$\frac{-\ln(\text{fraction of negative wells in PE plates})}{\text{Total number of wells in PE plates}}$$

$$\text{Total number of cells plated for PE}$$

MF was calculated as:
$$\frac{-\ln(\text{fraction of negative wells in MF plates})}{\text{Total number of wells in MF plates}}$$

$$\text{Number of cells plated for MFxPE}$$

Chapter 3: Results

Cell model used for these experiments was E18 human lymphoblasts, that are thymidine kinase heterozygotes (tk+/-), and therefore mutations at this locus (tk+/- → tk-/-) can be easily quantified by selecting cells in the pyrimidine analog TFT (tri-fluoro thymidine). E18 cells also contain a single unique I-SceI site built into the active allele. Therefore, if I-SceI enzyme is expressed in the cell, a single double strand break can be introduced within the target gene locus. It is known that this can lead to a significant increase in gene mutation frequency in the targeted cells (Honma et al., 2003), but it is not known whether this sort of damage is sufficient to elicit a significant level of bystander signal that can be transferred to other cells.

1. Thymidine Kinase locus characterization of E18 cells (Figures 3.1 and 3.2)

Extracted whole cell DNA from TK6 (parent cell line without I-SceI site) and E18 (modified cell line with I-SceI insert) was used for PCR amplification of a 223 base pair region of intron 2, in which the I-SceI sequence is present in E18 cells. The PCR product was electrophoresed on a 2% agarose gel (fig.3.1). The band of interest from E18 cell DNA is slightly larger than that from TK6 cell DNA suggesting that the I-SceI insert is intact. The same fragment of intron 2 (223 base pair) was then digested with I-SceI restriction enzyme to confirm the presence of I-SceI site (fig.3.2)

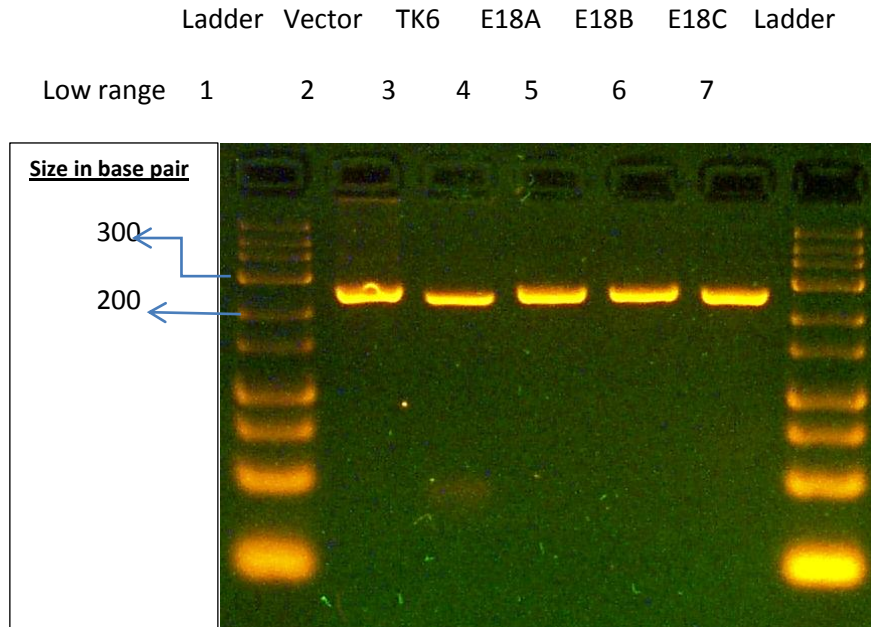


Fig3.1 Shows I-Sce1 site in E18 cells A, B and C (lanes 4,5,6). Notice that the band of interest in E18 cells and the Vector (lane 2) is slightly larger than the TK6 band since TK6 cell line does not have the I-Sce1 site.

The two commonly used methods to introduce restriction enzymes into the cells include the use of commercially-available enzymes that can be transfected directly, or an expression vector can be used. The plasmid vector pAdTrackCMV I-Sce1, was obtained from Dr. Jac Nickoloff's lab at Colorado State University. This expression vector not only contains I-SceI, but also GFP, so that transfection/expression frequencies can be monitored by green fluorescence.

Since the long-term objectives of this project involved the use of transfection it was tantamount to investigate the ambient delivery system and find out whether it could potentially cause additional bystander signal in E18 cells besides that caused by the DNA strand breaks. If electroporation or lipofection causes the release of bystander signals then medium transferred from targeted cells to naïve cells should result in increased mutation fraction.

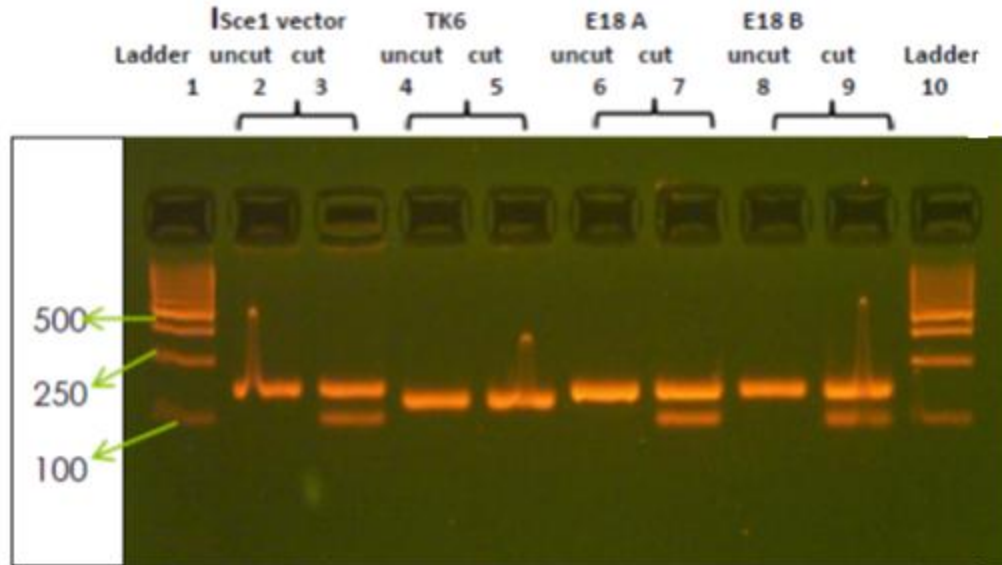


Figure 3.2. The PCR product of I-Sce1 site in Vector (pTKUAS) and E18 cells is 223 bp. TK6 is a control cell line that lacks the I-Sce1 site. The digested product size is approximately 192 and 31 bp respectively, making up a total of 223 bp hence the digested product size conforms to the undigested PCR product. Undigested and digested product of I-Sce1 restriction site in vector (lanes 2, 3), Tk6 (4, 5), E18 A (6, 7) and E18 B (8, 9). Lanes 1 and 10 contain the DNA ladder.

DNA Sequence of I-Sce1 site in intron 2 of E18 cells:

Since pTKUAS vector was used originally to construct the E18 cell line, the 700 base pair sequence within the ECOR47III site in the thymidine kinase locus was amplified and the product sequenced (at Colorado State University's Proteomics and metabolomics facility) to locate the I-Sce1 restriction sequence (***TAGGGATAA~CAGGGTAAT***). The 700 bp PCR product from E18 cells and the targeting vector with the following sequence and I-Sce1 site is highlighted in yellow and italicized:

E18 TKF1 PCR product of intron 2 with I-Sce1 site at 1692-1710 bp (667 bp upstream of Exon 3).

ACTTGCCACCACCGCGAAATGTGGTAGAGTATCATTGCCTTCTGGTAAGATCT
TGCTTCTAATTCATTGTTCCGGTAGCTGGGATTACAGATGTTGCCACCATGC
ACTGCCCAACATTCTTTTATGGCCCTGGGGATCCTTCTGCTCAAACCCCTTG
CTCCTAAAGATGTGGCTCACAGTTGGACTTCTTGGACCCAGAAGCAAGTGCTT
TTGACGCTGCACACAAAGACTTTCTGAAATTAATTTAGAAAAGCTGTATGCC
AGGTGTGGTGGCCACGCCTTTAATCCCAGC1692-

1710 **TAGGGATAA*CAGGGTAAT**

GCTTTGGAAGGCTGAGGTGCGTTGATCACTTGAGGTTAGGAGTTTGAGACCA
CCCTGGTCAACGTGGTAAAACCCCATCTCTACTGAAAAAAAAAACAAAAAT
TATCTGGGCATGGTGGCAGCCTCCTGTAATCCCAGCTACTCGGGAGGTTGAG
GCAGGAGAATCTCTTGAACCCGGAAGGCAGGGGTTGCAGTGAGCTGAGATCG
CTCCACTGCACTCTAACCTAGGCAACAGAGCGAGACTCCACCCTTTAAGAAA
GAAAGAAAACTCTGAACTCTGGAAACAACCTCTCGGATGAGGTTACTTTGGA
ATGCAGTCGCACGTTCCCTCTACATGTAGCCTTTGCTTCTGGTTCCCCACTTA
ATTTCCCGGGGGACCTCCGAGAGTCAGTAGCGTCCTGCGCGACGATGTGGT
GGAGACGACCTCTCTACACCCATTGTGCCCTCGATCTGCTGGCAGACCACTT
CTTTCGGCGCGGAGTCATACCTCCTAT

pTKUAS Vector PCR product (with I-Sce1 site):

CCCCGCACTAGCTGCGTCTTGCTATGTTGCCAAGCTGGTCTTGAACCTCCTGGT
CTCAAGCAATCCTCCTACTTCTTCATCCCAAAGTGCTGGGATTACAGATGTTA
GCCACCATGCCCTGCCCAACATTCTTTTATGGCCCTGGGGATCACTTCAGCT
CAAACCCCTTGCTCAGGAAGATGTGGCTCAGAGTTGGACTTCTTGGACCCAG
AAGCAAGTGCTTTTGACGCTGCACACAAAGACTTTCTGAAATTAATTTAGAA
AAGCTGTATGCCAGGTGTGGTGGCCCACGCCTTTAATCCCAGC **TAGGGATAA** C
AGGGTAAT GCTTTGGAAGGCTGAGGTGCGTTGATCACTTGAGGTTAGGAGTTT
GAGACCACCCTGGTCAACGTGGTAAAACCCCATCTCTACTGAAAAAAAAAAC
CAAAAATTATCTGGGCATGGTGGCAGCCTCCTGTAATCCCAGCTACTCGGGA
GGTTGAGGCAGGAGAATCTCTTGAACCCGGAAGGCAGGGGTTGCAGTGAGCT
GAAATCGCTCCACTGCACTCTAACCTAGGCAACAGAGCGAGACTCCACCCCA
AAAAGAAAGAAAGAAAACTCTGAACTCTGGAAACA ACTCTGGGATGAGGT
TACTTTGGAATGCAGTCACAGGTTCTCTCTACATGTAGCCTTTGTTCTGCTCCC
CCCCCAAAA

The first 192 nucleotide bases (of E18 PCR product) were analyzed for BLAST human sequence and identified to be the human thymidine kinase gene located on chromosome 17. This query confirmed that the E18 cell line, used for my experiments, has an I-Sce1 site in the thymidine kinase locus and since the cell line was constructed in 2002 by Wei Zou (working in Dr. Howard Liber's laboratory at that time) and the site was still intact and could be used to investigate the phenomenon of DNA strand break associated bystander effect (DSB-ABE).

The location of I-Sce1 site within *TK1* gene.

The location of I-Sce1 site was determined by PCR amplification of ECOR47III site from 1397-2097 bp followed by gel electrophoresis (2% agarose) to identify a 700 bp product (Figure 3.1 and 3.2). The product was gel purified and sequenced for I-Sce1 site identification (at CSU proteomics and metabolomics facility). BLAST sequence of the purified PCR product helped identify the exact position of the I-Sce1 site at 1692-1710 bp in intron 2 (Figure 3.3). The map shown here determined the position of I-Sce1 site, which was 694 bp upstream of exon 3.

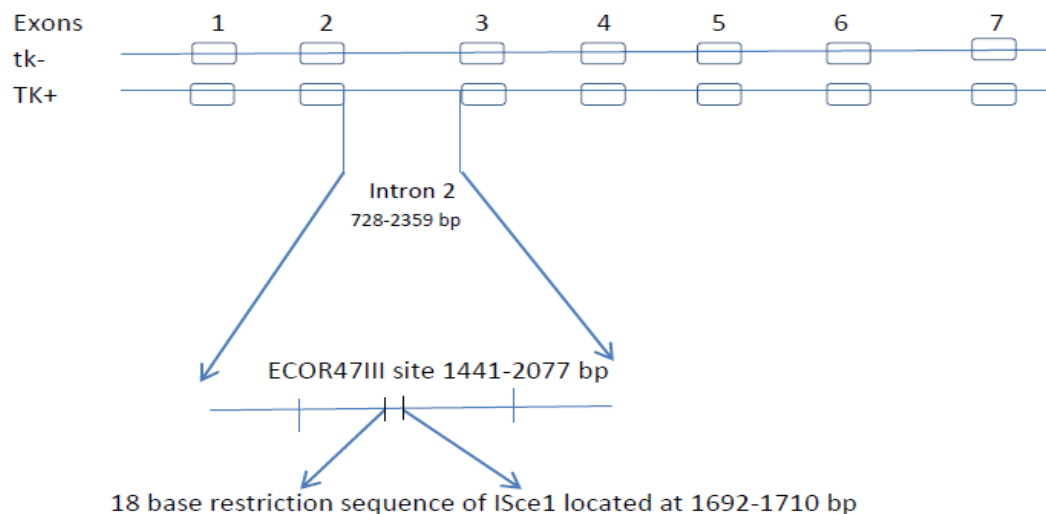


Fig. 3.3 Schematic of the location of I-Sce1 site in E18 cell line

The I-Sce1 site (1692-1710) directed breaks in E18 cell line could cause LOH in the active allele of *TK1* gene to delete some or all of either Exon 1 and/or Exon 2 to render the active allele inactive. Such mutants would be compound heterozygotes that are then isolated using mutation assay (Liber & Thilly 1982) as depicted in the schematic (Figure 3.4).

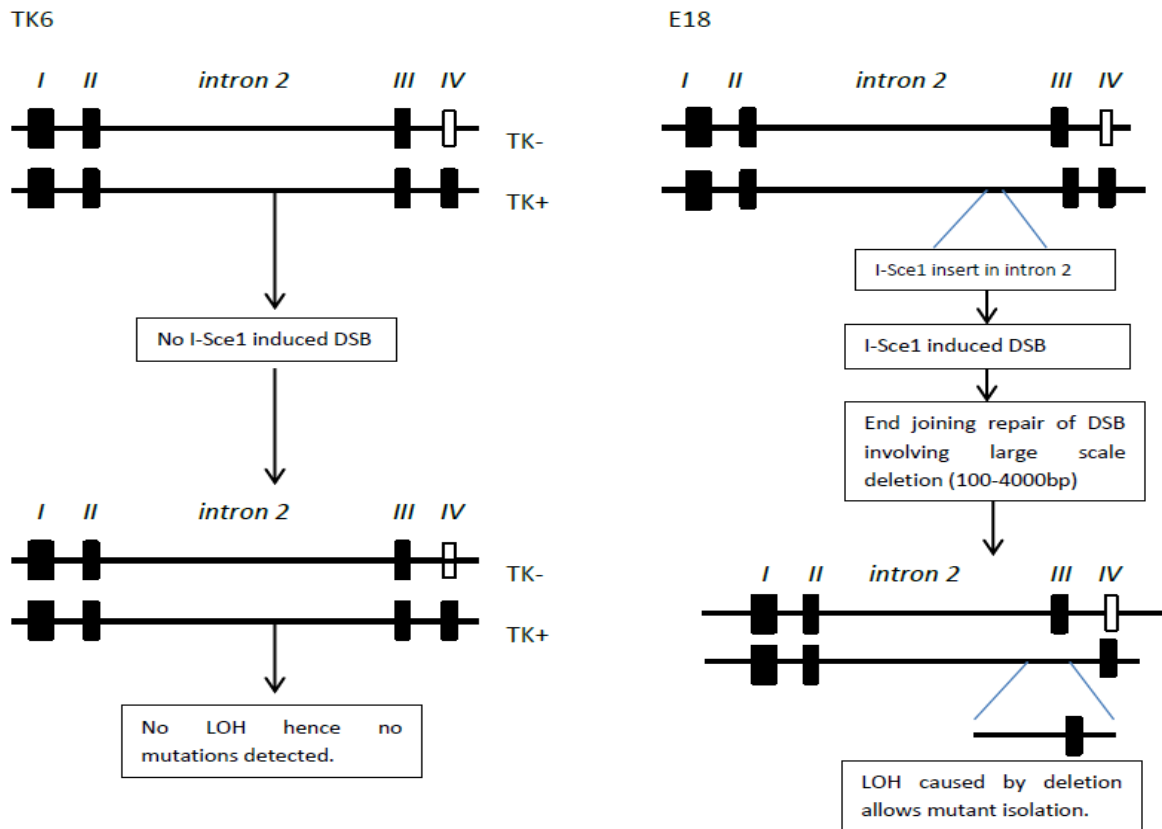


Fig. 3.4 Schematic showing how I-Sce1 induced deletions in intron 2 of cell model (E18) could have caused LOH as compared to the control parent cell line TK6.

2. Measuring transfection efficiency of electroporation of pAdTrackCMV I-Sce1 into E18 cells (Figures 3.5 and 3.6):

There were two approaches for transfection that were used:

- i. Electroporation.
- ii. Lipofection.

Once a potential bystander signal was generated, medium was transferred from targeted cells to naïve cells. A positive bystander effect was measured as an increase in gene mutations, at the thymidine kinase locus in naïve cells.

With the ability to measure transfection efficiency, plasmid pAdTrackCMV I-Sce1 proved to be advantageous, especially because of its GFP marker gene. When a GFP carrying pAdTrackCMV I-Sce1 was compared to non GFP plasmids (pQCXIH I-Sce1 and pIRES-Hyg3 I-Sce1) the self-inactivating factor of the latter plasmids allowed me to rule out their use for transfections because my preliminary experiments showed that maximum bystander signal generation occurred at 5 hours post-transfection and self-inactivating nature could cause the translations of I-Sce1 enzyme to stop prematurely which could affect the bystander signal generation. The GFP tagged plasmid pAdTrackCMV I-Sce1 was shown to cause transient transfection and the green fluorescent signal could be detected for up to 15 hours (Fig 3.5 and 3.6). This meant that the GFP plasmid, besides having a fluorescent marker gene could also maintain translation for up to 15 hours hence pAdTrackCMV I-Sce1 was preferred. Other data in chapter 3 also helped me to establish a suitable delivery system, transfection parameters and a suitable electroporation buffer for the new cell system. Data in figure 3.5 showed that using either PBS or electroporation buffer (EB) for transfection reactions did not affect the results much but the latter was preferred because of vendor specifications.

This experiment was set up to determine the expression and transfection efficiency using the GFP marker gene of pAdTrackCMV I-Sce1 plasmid. At 5, 10 or 15 hours after electroporation, cells were fixed in Methanol: Acetic acid (3:1) and counterstained with DAPI and those with green fluorescence were counted at 100X. (Fig.3.5). Five random

fields of view were scored for each slide and following formula used for determining the transfection efficiency.

$$\text{Transfection efficiency (TE\%)} = \frac{\text{average of total number of green cells in 5 random fields of view}}{\text{average of total number of cells per view}} \times 100$$

It was important to determine the maximum transfection efficiency that could be achieved with electroporation in order to proceed with experiments that would use electroporation as the means of delivering experimental plasmid into the cell model system. Fig 3.5 shows results of transfection efficiency (TE) in three panels. Panel A shows the control cells that were added with pAdTrackCMV I-Sce1 plasmid but not electroporated, fixed and counterstained. Panel B shows the transfected cells using DAPI channel while panel C shows the same cells as panel B but viewed under the FITC channel.

Establishing Transfection efficiency of the plasmid pAdTrack CMV I-Sce1

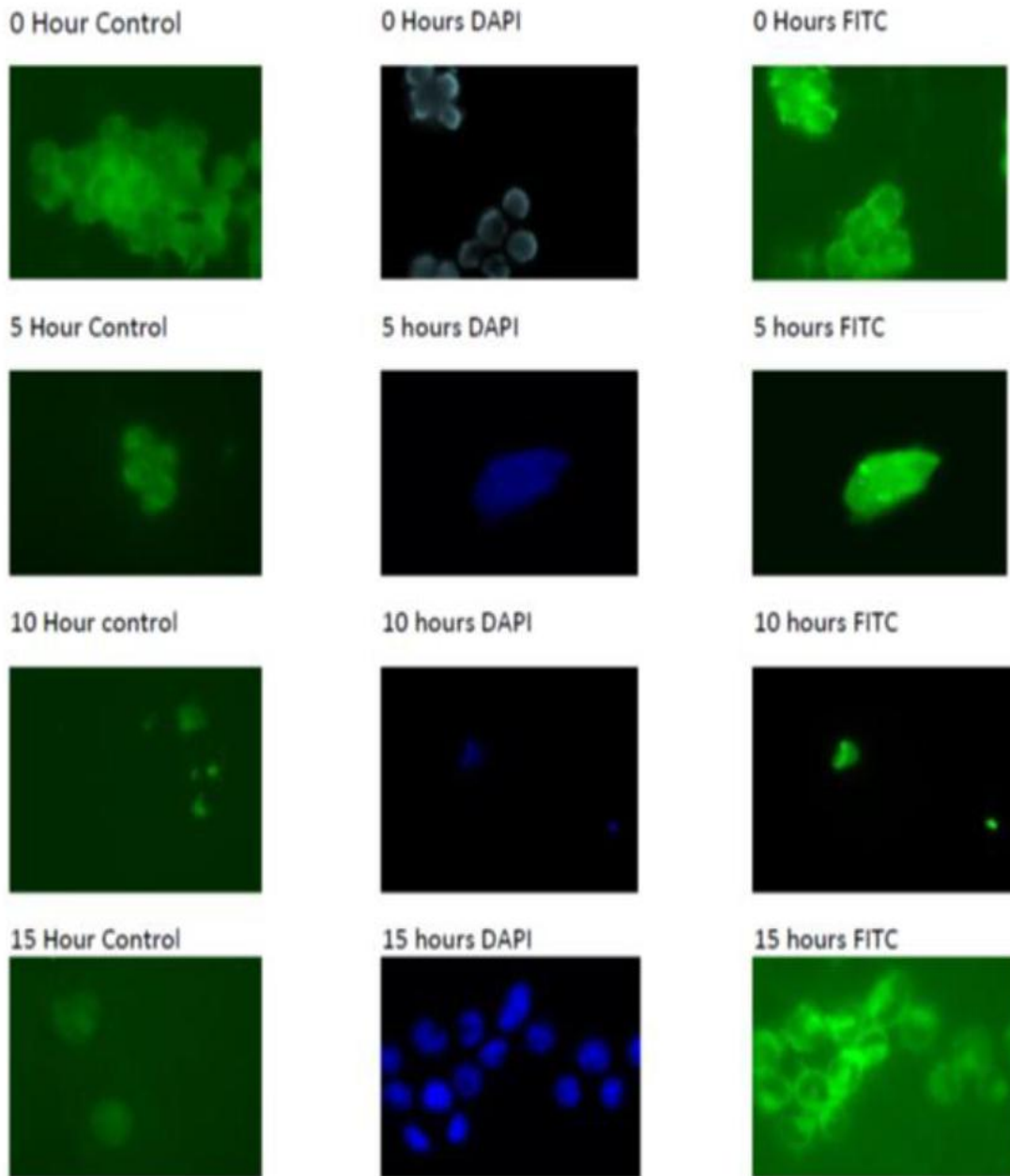


Fig 3.5 Panel A shows the control cells that were not transfected with experimental plasmid pAdTrack CMV I-Sce1

Panel B shows the I-Sce1 transfected cells at 0, 5, 10 and 15 hours after electroporation using DAPI filter.

Panel C shows the same field of view as panel B but using FITC filter at 0, 5, 10 and 15 hours.

In figure 3.5 five random fields of view were scored for cells expressing GFP, the cells that showed positive transfection for experimental plasmid pAdTrack CMV I-Sce1 nuclease, fluoresced green, under the FITC channel, and these cells were counted to determine TE (transfection efficiency). In figure 3.6 plotting the TE against time showed a maximum average TE of 54 % at 5 hours and transfection could be detected for up to 15 hours post electroporation. At 5 hours maximum green fluorescence signal could be detected from inside the cells. Fluorescence at 0 hours is due to autofluorescence. It was difficult to observe live cells in suspension, therefore fixing them was the alternative.

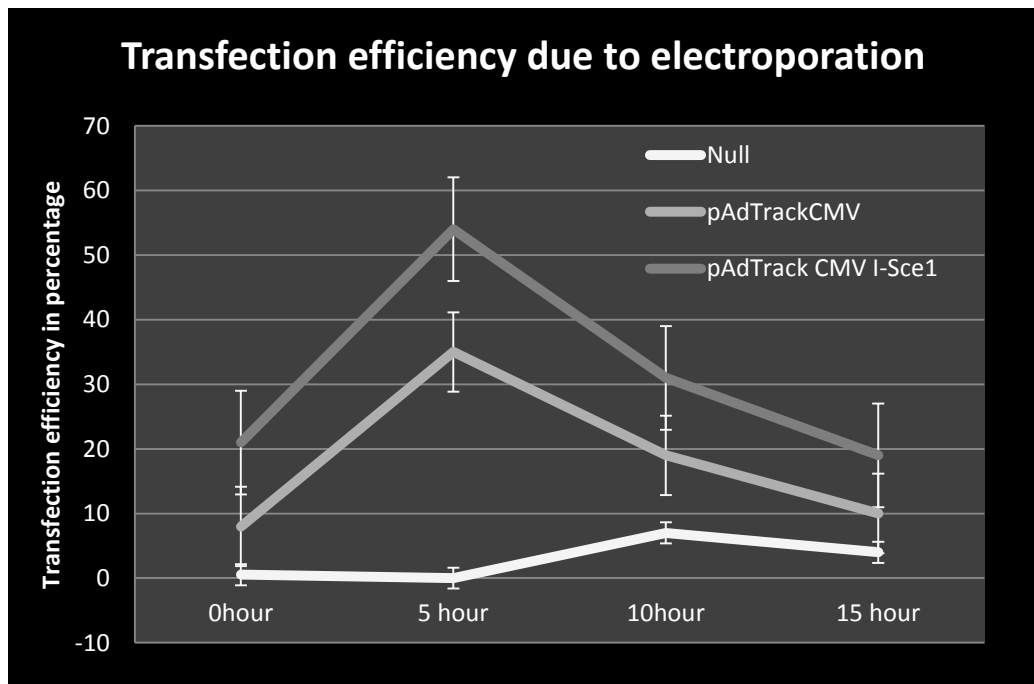


Fig. 3.6 Transfection efficiency calculated at 0,5,10 and 15 hours post-electroporation as a measure of fluorescing green cells in up to five random fields of view observed under 100X magnification using FITC channel. DAPI was used as counterstain.

3. Determining the efficacy of electroporation buffer and PBS for direct and bystander mutagenesis (Fig.3.7)

This experiment was aimed at finding out whether the electroporation buffer or PBS (phosphate buffered saline) is less mutagenic for the electroporation reaction mixtures. For each 250uL reaction mixture the E18 cells were either resuspended in salt based electroporation buffer or PBS. Immediately after electroporation the cells were transferred to warm RPMI and allowed to grow in an incubator at 37°C for 48 hours to give the plasmid enough time to express the restriction endonuclease I-Sce1 and to make DNA cuts at the I-Sce1 site to generate mutants. The control plasmid used in this experiment was pUC19 and it was electroporated either in the presence of electroporation buffer (EB) or phosphate buffered saline (PBS). Whereas the experimental plasmid was pAdTrackCMV I-Sce1 which was also electroporated in to E18 cells either in the presence of electroporation buffer (EB) or phosphate buffered saline (PBS). At the end of 48 hours the cells were plated for direct as well as bystander MF. As already mentioned, mutants were selected with TFT supplemented medium.

The rationale for this experiment was to be able to compare the mutagenic effects of two buffers for electroporation, i.e., vendor specified electroporation buffer versus PBS to set optimum parameters for transfection and at the same time find out if either of these parameters could affect direct or bystander mutation fractions. Identical conditions were used for testing both buffers.

Electroporation buffer and PBS both showed similar results for mutation fraction in direct as well as bystander MF. Electroporation in the presence of electroporation buffer (EB) increased the bystander MF to 15×10^{-6} from a baseline of 4×10^{-6} (control) whereas

electroporation with PBS increased the bystander MF from a baseline of 5×10^{-6} to 17×10^{-6} . The difference between the use of electroporation buffer (EB) and PBS **was not significant** in this experiment with a p-value of 0.205. The p-value for control+EB versus experimental+EB was 0.014 **which was significant**. Hence it was concluded that either buffer could be used for electroporation but the vendor specified electroporation buffer was preferred to achieve maximum transfection efficiency using the BioRad electroporator. Having seen a significant increase in bystander MF due to electroporation of experimental plasmid it was essential to set up a time course experiment to determine at what time point maximum bystander mutagenesis could be induced.

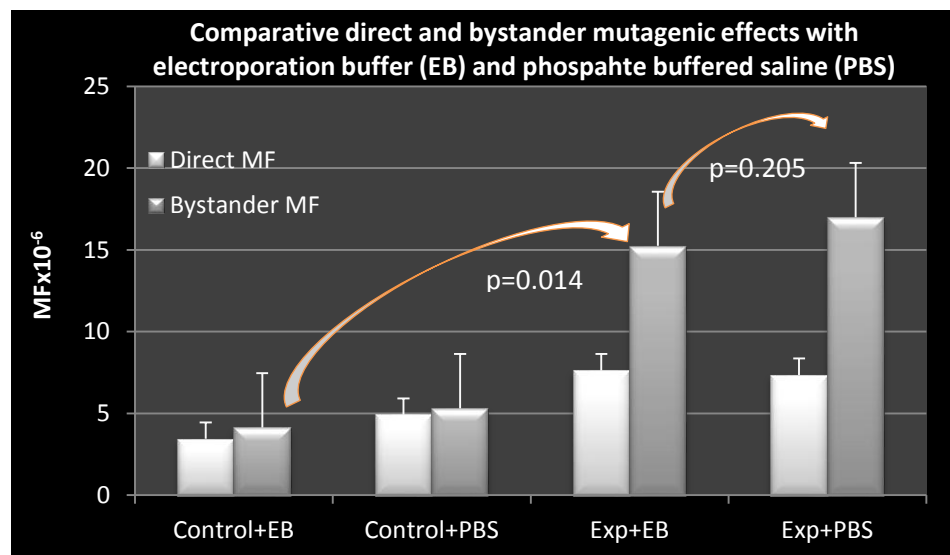


Fig 3.7. The graph shows mutation fraction when E18 cells are electroporated with pAdTrackCMV I-Sce1 as experimental plasmid or pUC19 as control plasmid. Controls for direct and bystander were mixed with two buffers i.e., electroporation buffer or PBS but not electroporated while the experimental plasmid pAdTrackCMV I-Sce1 was transfected either in the presence of electroporation buffer (EB) or phosphate buffered saline (PBS).

4. Determining the time required to generate maximum bystander mutagenesis

(Figure 3.8)

To determine at what time point after I-Sce1 expression in the cell model, maximum bystander signal could be generated, a time course experiment was set up to record bystander mutagenesis at 0,5, 10 and 15 hours.

In fig.3.8 the (C1A) negative control had pAdTrackCMV I-Sce1 but was not electroporated, (C2A) was the positive control for electroporation using pUC19 control plasmid transfected in to E18 cells by electroporation and the experimental electroporated cells (E2A) had pAdTrackCMV I-Sce1 plasmid electroporated into E18 host cells. These were all allowed an incubation time of either 5, 10 or 15 hours after electroporation and then the medium was transferred to T-75 flasks of **naïve bystander cells correspondingly labeled as (C1B, C2B and E2B)** which were later incubated for 72 hours before plating to determine the bystander mutation fraction (fig. 3.8). Electroporation conditions were the same as outlined in materials and method section.

When compared to C1B (negative control using pAdTrackCMV I-Sce1 but not electroporated) the bystander mutation Fraction (MF) results for C2B (positive control using pUC19 plasmid transfected into E18 cells by electroporation) suggest that the highest bystander signal was being generated at 5 hours although some bystander signal was also detected at 10 and 15 hour time points. A paired t-test analysis of three replicate experiments using E2B compared at 5 and 10 hours gave a **p-value of 0.014** which is significant. The p-value for **C2B at 5 hours versus C2B at 10 hours was 0.034** which was also significant. It was not clear from these experiments if electroporation or the

experimental plasmid or both could have been the possible cause of increased bystander mutation fraction, therefore it was necessary to test an alternate delivery system such as lipofection.

Having performed several experiments with lipofection (appendix 1) this delivery proved to be more toxic and more mutagenic than electroporation, therefore further testing with lipofection was discontinued.

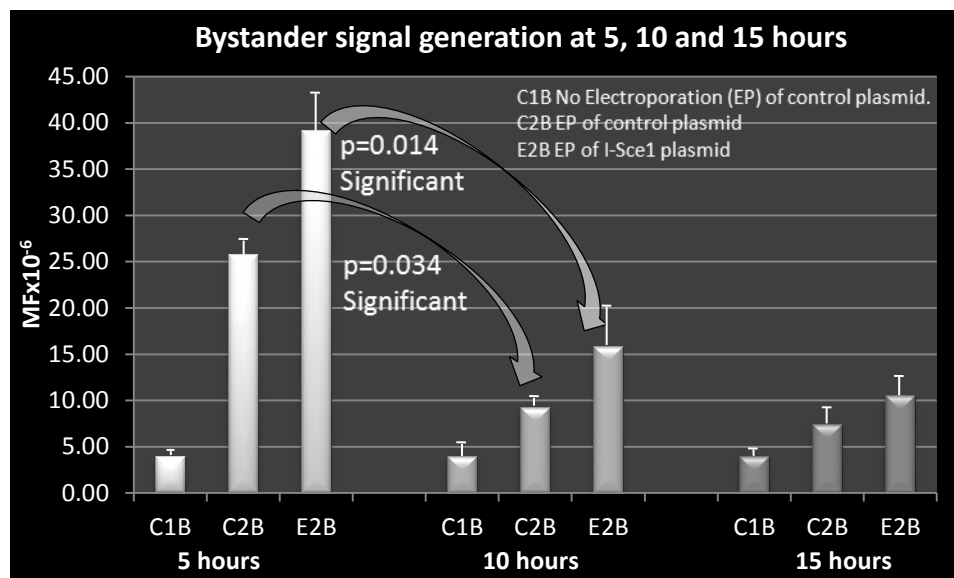


Fig. 3.8. Graph shows the increase in bystander mutation fraction due to electroporation of experimental plasmid pAdTrackCMV I-Sce1 at 5, 10 and 15 hours of medium transfer from directly electroporated E18 cells, to naïve E18 cells. C1B (negative control using pAdTrackCMV I-Sce1 but not electroporated), C2B (positive control using pUC19 plasmid transfected into E18 cells by electroporation), E2B (experimental data point with pAdTrackCMV I-Sce1 electroporated in the presence of electroporation buffer).

5. Comparing the mutagenic effect of GFP marker in the experimental plasmid pAdTrackCMV I-Sce1 with pIRES-Hyg3 I-Sce1 and pQCXIH I-Sce1 (Figure 3.9):

The experimental plasmid pAdTrackCMV I-Sce1 carries a GFP marker for establishing transfection efficiency, however the GFP protein, due to its size (26 kD) could affect the fidelity of my experimentation, therefore it was logical to compare the mutation effects of this plasmid with one that does not have GFP but carries an I-Sce1 gene. The non-GFP plasmids used for comparison were, pQCXIH I-Sce1 and pIRES-hyg3 I-Sce1 and their results are reported in figure 3.9. The three I-Sce1 plasmids (with and without GFP) were electroporated into E18 cells in a 250uL reaction and immediately put into warm RPMI for recovery and bystander signal generation and incubated for 5 hours. After 5 hours the conditioned medium from directly targeted cells was removed by centrifugation and put on naïve E18 cells. A control vector pAdTrack CMV was also used during the experiment, besides an absolute control and mock for electroporation.

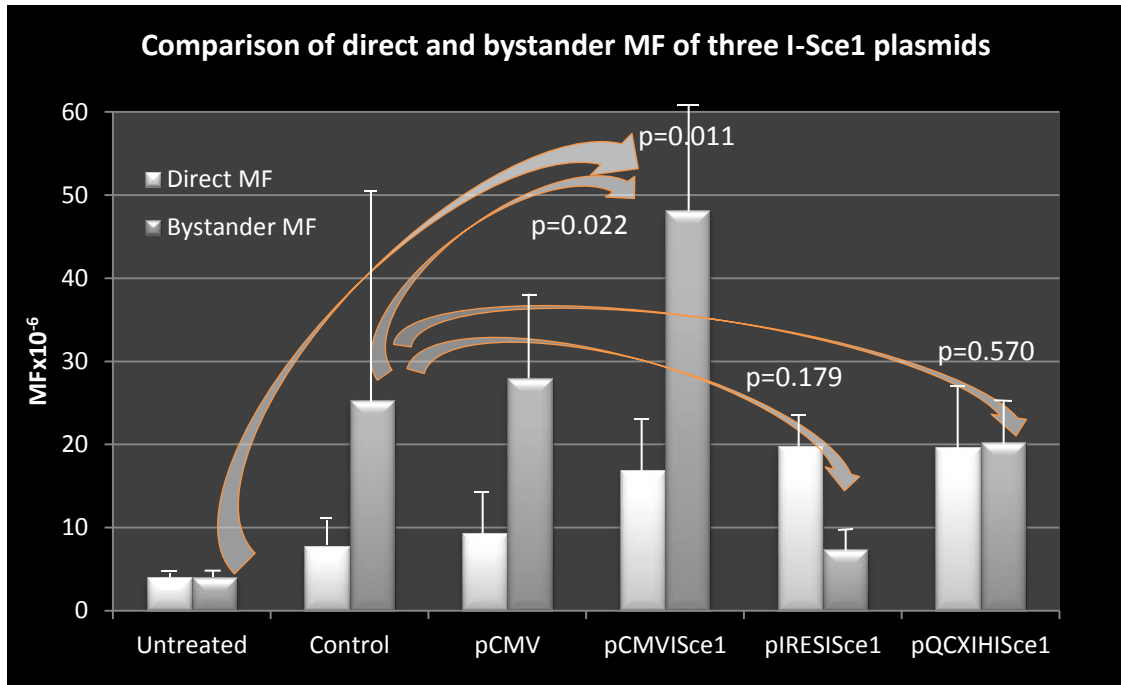


Figure 3.9: Comparison of three I-Sce1 plasmids: pAdTrack CMV I-Sce1, pQCXIH I-Sce1 and pIRES-Hyg3 I-Sce1. The direct and bystander mutation fractions for these three I-Sce1 containing vectors were plotted with three controls: absolute, mock (electroporation of E18 cells only) and CMV control vector (pAdTrackCMV backbone without I-Sce1 gene). The lower bystander MF for pQCXIH I-Sce1 and pIRES-Hyg3 I-Sce1 (as compared with pAdTrackCMV I-Sce1) is indicative of the self-inactivating nature of the two plasmids. Please refer to table 3.01 for statistical analysis of the data shown in this figure.

Plasmid pIRES hyg3 I-Sce1 is a 3.7 kb retroviral vector and contains the internal ribosome entry site (IRES) of the encephalomyocarditis virus (ECMV) which permits the translation of two open reading frames from one messenger RNA under the CMV major immediate early promoter. It is hypothesized in these experiments that this could have led to the production of a higher Direct MF than the bystander MF. By decreasing the level of expression of the antibiotic resistance marker, the selective pressure on the entire expression cassette is increased, resulting in selection for cells that express the entire

transcript, including the gene of interest at high levels. The optimal concentration for transfection was not established for this plasmid.

Plasmid pQCXIH I-Sce1 is 7.8 kb retroviral vector which is a self-inactivating bicistronic expression vector designed to express a target gene along with the hygromycin resistance gene. Upon transfection into a cell line, this vector can transiently express or integrate and stably express a viral genomic transcript containing the CMV immediate early promoter, gene of interest (GOI), internal ribosome entry site (IRES) and hygromycin resistance gene. The GOI and the hygromycin resistance gene are co-translated via the internal ribosome entry site (IRES) as a bicistronic message in mammalian cells. The optimal concentration for transfection was not established in these experiments. This plasmid behaves similar to pIRESHyg3 I-Sce1 in the sense that it immediately begins production of I-Sce1 enzyme and then undergoes self-inactivation. Hence Direct MF is equal to the bystander MF. The virus cannot replicate within host cells due to the absence of structural genes.

The GFP containing vector is pAdTrack CMV I-Sce1 which is a 9.2 kb adenoviral vector that has Kanamycin resistance has two CMV promoters, one for GFP and the other one for I-Sce1 endonuclease gene. The optimal concentration for transfection was established to be 5 ug/250 uL reaction mix.

The results in figure 3.9 indicated a higher direct mutation fraction for pQCXIH I-Sce1 and pIRES-Hyg3 I-Sce1, which could be associated to their smaller molecular weights and thus higher transfectability and also to the internal ribosome entry sites, that cause the vectors to immediately translate the I-Sce1 protein and cause DNA cutting. These direct MF values, however, are not significantly different from the control direct MF (table

3.01). The lower bystander MF for pQCXIH I-Sce1 and pIRES-Hyg3 I-Sce1 is indicative of the self-inactivating nature of the two plasmids.

Due to the self-inactivating nature of the two non-GFP I-Sce1 plasmids i.e., pQCXIH I-Sce1 and pIRES-Hyg3 I-Sce1 the direct mutation fraction is more important than bystander. Statistical analysis of pAdTrack CMV versus pQCXIH I-Sce1 and pIRES-Hyg3 I-Sce1 showed non-significant results only for pIRES-Hyg3 I-Sce1 (table 3.01). Hence it can be concluded that GFP does not affect the transfection or DNA cutting ability or mutagenicity of the host (E18). However the biggest advantage of pAdTrack CMV I-Sce1 outweighs all the rest which is to be able to establish the transfection efficiency due to the GFP marker.

Statistical analysis: Student's t-test was employed to analyze the data and Sigma plot version 11.0 was used for determining p-values at a confidence interval of 95%.

Table 3.01: Statistical analysis of comparison between the direct and bystander MF from three I-Sce1 Plasmids.

Analysis type	Direct MF t-test p values at 95 % confidence interval		Bystander MF t-test p values 95 % confidence interval	
Untreated versus pAdTrackCMV I-Sce1	0.039	Significant	0.011	Significant
Untreated versus pIRES-Hyg3 I-Sce1	0.006	Significant	0.83	Not Significant
Untreated versus pQCXIH I-Sce1	0.040	Significant	0.006	Significant
Control versus pAdTrack CMV I-Sce1	0.222	Not significant	0.022	Significant
Control versus pIRES-Hyg3 I-Sce1	0.059	Not significant	0.179	Not significant
Control versus pQCXIH I-Sce1	0.097	Not significant	0.570	Not significant
pAdTrackCMVI-Sce1 versus pIRES-Hyg3 I-Sce1	0.605	Not significant	Not applicable	
pAdTrackCMVI-Sce1 versus pQCXIH I-Sce1	0.7	Not significant	Not applicable	

6. The transfection of rare cutting restriction enzymes into E18 cells causes a measurable increase in mutation fraction (Figure 3.10)

This experiment encompassed the use of electroporation for transfecting a pAdTrack CMV I-Sce1 (pSce) plasmid and three restriction endonucleases (Not1, Sfi1 and I-Sce1) into E18 cell line, making one to several DNA breaks and collecting mutation data to see if one induced double strand break can generate sufficient bystander signal and if electroporation could have additional possible effects on generating a bystander signal. Most of my investigations were based on monitoring the direct and indirect effects of electroporation and restriction endonuclease mediated DNA breaks. The rationale for using this strategy was to increase the number of double strand breaks from 1 to many in order to evaluate the extent of bystander signal generation in terms of mutation fraction. Not 1 is an 8 base cutter with recognition sequence GC[^]GGCCGC but being methylation dependent it cuts less frequently. This sequence occurs 3000 to 5000 times in the human genome (Zabarovsky et al., 1994) the lower range corresponding to the methylation dependence. Sfi1 is a 13 base cutter with a recognition sequence of GGCCNNNN[^]NGGCC (Nolin, and Dobkin 1991). This sequence occurs almost 20,000 times in the human genome and interestingly makes 4 DNA breaks instead of the usual 2 (Wentzell et al., 1995). Sfi1 works like an 8 base cutter, due to its non-specific restriction sequence recognition and therefore cuts more frequently than expected because it is a tetrameric protein and methylation independent (Wentzell et al., 1995). I-Sce1 is an 18 base cutter (TAGGGATAA[^]CAGGGTAAT) and presumably cuts only once at the I-Sce1 site within the *TK1* gene (17q23.3-q25.3). There are five non-specific sequences for I-Sce1 endonuclease in the human genome (Petek et al., 2010) however, the effect of one to five DNA breaks on generating the bystander signal can be determined. Ten units of

each enzyme were mixed individually with E18 cells and electroporated at set parameters. Untreated cells were not electroporated, while controls for each enzyme mixture were. Immediately after electroporation the transfected cells were incubated in warm RPMI for 5 hours to allow recovery and bystander signal generation. At the end of 5 hours the medium (potentially containing bystander signal) was transferred from electroporated cells to naïve cells to observe any bystander effect (BE), using mutation fraction as end point. The directly electroporated cells were analyzed to determine directly-induced mutation.

This experiment was designed to answer the following questions:

1. Is the number of (dsb) sites in and around *TK* gene directly proportional to direct MF?
2. Is one double strand break (dsb) able to produce sufficient bystander effect (BE) to increase bystander mutagenesis?

If yes: Is BE dose dependent. i.e., could a higher number of (dsb) generate a higher MF in naïve (bystander) cells?

If no: A double strand break could only increase the MF in directly targeted cells.

This experiment helped address the specific aims A and B of Aim 2 which would investigate whether one DNA double strand break is sufficient to induce a bystander signal and if there could be a dose response in terms of the number of DNA breaks induced by transfecting restriction enzymes that cut DNA at rates dependent on the frequency of occurrence of restriction sites. Because ionizing radiation generates many different types of damage, the plan was to utilize restriction enzyme-induced breaks to limit the damage in the targeted cell to double strand breaks (DSB). In addition the

effects of electroporation on possible generation of bystander signal are also investigated herein. This led me to frame the following hypotheses.

(a) Hypothesis 1 (for direct effects of DNA damage):

A single double strand break caused by targeting plasmid pAdTrack CMV I-Sce1 (pSce) at the I-Sce1 site and transfecting rare cutting restriction endonucleases through electroporation will increase mutation fraction of E18 cells, compared to the control.

(b) Hypothesis 2 (for bystander mutagenesis of DNA damage):

A single double strand break will produce and release sufficient bystander signal into the medium, and conditioned medium transferred from electroporated cells to naïve cells will give a higher bystander mutation fraction when compared to control.

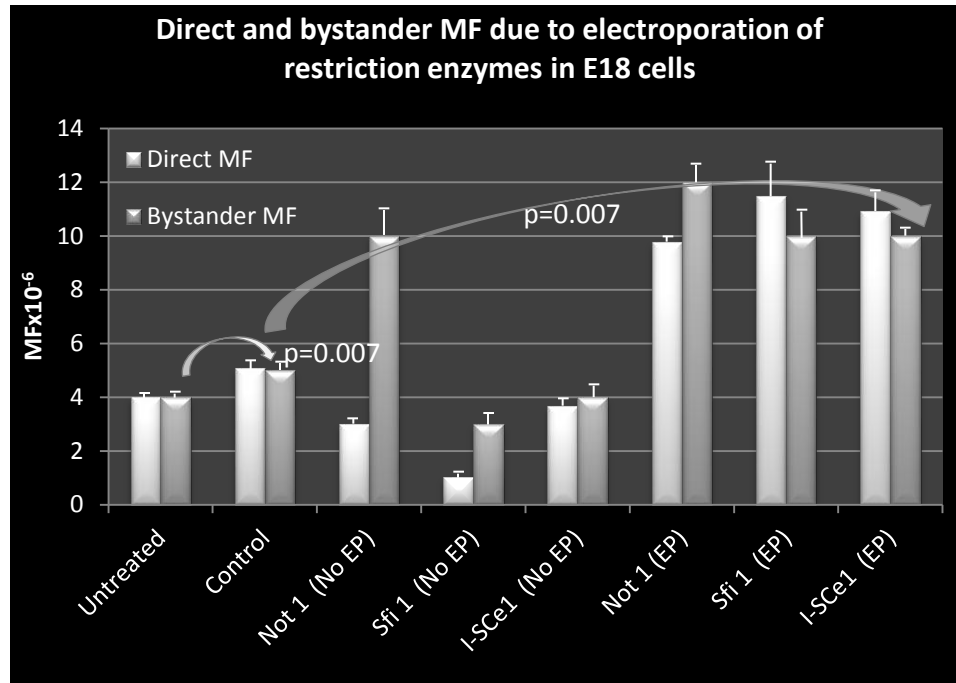


Fig. 3.10 The comparative effects of electroporating rare cutting restriction endonucleases (Not1, Sfi1 and I-Sce1) into E18 cells on direct and bystander mutation fraction. The direct and bystander effects are shown side by side for clear comparison. 'No EP' and 'EP' refers to the reaction mixture that was either not electroporated (No EP) or electroporated (EP). For each enzyme Not1 (No EP), Sfi1 (No EP) and I-Sce1 (No EP) refers to the reaction mixtures that were not electroporated but corresponding enzyme was added. Control refers to the reaction mixture consisting of E18 cells only that were resuspended in electroporation buffer and electroporated to monitor the mutagenic effects of electroporation.

Table 3.02 Statistical analysis of direct and bystander MF due to electroporation of restriction enzymes into E18 cells.

	Direct MF	Remark	Bystander MF	Remark
Untreated vs control	0.167	Not significant	0.007	Significant
Control vs Not1 (not Electroporated)	0.073	Not significant	0.09	Not Significant
Control vs Sfi1 (not Electroporated)	0.009	Significant	0.069	Not Significant
Control vs ISce1 (not Electroporated)	0.203	Not significant	0.230	Not Significant
Control vs Not 1 (Electroporated)	0.005	Significant	0.056	Not Significant
Control vs Sfi1 (Electroporated)	0.139	Not significant	0.099	Not Significant
Control vs ISce1 (Electroporated)	0.138	Not significant	0.007	Significant
Not 1 vs Sfi1 (Electroporated)	0.644	Not significant	0.607	Not Significant
Not 1 vs ISce1 (Electroporated)	0.732	Not significant	0.830	Not Significant
Sfi1 vs ISce1 (Electroporated)	0.907	Not significant	0.643	Not Significant

An average of three replicate experiments showing the effect of three restriction endonucleases into E18 cells is shown in Fig. 3.10. The graph presents both direct and bystander mutagenesis. Direct electroporation of all three enzymes resulted in increased MFs and all three conditions produced a bystander effect as evident from the bystander mutagenesis. Interestingly, the I-Sce1 bystander mutagenesis was significantly higher than the control for bystander MF, while the control for bystander MF was also significantly higher than the untreated. It was also interesting to observe that the bystander MF values (for electroporation of all three restriction enzymes regardless of their cutting frequencies) were not significantly different from each other

The results indicate three important conclusions:

1. One to six DNA breaks (Petek et al., 2010) at one I-Sce1 site inserted at the *TK1* locus plus five non-specific I-Sce1 restriction sites, caused by I-Sce1 enzyme can generate a bystander signal.
2. Electroporation itself has an additional effect on bystander mutagenesis as evident from the statistical analysis of untreated versus control bystander MF values (table 3.02).
3. Not1 and Sfi1 induced breaks (ranging in number from 5000 to 20,000) have the same effect on increasing bystander mutagenesis as a single DNA break caused by I-Sce1 hence an absence of dose response.

To further elucidate the additional effects of electroporation on bystander mutagenesis it was decided to replicate these results using lipofection as the delivery system.

7. Temporal aspects in bystander effect (Figure 3.12):

Preliminary data from my own experiments and pre-existing data on the existence of temporal aspects in radiation induced bystander effect (RIBE) led me to develop the following hypothesis.

Hypothesis:

If transfection of plasmid pAdTrackCMV I-Sce1 into E18 cells cuts only once at the I-Sce1 insert in intron 2 of *TK1* gene then it must cause an increase in the direct as well as bystander mutation fractions indicating the mutation fraction induced by the cutting action of enzyme alone. This I-Sce1 induced bystander effect can be mathematically separated from the overall bystander effect due to all sources.

To test this hypothesis time course mutation experiments were set up to investigate the possible temporal aspects involved in bystander signal generation and to see how soon after electroporation of experimental plasmid the cells can generate a bystander signal. These experiments also helped me to answer questions about the relationship between direct and bystander MF and if I-Sce 1 plasmid or the electroporation buffer, in itself, has the ability to upregulate direct and bystander MF.

It was important to find out how soon after electroporation the targeted cells were able to produce a bystander signal that can increase the MF in naïve bystander cells. For this investigation experiments were set up to transfer medium from E18 cells electroporated with the experimental plasmid pAdTrackCMV I-Sce1 at 0, 2, 3, 4, 5 and 10 hour time points and both direct and bystander mutation fractions (MFs) measured. The following diagrammatic representation of the experiment explains what was done.

Comparison between the direct effects and the bystander effects were carried out to measure the total overall increase and the total actual increase in mutation fractions due to the transfer of conditioned medium containing the bystander signal from direct to naïve cells.

Using statistical analysis and mathematical relationships of the data actual bystander MF produced by the I-Sce1 plasmid was separated from total bystander MF (an aggregate of background sources, electroporation and the cutting action of I-Sce1 plasmid).

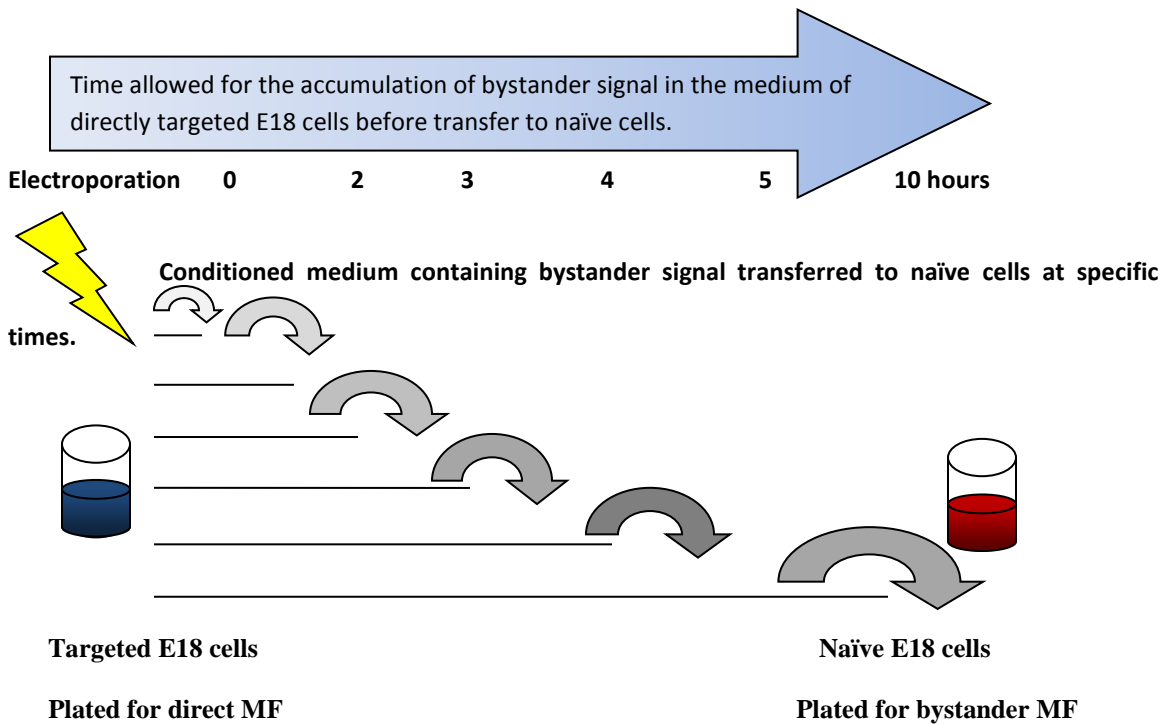


Fig.3.11 Experimental design of the time course experiment.

Other investigators (who investigated radiation induced bystander effect RIBE) and also the (DSB-ABE) data presented here showed that bystander effect begins to diminish at 15 hours (reference figure 3.8). The minimum time required to generate bystander effect was therefore investigated and the conditioned medium separate immediately after electroporation of plasmid pAdTrackCMV I-Sce1 into E18 cells. Having seen some

initial experimental evidence which indicated that electroporation of experimental plasmid pAdTrack CMV I-Sce1 has limited effect on increasing the mutation fraction, it was decided to replicate these experiments to obtain more reliable data. Measurements were made by transferring the medium from directly electroporated cells at 0*, 2, 3, 4, 5 and 10 hour time points to naïve cells and incubated for another 72 hours so that mutants can emerge in the medium. These cells were plated to determine the mutation fraction and mutants selected for, in a TFT supplemented RPMI medium. Both Direct and Bystander effects of electroporating the experimental plasmid were measured and shown in figure 3.12. (**Note: The medium separation took about 10 minutes and therefore technically it was not '0' hour per se*).

Several data points were set up to establish the dynamics involved in DSB-ABE and to answer the questions mentioned above. The controls included an (1) untreated i.e., E18 cells that were not electroporated, (2) plasmid suspended in electroporation buffer, not electroporated and (3) E18 cells with plasmid suspended in buffer but not electroporated. The experimental data points (4, 5 and 6) included all of the conditions 1, 2 and 3 but were electroporated at set parameters (see materials and method section). Results are shown in figure 3.12.

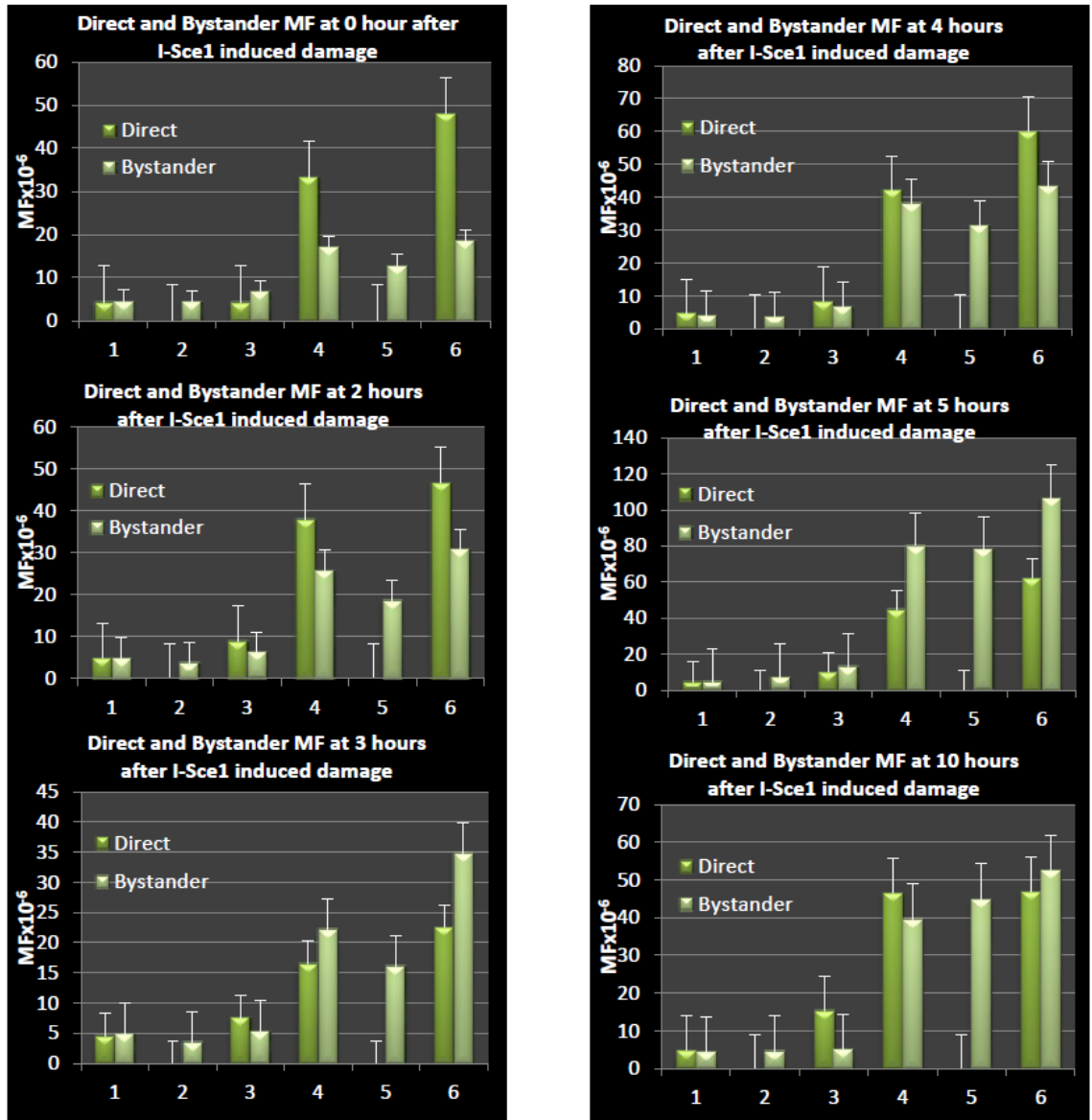


Fig. 3.12 Direct and Bystander effects of electroporating experimental plasmid pAdTrack CMV I-Sce 1 into E18 cells. The first three bars sets (1, 2 and 3) are controls for no electroporation namely (1= E18 cells only, 2= Plasmid only, 3=E18 cells plus plasmid only) while the last three bars (4, 5 and 6) in each graph are subsequent experimental conditions for electroporation. Averages of four successive experiments were plotted for direct and bystander mutagenesis at 0, 2, 3, 4, 5 and 10 hours post- electroporation. **In the results analysis section for every data point the post-fix ‘D’ for direct or ‘B’ for bystander has been used. So 6D would refer to the direct effect for data point 6 while 6B would refer to the bystander effect of the same data point.**

Statistical analyses of time course experiment (figure 3.12):

Several comparisons of data points were made to statistically analyze the data using Sigma plot version 11.0. The raw data was grouped into several categories by arranging it into 24 data points (6 data points/4 replicates, hence $6 \times 4 = 24$) and analyzing them statistically to answer the four questions outlined above.

a. Time response of mutagenic effect due to I-Sce1 Vector alone

The results in fig. 3.12 were first analyzed to see if the plasmid induced direct and bystander MFs follow a time response. In order to investigate I-Sce1 induced DNA strand breaks as a possible cause of bystander signal generation, induced direct (**D**) and induced bystander (**B**) MF due to plasmid I-Sce1 were calculated by **subtracting the MF values of 4D from 6D for direct MF** i.e., (subtracting the direct MF value of directly electroporated E18 cells only from E18 cells electroporated in the presence of plasmid pAdTrack CMV I-Sce1) **and similarly subtracting 4B from 6B for bystander MF** (subtracting the bystander MF value of electroporated E18 cells only from E18 cells electroporated in the presence of plasmid pAdTrack CMV I-Sce1). The averages of $A6D - A4D$ and $A6B - A4B$ from four replicate experiments were plotted for both Direct and Bystander MF respectively at each time point and shown in fig.3.13.

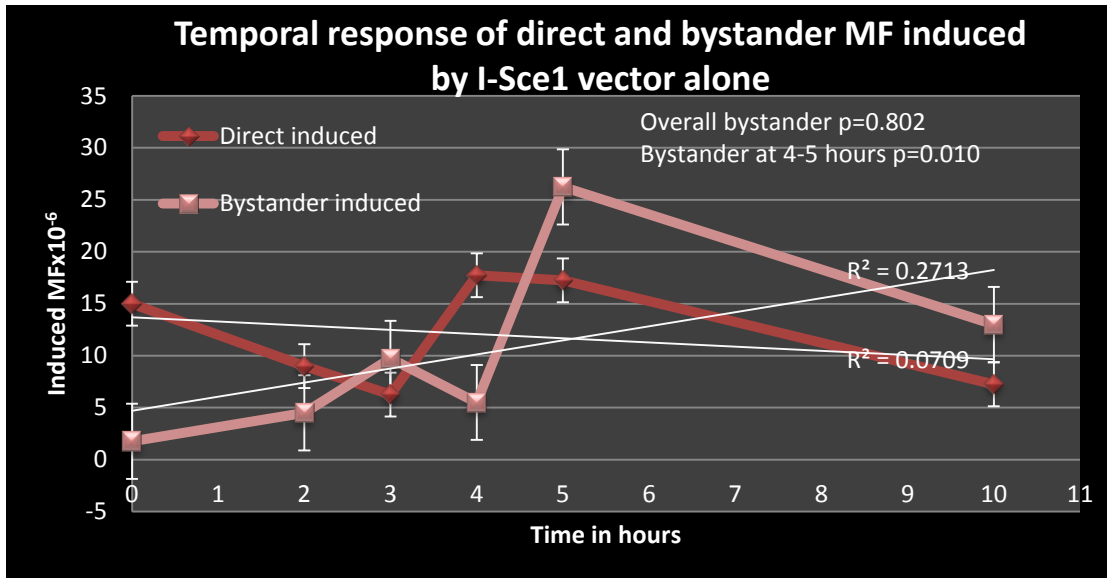


Fig. 3.13 Induced direct and bystander MF of data points 4 and 6 explained in the legend of fig.3.12 at 0, 2,3,4,5 and 10 hour time points. (R^2 for Induced Direct= 0.0709, R^2 for Induced Bystander=0.27133).

The t-test analyses of these relationships: Paired t-test (at 95% confidence interval) was used to compare the induced direct MF (6D-4D) with induced bystander MF (6B-4B) values from 0-10 hours. In direct and bystander mutagenesis there were no significant differences between any of the data points as the p-value was 0.802 which is far greater than the significant value of 0.050. However when the graph was plotted for induced bystander MF a surge could be observed between 4 and 5 hours. Therefore further analysis were carried out from 0-4 hours and found it to be non-significant but from 4-5 hours the surge gave a p-value of 0.010 which is highly significant. Therefore it can be concluded that there is a time-dependent response for bystander mutagenesis and it requires at least 5 hours of signal generation from directly targeted cells to cause a significant change in naïve cells.

The induced DSB-ABE by vector transfection alone demonstrated that between 2 and 3 hour time points the direct and bystander MFs transect, indicating that the bystander signal generated by directly targeted cells could be affecting the direct MF within the time period before which conditioned medium was transferred to naïve cells.


In order to address additional questions the data was analyzed as single groups; thus each of the six conditions shown in fig.5.12 and 5.13 now consisted of 24 points.

b. Other possible relationships that can be looked at from statistical analyses

The following criteria was used to investigate if:

- i. DSB induced by I-Sce1 plasmid and electroporation can increase the direct MF.
- ii. Electroporation has an individual mutagenic effect and increases direct MF.
- iii. I-Sce1 plasmid can also individually increase the direct MF.
- iv. Electroporation of buffer alone can increase the bystander MF.
- v. Electroporation of I-Sce1 plasmid into cells significantly enhances the bystander MF.
- vi. Electroporation of I-Sce1 plasmid causes significant increase of bystander MF when compared with electroporation of buffer alone.
- vii. Electroporation of I-Sce1 plasmid alone causes a significant increase of bystander MF.
- viii. Direct mutagenesis also affects the bystander mutagenesis when I-Sce1 plasmid is electroporation in directly targeted cells.

Table 3.03: Statistical analysis of time course experiment for data sets in figure 3.12

Observation	Types of Comparison Direct Vs. bystander  Direct vs bystander	N (number of values)	P- value
i	Direct/EP** plasmid vs EP cells (4D vs 6D)*	24	<0.001
ii	Direct/ EP vs No EP** (1D vs 4D)*	24	<0.001
iii	Direct/EP of plasmid vs No EP of plasmid (3D vs 6D)*	24	<0.001
	A2D vs A5D***	Not relevant***	
iv	BSE/EP** of buffer vs EP of cells (4B vs 5B)*	24	0.345
v	BSE/EP** of plasmid vs EP of cells (4B vs 6B)*	24	<0.001
vi	BSE/ EP** of plasmid vs EP of buffer (5B vs 6B)*	24	<0.001
vii	BSE/EP** of plasmid vs No EP** of plasmid (3B vs 6B)*	24	<0.001
viii	Observed direct vs bystander effect (6D vs 6B)*	24	0.998
<p><i>*Note: In this table, for every data point the post-fix 'D' for direct or 'B' for bystander has been used. So 6D would refer to the direct effect for data point 6 while 6B would refer to the bystander effect of the same data point.</i></p> <p><i>Abbreviations used **EP: Electroporation, ** NO EP: No electroporation</i></p> <p><i>***Direct MF for A2D and A5D is not relevant since these conditions only had plasmid suspended in RPMI and electroporation buffer and they were either not electroporated or electroporated respectively)</i></p>			

A paired t-test was used to analyze these data. Statistical analyses of all relationships in table 3.03, except relationships iv and viii, were significant when tested at 95 % confidence interval.

Some questions answered on the basis of statistical analysis:

- i) **Do the studies of progression of direct or bystander mutagenesis indicate a time-dependent response?**

Results and data analysis show temporal kinetics exist between 4 and 5 hours. However an overall change could not be measured. Hence it can be concluded that DNA strand break associated bystander effect does give a time-dependent response.

- ii) **What are the direct effects of Electroporation (EP) of plasmid?**

Even though the emphasis of this project is on determining if double strand breaks lead to bystander signals, the potential ‘direct’ effects of the treatment in the transfected cells were also measured. If ‘**D**’ is the observed overall direct MF (6D), which could include an MF due to the bystander signal generated by directly targeted cells with electroporation of plasmid, and ‘**d**’ is the actual induced direct MF due to plasmid alone (6D-4D), while ‘**bse**’ refers to the MF due to bystander signal generation by directly electroporated cells (6B-4B), then the simple relation between these factors could be expressed as:

$$D = d + bse \text{ (refer to figure 3.14 also)}$$

(i.e., to evaluate if bystander signals generated by directly targeted cells could contribute to the overall direct MF after electroporation of the plasmid pAdTrackCMV I-Sce1?)

It is important to note that from table 3.03 it can be concluded that there is no significant difference between observed direct and bystander mutagenesis (6D and 6B, comparison viii in table 3.03). There can be two possible cases:

- i. For $D=d+bse$, if there is no significant difference between overall direct MF 'D' and induced bystander MF 'bse' then true direct MF 'd' must be zero, meaning that a true induced direct effect does not exist.
- ii. Directly electroporated (hit) cells are refractory to bystander signal therefore 'bse' in directly hit cells is zero and thus $D=d$. There are several suggestions in the literature for this sort of behavior (Zhang et al., 2009)

Some possible explanations for an absence of true induced direct effect 'd' in case (i) are that:

- a. The overall direct effect 'D' is a product of mutations due to electroporation, plasmid and the background which would otherwise cause a positive feedback loop in directly electroporated cells, but upon medium transfer that loop affects the naïve cells instead to give a larger bystander response than the direct response.
- b. The direct cells become refractory to the bystander signal possibly due to an adaptive response.

Investigating the second case was beyond the scope of this project.

iii) What are the Indirect mutation effects of Electroporation (EP) and:

(a) Is EP of buffer different from EP of cells?

(b) Is EP of cells/plasmid different from either of these controls?

(a) Based on the statistical analysis performed in table 5.01 (comparison # iv) it can be argued that electroporation of cells is not different from the electroporation of buffer since the p-value of 0.345 is not significant. This also suggests that the overall bystander

signal being generated in these experiments could be a product of DNA damage from I-Sce1 plasmid as well as electroporation.

(b) Similarly electroporation of plasmid also has the ability to increase MF since comparison # v in table 3.03 has a p-value of <0.001.

iv) Does Bystander MF 'bse' contribute to the overall direct mutagenesis?

In order to evaluate the efficacy and possible mutagenic role of electroporation and other factors involved and contributing towards MF the relationship $D=d+bse$ has proved beneficial.

As the overall induced Direct MF due to plasmid alone was calculated (referred to as 'D') it was less than the sum of $d+bse$, hence bystander effect does contribute towards the overall Direct MF 'D' (refer to figure 3.14).

When all 24 values (from 6 data points and 4 replicates) were plotted for $D=d+bse$, 13/24 values were less than zero, 10/24 values were more than zero and 1/24 value showed no difference. When a graph was plotted for 'D' (figure 3.14) most of the time 'D' was less than the product of $d+bse$, but when D was more than zero, the induced bystander signal (bse) must have been contributing towards the overall direct mutagenesis (D) in directly targeted cells. This suggests that the bystander signal does affect the directly induced mutation fractions.

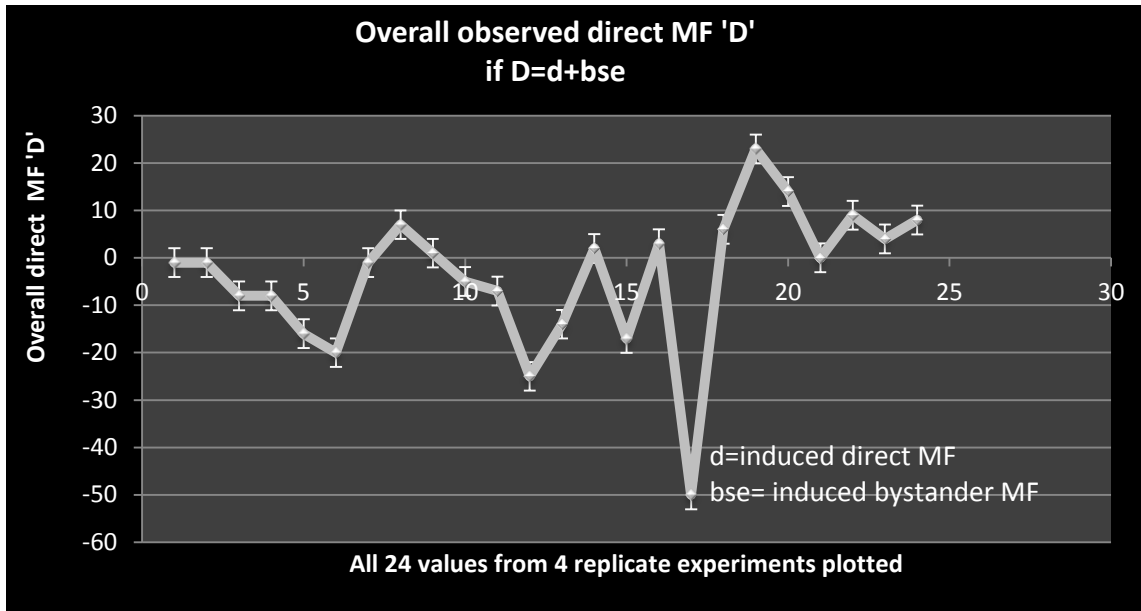


Figure 3.14 shows a line graph in support for the equation $D=d+bse$. 'D' (overall observed direct MF) being smaller than zero suggests that the induced bystander effect 'bse' in the time-course experiment was not only due to the background sources of DNA damage and that when the bystander signal was separated from directly targeted cells, it had an effect on direct MF.

1. These experiments and analyses allowed to answer several questions and understand the dynamics of bystander effect to some degree.
2. The time course experiments produced replicable results re-affirming the previous findings where electroporation caused an elevated direct MF compared to the background non-electroporated conditions (also evident in figure 3.12) at all time points.
3. Once again all results from current experiments coincided with previous experiments to show that bystander MF is indeed increased when medium from directly electroporated cells is transferred to naïve cells.

4. Results indicate that direct MF of electroporated cells is **increased by a factor of 8** when compared to the non-electroporated background Direct MF.
5. Bystander MF of naïve cells, in which medium was transferred from directly electroporated cells, **increased by a factor of 9** when compared to the background of non-electroporated bystander MF.
6. Results also indicated that the electroporation buffer itself could become mutagenic when electroporated as evident from 5B (bystander MF due to electroporation of buffer) bars in (fig.3.12). This observation demands more insight and further testing.
7. The ratio between direct and bystander MF was 1 (since the factor by which they increased was 8:9).

Direct MF: Bystander MF

Since this *relationship* helped to evaluate that overall direct MF ‘D’ is not equal to the sum of induced direct MF ‘d’ and induced bystander MF ‘bse’; it was reasonable to assume that the overall direct MF ‘D’ could have been a sum of mutations from various other sources like regular DNA replication or background mutations.

8. **Estimating the number of DNA double strand breaks induced by restriction enzymes (Figure 3.15):**

Because Not1 and Sfi1 should induce double strand breaks randomly throughout the genome it was reasonable to compare the mutagenicity of these restriction enzymes (REs)

with that of ionizing radiation (IR) which is known to induce 40 DSB/Gy of low LET γ -rays (Lobrich et al., 1994).

E18 cells were grown to a density of 1×10^5 cells/mL in T-75 flasks and irradiated at 0.0, 0.25, 0.50, 0.75 and 1.0 Gy with γ -source irradiator (G. L. Shepherd Mark-I/68A (SS-056)) and allowed a recovery period of 3 hours in an incubator set at 37 °C. At the end of 3 hours these cells were plated in 96 well plates to determine the mutation fraction. Once the mutation fraction was measured and plotted on the graph, I used the known fact that 1 Gy of exposure can cause almost 40 double strand breaks to estimate how many breaks could be expected in the E18 cell model at a specific range of mutation fraction. The experiment was done in three replicates to plot averages of the mutation fraction against dose figure 3.15.

As can be seen when comparing the MFs shown in figure 3.15 to those in figure 3.10, the direct MFs obtained for Not1 and Sfi1 are approximately equal to those induced by 0.5 Gy γ -rays. Therefore it can be estimated that the electroporated restriction enzymes were effectively creating about 20 DSB/cell. This relatively low level of effective digestion (there are thousands of sites per cell, but many or most of the induced breaks may be easily repaired- much more so than for IR where the ends created by the break are not religatable) is consistent with the fact that electroporation of the REs were not particularly toxic to the cells.

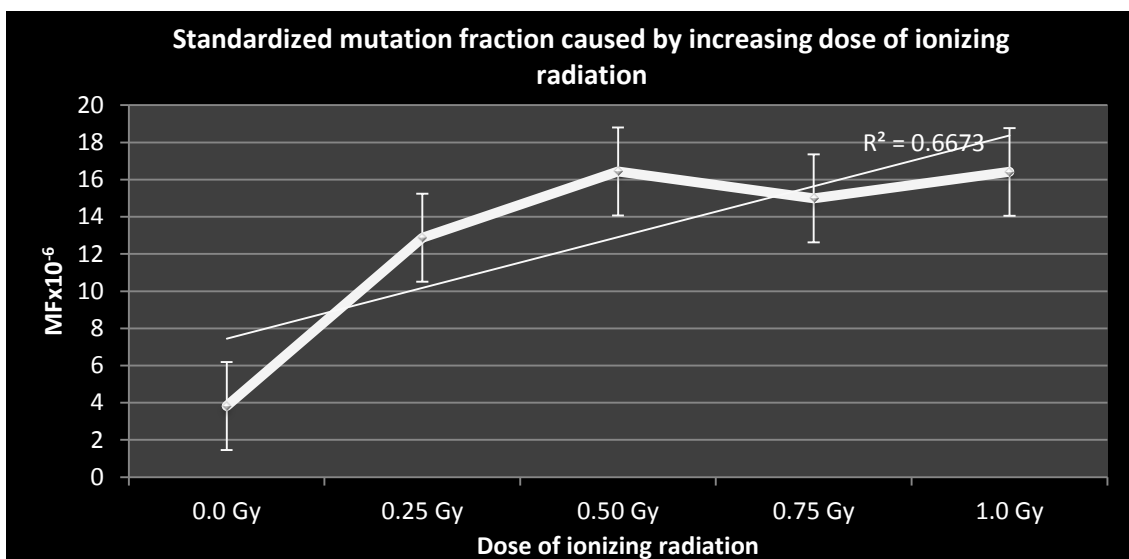


Figure 3.15. Standardized mutation fraction produced by increasing dose of ionizing radiation. Averages of three replicate experiments were plotted. The R^2 value is also shown on the line graph and was calculated to be 0.6673.

9. Effect of inhibition of DNA repair enzyme DNA PK on DSB-ABE (Figure 3.16)

The experiment was designed to measure the effect of inhibition of DNAPK, a DNA repair enzyme on direct and bystander MF induced by DNA damage from electroporation of plasmid pAdTrackCMVI-Sce1. The directly targeted cells were treated with 10 μ M of DNA PK inhibitor NU 7026 for 16 hours prior to transferring the medium containing the bystander signal to naïve bystander cells. Regular lab protocol was used for inhibition (reference materials and method section of this chapter).

It was hypothesized that if DNA strand breaks induced a bystander effect then it was formally possible that inhibiting one or more of the pertinent DNA repair enzymes might modify the bystander MF. For example, by inhibiting DNA PK the mutation fraction of bystander naïve cells (that were exposed to bystander signal produced by the cells

targeted directly with the DNA damaging plasmid) could change. If such a change in bystander MF occurred following DNA PK inhibition, this might indicate that the DNA strand break induced bystander signal can be suppressed by reducing the DNA damage and bystander signal produced thereof.

E18 cells directly electroporated with pAdTrack CMV I-Sce1 were treated with NU7026 (a DNA PK inhibitor) for 16 hours (a standard lab protocol) and transferred the conditioned medium to naïve bystander cells at the end of that time period. The direct and bystander mutation fractions were then compared with a number of controls. Untreated cells were compared with a control batch that was electroporated with the control plasmid pAdTrackCMV, a batch that was electroporated with the experimental plasmid pAdTrackCMVI-Sce1 and the last batch was treated with the inhibitor after electroporating the cells with pAdTrackCMVI-Sce1.

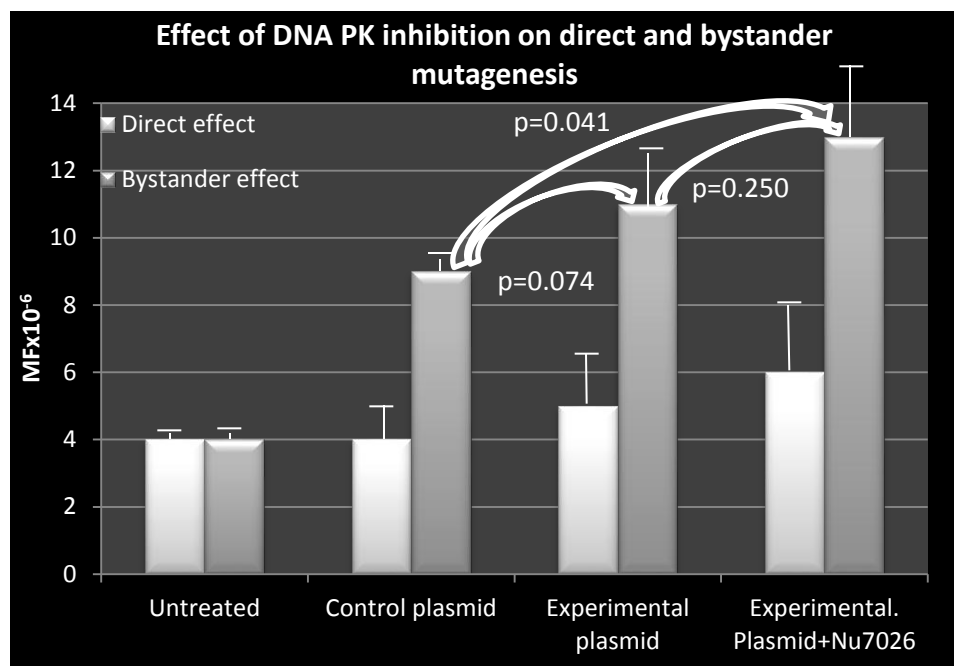


Figure 3.16. The effect of inhibition of DNA repair enzyme DNAPK with NU7026 (10 μ M) on the direct and bystander mutation fraction (averages of three replicate experiments plotted). Absolute control shows the background MF, pAdTrackCMV was used as the control plasmid to differentiate and measure the actual MF due to the cutting action of experimental plasmid pAdTrackCMV I-Sce1 and separating it from the DNA damage caused by electroporation.

Statistical analyses of the results indicated that there was a significant difference between the direct and bystander effect, when all 12 values were considered for each category. The student's t-test gave a p-value of 0.006. Hence it can be concluded that a definite bystander effect existed in this experiment. When control plasmid bystander mutagenesis was compared to bystander mutagenesis due to I-Sce1 plasmid the p-value indicated a non-significant difference ($p=0.074$). The difference between uninhibited bystander mutagenesis and DNA PK inhibited bystander mutagenesis was also not significant ($p=0.250$).

Comparing the control to inhibited DNA PK bystander mutagenesis gave a p-value that was significant i.e., 0.041 indicating that a bystander signal was generated by I-Sce1

plasmid and that DNA PK inhibitor NU7026 did not cause the bystander signal to increase ($p=0.250$). These results were complementary to the findings of other researchers who have shown that DNA repair capacity is independent of bystander mutagenesis. The lack of correlation between DNA repair capacity and bystander effect has been discussed in the following ways by investigators working on RIBE:

- a. Evidence exists to support the idea that when one DNA repair enzyme (DNA PK in this case) is inhibited with NU7026 other repair enzymes like ATM and ATR can take over the function of repair (Zhang et al., 2009).
- b. DNA repair capacity and DNA strand break associated bystander effect are not dependent on each other (Kashino et al., 2007).
- c. With regards to the reception of bystander signal by naïve cells, ATR inhibition is important while ATM and DNA PK do not have a role to play (Burdak-Rothkamm et al., 2007).
- d. DNA strand breaks have nothing to do with DSB-ABE.
- e. It can be argued here that when only one of the three known DNA repair enzymes is inhibited the other two repair enzymes may take over and hence a significant difference could not be observed. Having observed an increase in bystander MF null hypothesis was rejected and DNA PK could be considered as one of the most important enzymes of DNA repair. It was now important to investigate the effect of inhibition of all three known enzymes of DNA repair and their effect on DSB-ABE.

10. Effect of inhibition of 3 known DNA repair enzymes on direct and bystander mutation fractions (Figure 3.17):

This experiment was aimed at testing the hypothesis that if DNA strand break associated bystander effect is in fact generated by strand breaks then the inhibition of DNA repair enzymes in the directly targeted cells should effectively cause an additional increase in the mutation fraction of naïve cells. Three major enzymes known to play a part in DNA repair were either inhibited individually or in tandem. The three repair enzymes, namely ATM, ATR and DNA PK have been known to act as DNA damage sensor enzymes and recruit other proteins to carry out the repair process. ATM was inhibited by using a low concentration (600 nM) of a chemical inhibitor called CGK 733 while ATM and ATR were inhibited by a higher concentration (10 uM) of the same chemical. DNA PK inhibition was carried out with NU7026 at a concentration of 10uM as above (refer to the materials and method section for details). A 16 hour inhibition treatment was given to direct cells immediately after transfection with control or experimental plasmids, at the end of that time the conditioned medium was transferred to naïve bystander cells (while direct cells were supplemented with fresh RPMI medium). Both direct and bystander cells were further incubated for 72 hours to allow mutant expression.

The rationale for the experiment was to establish that DNA breaks if left unrepaired could cause a higher increase in the mutation fraction of directly targeted as well as naïve bystander cells. One of the functions of DNA damage sensor enzymes is to induce cell cycle arrest so damage can be repaired but if this damage persists then there can be two logical end-points:

- a. *The cells undergo apoptosis due to the heavy unrepaired damage,*
- or,*
- b. *They re-enter the cell cycle with damaged DNA and cause an increase in mutation fraction of directly targeted cells.*

If (a) is correct then a loss of viability of the directly targeted cells must be exhibited and hence a lower mutation fraction in the population due to loss of cells that contribute towards mutant expression. However if condition (a) is wrong and instead (b) is correct then the load of DNA damage persists and the cells produce a DNA strand break associated bystander signal, which when transferred to naïve cells could cause an increased bystander mutation fraction in naïve cells. It could also generate a higher direct mutation fraction since the DNA damage was not allowed to undergo repair. If both (a) and (b) are incorrect then DSB-ABE and DNA repair capacity do not have a positive correlation.

In the absence of one DNA damage repair enzyme another can take over the function and effectively repair the damage. Taking into consideration this fact inhibiting individually each known DNA repair enzyme in the directly targeted cells was tested. It is worthwhile to mention that a specific ATR inhibitor does not exist. One commercially available inhibitor known as CGK 733 can inhibit ATM at a lower concentration and ATM/ATR together at higher concentrations. This inhibitor was used to inhibit either ATM or ATM/ATR. But for DNA PK inhibition NU7026 was used.

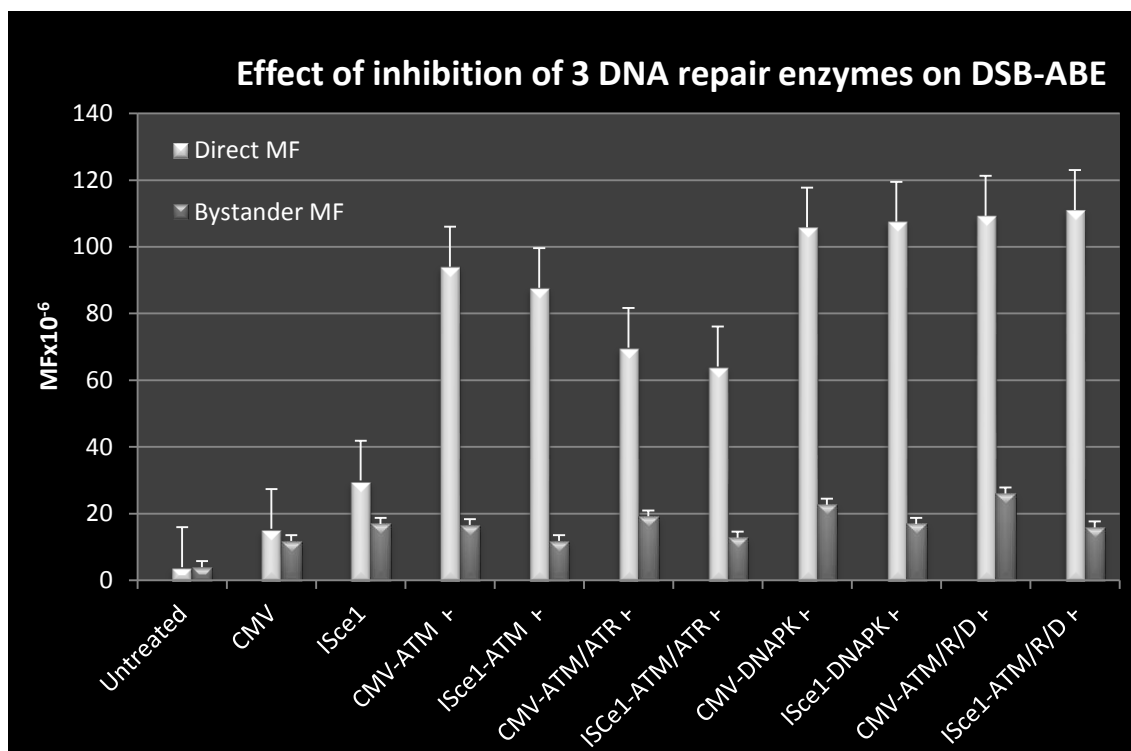


Figure 3.17: The effect of inhibition of three known DNA repair enzymes ATM/ATR and DNA PK on the mutation fractions of directly targeted and naïve bystander cells. ATM was inhibited by using a lower concentration (600nM) of CGK733, ATM/ATR were inhibited by using a higher concentration (10uM) of CGK 733, while DNA PK was inhibited by using 10uM of NU7026. Abbreviations used: Untreated (absolute control), CMV (pAdTrack CMV control vector transfection), ISce1 (pAdTrack CMV I-Sce1 experimental vector transfection), CMV-ATM \ominus or ISce1-ATM \ominus (ATM inhibition in control or experimental vector transfections), CMV-ATM/ATR \ominus or ISce1-ATM/ATR \ominus (ATM and ATR both inhibited in control or experimental vector transfections), CMV-DNAPK \ominus or ISce1-DNAPK \ominus (DNA PK inhibited with control or experimental vector transfections), CMV-ATM/R/D \ominus or ISce1-ATM/R/D \ominus (ATM, ATR and DNAPK inhibited in control or experimental vector transfections). Results indicate a higher influence of DNA repair enzyme inhibition on the mutation fraction of directly targeted cells than bystander cells. Also notice a 10 fold increase in direct MF (compared to uninhibited CMV or ISce1 transfectants) when DNA PK is inhibited in both control and experimental transfectants. While notice that when either or both ATM and ATR are inhibited the direct MF increases 4 to 8 fold but with DNAPK inhibition this increase is almost 10 fold. This increase suggests a greater role for DNA PK in the repair of I-Sce1 induced DNA damage in direct cells. The same trend is also exhibited in bystander MF but not to the same extent as shown in directly targeted cells.

These results have not yet been replicated, however the data in figure 3.17 suggests that:

1. Transfection of experimental plasmid (pAdTrackCMVI-Sce1) did increase the MF from baseline levels by a factor of 8, which is consistent with my earlier findings (please refer to figure 3.12).
2. When DNA repair enzyme ATM was inhibited after transfection with pAdTrackCMV I-Sce1, in directly targeted cells, the direct MF increased from 30×10^{-6} to 88×10^{-6} an increase by a factor of 3.
3. When DNA repair enzymes ATM/ATR were inhibited after transfection with pAdTrackCMV I-Sce1, in directly targeted cells, the direct MF increased from 30×10^{-6} to 64×10^{-6} an increase by about a factor of 2.
4. When DNA repair enzymes ATM/ATR and DNA PK were inhibited after transfection with pAdTrackCMV I-Sce1, in directly targeted cells, the direct MF increased from 30×10^{-6} to 111×10^{-6} an increase by about a factor of 4.
5. There was virtually no effect of DNA repair inhibition on bystander MF, whether one two or all three repair enzymes were inhibited.
6. These observations indicate that DNA PK is a major DNA damage repair enzyme but DNA repair capacity does not affect the bystander signaling phenomenon. Since these results need to be replicated before any conclusions can be made based on statistical analysis, I plan to take this aspect as my future project for DSB-ABE investigations.

11. Nature of DNA strand break associated bystander signal through inhibition studies (Figure 3.18):

This experiment was aimed at determining the nature of signal released in DSB-ABE. It has already been argued in the background section (reference 1.02, 1.03, 1.06 and 1.07) that bystander signal can be of many chemical forms but this investigation was limited only to testing the reactive oxygen species (ROS) as a possible bystander signal or the reception of a cytokine based signal in naïve cells that follows the Mitogen activated protein kinase (MAPK) pathway.

The release of ROS and its possible role as a bystander signal in RIBE has already been discussed in the background section. In order to apply the same logic to non-radiation based DNA damage that could produce ROS, I decided to test the hypothesis of degrading ROS with superoxide dismutase SOD and measuring the direct and bystander MF. ROS degradation with SOD was mainly targeted at inhibiting the bystander signal produced by directly targeted cells while MAPK pathway inhibition with PD 98059 was targeted at inhibiting the reception of bystander signal by naïve cells.

The directly targeted E18 cells were centrifuged 5 hours after transfection (electroporation with plasmid) and separated the medium containing the bystander signal. The medium was treated with SOD or PD98059 for 1 hour (as per vendor specifications) and applied the medium to naïve cells. Both direct and bystander cells were plated for mutation fraction after 72 hours of incubation to allow mutant expression. Results of three replicate experiments are shown in Figure 3.18.

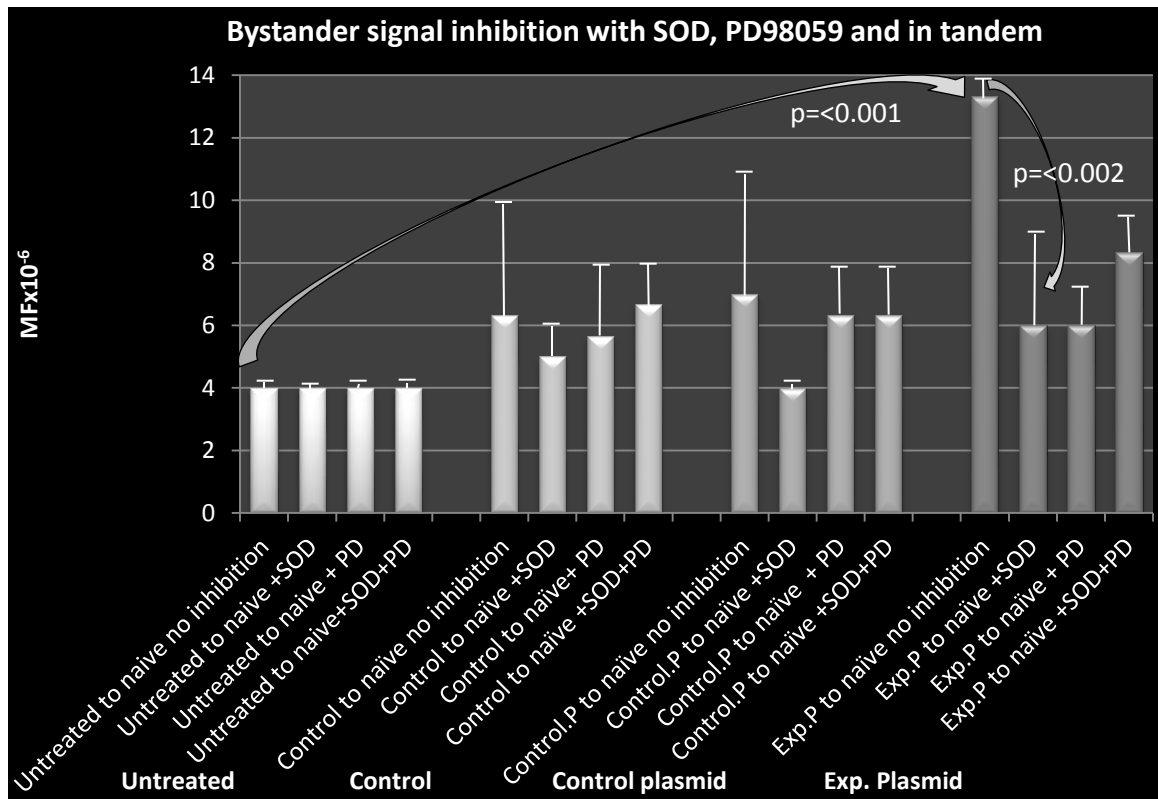


Fig. 3.18 Data plotted from an average of three replicate experiments. The four bars in group one (untreated) depict Bystander MF of untreated cells either not inhibited or inhibited with SOD or PD98059 or SOD and PD98059. Group 2 (control) shows mock electroporation of E18 cells either not inhibited or inhibited with SOD or PD98059 or SOD and PD98059. Group 3 (Control Plasmid) shows E18 cells electroporated with control plasmid (pAdTrack CMV) either not inhibited or inhibited with SOD or PD98059 or SOD and PD98059. The last group (Experimental plasmid) shows the bystander MF of E18 cells that were transfected with plasmid pAdTrackCMV I-Sce1 and either not inhibited or inhibited with SOD or PD98059 or SOD and PD98059. The cells that released bystander signal with no plasmid (Abs), electroporation only (Mock), control plasmid (CMV) and experimental plasmid (ISce1) were centrifuged after 5 hours and the separated conditioned medium was treated for 1 hour with enzyme SOD (20 units) or chemical inhibitor PD98059 (5uM) or in tandem with SOD and PD98059. This bystander inhibited conditioned medium was then applied to naïve cells and incubated for 72 hours to express mutants. The Bystander MF shown here represents the results 4 replicate experiments aimed at inhibition of bystander signal due to reactive oxygen species or MAPK pathway.

Following a 1 hour treatment of conditioned medium containing the bystander signal with PD98059 the bystander mutation fraction was decreased significantly, compared to the control uninhibited bystander MF. This decrease indicated that the nature of bystander signal follows the MAPK pathway. The p-value associated with this decrease was <0.002, which is significant. Several statistical comparisons were made using paired t-test at a confidence interval of 95%. The results are tabulated in table 6.01.

Table 3.04: Statistical analysis of bystander signal inhibition.

Comparison	p-value at 95% confidence interval	Remark
Untreated versus I-Sce1 (experimental plasmid) induced bystander MF	<0.001	Significant
I-Sce1 (experimental plasmid) induced bystander MF versus SOD inhibition	0.058	Not significant
I-Sce1 (experimental plasmid) induced bystander MF Versus PD98059 inhibition	<0.002	Significant
I-Sce1 (experimental plasmid) induced bystander MF versus SOD/PD98059 inhibition	0.013	Significant

Since the experiment was replicated three times and their averages used for plotting the graph, the statistical analysis compared means of these values to show whether a relationship is significantly different or not. From table 3.04 it was indicated that it was not super oxide dismutase that degraded the signal but inhibition due to PD98059. Based on these experiments and subsequent statistical analysis my null hypothesis can be

rejected and it is therefore concluded that Mitogen activated protein kinase pathway (MAPK) is in some way involved in the reception of bystander signaling by naïve cells.

It is known from radiation induced bystander signaling research that MAPK pathway is involved. If MAPK pathway activates c-Myc by heterodimerization with Miz1 then p-21 is inhibited which leads to cell cycle arrest or escaping the apoptotic pathway. Ceballos et al. (2005) have reasoned that higher p-53 levels in a cell type can induce apoptosis while lower levels promote cell cycle arrest. They have also shown that this cell cycle arrest is promoted by p-21 which inhibits cyclin dependent kinase (CDK). p-21 on the other hand is inhibited by a c-Myc/Miz1 heterodimer complex and that this complex is required for c-Myc mediated repression of many genes besides p-21. A c-Myc/Max complex on the contrary upregulates certain genes upon binding with specific DNA sequences called (E-boxes). Since p-53 is upregulated in DNA damaged cells, c-Myc activation through MAPK pathway (present in the bystander signal) can cause inhibition of p-53 thus allowing the naïve cells to evade apoptosis and accumulate mutations caused by a separate DNA damaging pathway to raise the bystander mutation fraction (as shown in by my experimental data). Inhibition of the MAPK pathway (using PD98059) removes the c-Myc induced inhibition of p-53 and reactivates the p-53 mediated apoptotic response thus cells die instead of accumulating the DNA damage and mutations, therefore the bystander MF is reduced.

Given the scope of this project it is not possible to extrapolate my studies at this time to investigate the level at which MAPK pathway is involved, however this could be an interesting future project. As far as the aims for this particular project are concerned

evidence was found in support of aim 3 that DSB-ABE can be inhibited by blocking the MAPK pathway.

12. Comparison of DNA strand break associated bystander effect (DSB-ABE) induced by I-Sce1 plasmid in control (TK6) and experimental (E18) cell lines (Figure 3.19):

In all the preceding experiments it was demonstrated that the bystander effect was generated by I-Sce1 induced DNA strand breaks in E18 cell line, which has an I-Sce1 insert. To compare those results with a control cell line, TK6 was chosen since this is the parent cell line form which E18 was derived. TK6 has the same genotype as E18 except the I-Sce1 insert in intron 2 of the *TK1* gene.

TK6 does not have an I-Sce1 insert, so electroporation of I-Sce1 plasmid should not cut at the I-Sce1 site and therefore must exhibit a low direct and bystander mutation frequency compared to E18. It was expected that electroporation itself would cause some DNA damage in TK6 and therefore generate some bystander signal (measured in terms of direct and bystander MF) but this increase would be significantly lower than the MF generated by using E18 cell line.

Both cell lines TK6 and E18 were grown to a density of 10×10^5 or 1 million cells/mL and used to prepare 250uL reactions for electroporation. Both cell lines were transfected with the control vector (pAdTrackCMV) and experimental vector (pAdTrackCMV I-Sce1) in a 4mm cuvette gap and immediately transferred to warm RMPI. The transfected (directly targeted) cells were allowed to recover and produce bystander signal for 5 hours and then

the medium was transferred to 1×10^5 cell/mL naïve cells in a T-75 flask. Both directly targeted and naïve cells were grown for 72 hours to allow mutant expression and plated on the third day for direct and bystander mutant frequencies. Results of the experiment are shown in figure 3.19.

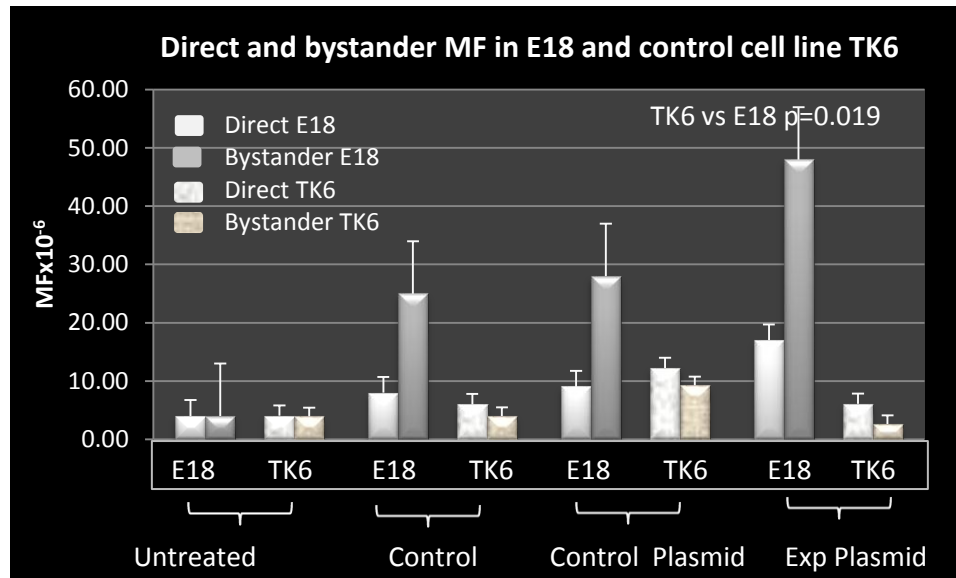


Figure 3.19: Figure shows the induction of E18 cells to produce a bystander signal when transfected with pAdTrack CMV I-Sce1 compared to the control cell line TK6. The directly targeted cells produce bystander signal, which is isolated as conditioned medium and applied to naïve cells. The direct cells respond by an increase in direct mutation fraction (DMF) while the naïve cells respond by an increase in bystander mutation fraction (BMF). Measurement of both mutation fractions in E18 cell line and control TK6 cell line, shows that TK6 does not respond to transfection of control or experimental plasmid, hence the absence of induced DNA damage in TK6 versus its presence in E18 clearly shows that DNA strand break associated bystander effect is a significant occurrence.

The data measurements show that TK6 being the control cell line for E18 (not having the I-Sce1 site for I-Sce1 enzyme to act upon) cannot be induced for DNA strand break associated bystander effect (DSB-ABE). Several controls were set up for comparison of increase in bystander MF with the background. The controls for both E18 and TK6

included absolute, mock electroporated cells in the presence of electroporation buffer, cells electroporated with control plasmid (pAdTrackCMV) and the experimental data point of cells electroporated in the presence of experimental plasmid (pAdTrackCMV I-Sce1). Electroporation of E18 cells either in the presence or absence of control and/or experimental plasmid could generate a bystander signal, measured as increase in bystander MF. However TK6 cell line consistently showed no response to any of the treatment conditions. In mock electroporated, control plasmid electroporated and experimental plasmid electroporated conditions TK6 responded probably to electroporation to a minimal extent.

Statistical analysis:

The p-value for E18 versus TK6 bystander mutation fractions was 0.019 (at 95% confidence interval) which is significant. The experiment provided support for the occurrence of DSB-ABE as a bystander phenomenon that can be associated strictly with induced double strand breaks in E18 cells which the control cell line could not demonstrate.

Summary of results:

Results of preliminary experiments showed that up to 54% transfection efficiency (figures 3.6) could be achieved with electroporation and that the transfection was stable until 15 hours. In figure 3.7 the results indicated both PBS (phosphate buffered saline) and EB (electroporation buffer) give the same results as far as bystander mutation

fraction is concerned since the p-value calculated with student's t-test was non-significant ($p=0.205$). However the use of electroporation buffer was preferred based on the BioRad electroporator vendor recommendations. In the third preliminary experiment (figure 3.8) the highest bystander mutation fraction was observed at 5 hour time point after transfection. The bystander MF at 5 hours was significantly different from the one at 10 hours ($p=0.014$, which is significant) and therefore it was decided to use the 5 hour time point as a standard for later experiments. Experimental data in figures S1 and S2 (see appendix 1) showed that lipofectamine was less efficient than electroporation in delivering the plasmid into the host E18 cells. The high toxicity level of lipofection and non-significant difference between bystander MF with lipofection of control and experimental plasmids into E18 cells ($p=0.333$) suggested the possibility that the high cell mortality associated with lipofection meant that a fewer number of cells in the directly targeted population were available to generate sufficient bystander signal to increase the bystander MF.

While exploring possible mutagenic effects of green fluorescent protein (GFP) marker comparison, of the mutation fractions induced by pAdTrackCMV I-Sce1 with non GFP plasmids pIRES-Hy3 I-Sce1 and pQCXIH I-Sce1 was essential.

The comparison of direct MF induced by the electroporation of GFP marker carrying plasmid pAdTrackCMV I-Sce1 with non GFP plasmids pIRES-Hy3 I-Sce1 and pQCXIH I-Sce1 gave non-significant p-values of 0.605 and 0.7 respectively (refer to table 3.01). This indicated that GFP in pAdTrackCMV I-Sce1 was not causing any additional mutagenic effect in the directly targeted cells. Comparison of direct MF due to all three I-

Sce1 plasmids was also significantly higher than the absolute background, indicating that the I-Sce1 enzyme was being synthesized in the host cells to induce DNA damage. The advantage of using pAdTrack CMV I-Sce1 plasmid was the ease of determining the transfection efficiency. The bystander MF of non-GFP plasmids (pQCXIH I-Sce1 and pIRES-Hyg3 I-Sce1) is significantly lower than that of GFP-containing plasmid (pAdTrack CMV I-Sce1). This is postulated to be due to the self-inactivating roles of both the non-GFP plasmids. It is possible that it is important for the plasmid to continue to produce the I-Sce1 enzyme and induce DNA double strand breaks at the I-Sce1 site in *TK1* intron 2 and offset the continual repair process associated with DNA damage.

The data for electroporation of restriction enzymes into E18 cells (Figure. 3.10) indicated that restriction enzymes did in fact increase both the direct and bystander mutation fraction. But only Not1 produced a significant increase in Direct MF compared to control. The bystander MF comparisons of Not1, Sfi1 and I-Sce1 with the control showed that although only I-Sce1 was statistically significant the other two were also close to being significant. However the fact that all three enzymes, regardless of their cutting frequency were producing almost the same level of bystander MF indicated a no-dose response. This means that a dose response of the number of DNA breaks on bystander signal generation does not exist.

This conclusion is consistent with IR data from RIBE which also shows no dose response for DSB-ABE. In order to interpret the results reliably the number of Not1, Sfi1 and I-Sce1 sites within the *TK1* gene of E18 cells were estimated. There were 4 Sfi1 restriction sites, one I-Sce1 site but no Not1 sites were identified within the *TK1* gene.

If MF is proportional to the number of double strand break sites within the *TK1* gene then the expected MF of direct effect as per hypothesis should be:

Sfi1> I-Sce1> Not1

And the observed direct MF corresponded with the expected MF:

Sfi1> I-Sce1> Not1

Similarly, the expected MF for bystander effect was:

Sfi1~Not1~I-Sce1

Which corresponded to the observed bystander MF:

Sfi1~Not1~I-Sce1

The direct mutagenesis data corresponded to the fact that increase in mutagenesis was observed with regard to the electroporation background for the direct effect using all three restriction enzymes and regardless of their cutting frequency the same direct mutation frequency (Not1=10, Sfi1=11 and I-Sce1=11) was being exhibited. The increase in MF for the direct mutagenesis does not correspond to the original hypothesis of MF being proportional to the number of double strand breaks in or near *TK1*. One possible complication in the experiment was that the number of E18 cells that were permeabilized by electroporation and took up the restriction enzymes may vary according to the size of respective protein that can diffuse through the pores to enter a cell and cause DNA breaks. The cutting efficiency may vary and methylation status may alter the Not1 pattern.

Investigation into the existence of temporal aspects of DSB-ABE (Figure 3.12) allowed me to answer some key questions:

1. Do the various data points used to study progression of direct or bystander mutagenesis indicate a time-dependent response?
2. What are the direct mutation effects of Electroporation (EP) of plasmid?
3. What are the Indirect mutation effects of EP and:
 - (a) Is EP of buffer different from EP of cells?
 - (b) Is EP of cells/plasmid different from either of these controls?
4. Do bystander induced mutations contribute to the overall direct mutagenesis?

The electroporation of experimental plasmid (pAdTrackCMV I-Sce1) into E18 cells and allowing the signal release into the medium for 0, 2, 3, 4, 5 and 10 hours gave some interesting results. These results indicated that it was difficult to measure from the raw data as to how much bystander MF increase was purely due to the I-Sce1 plasmid. It was clear however that in keeping with previous data, the highest bystander MF could be measured at 5 hours post-electroporation. Another surprising observation was that electroporation of the buffer could also produce a bystander MF when applied to naïve cells. Some pre-existing literature refers to the fact that there is heat (Bruskov et al., 2002) and radiation (Gudkov et al., 2010) induced production of reactive oxygen species in aqueous medium. It was postulated, based on the literature that free radicals or superoxides produced in the process of electroporation of plasmid could be the source of increased bystander mutation fraction when electroporated medium was transferred to naïve cells (reference figure 3.12, data point 5). To find answers for these questions

detailed statistical analysis were carried out and the results have been discussed in the light of those analyses in table 3.03.

To predict the number of DNA double strand breaks that can be induced by electroporation of restriction enzymes (figure 3.15) E18 cells were irradiated with γ -rays (0.0, 0.25, 0.50, 0.75 and 1.0 Gy) and the resulting mutation fraction was used for prediction of I-Sce1 induced double strand breaks. Based on the fact that 40 DSBs can be induced by 1Gy of radiation exposure (Löbrich et al., 1994) it was easy to graphically estimate the number of double strand breaks induced by electroporation of restriction enzymes into the host cell line. However this estimation would give the total number of double strand breaks present in the whole genome and not in the gene of interest i.e., *TK1*. To be able to establish the number of DSBs in *TK1* it is possible to extrapolate the analysis by comparing results using data from figure 3.12. The induced MF from electroporation of I-Sce1 plasmid (6D) can be subtracted from MF due to electroporation only (4D) and used to establish the DSBs induced purely by I-Sce1. The analysis revealed that a total of 20-40 DSBs are produced by 6D and approximately 10-12 DSBs are due to I-Sce1 alone. Hence the total DSBs due to I-Sce1 alone are only 10-12. This accounts for DSBs from all sources in a genome of 6×10^9 base pairs. Since the MF is calculated on a logarithmic scale of $\times 10^{-6}$ it can be assumed that one DSB can be expected at every 3×10^8 base pair. This also conforms to the total number of six breaks that I-Sce1 can potentially cause in the human genome (i.e., 5 breaks at non-specific sequences and one break at the I-Sce1 inserted sequence in intron 2). It is assumed that

the 4-6 additional DNA breaks are being caused by electroporation, hence bringing the total predicted breaks to 10-12.

Inhibition of DNA repair enzyme DNA PK, gave a significantly higher bystander mutation fraction compared to uninhibited bystander MF data point (Figure 3.16). If DSB-ABE is a kind of bystander effect that originates from induced DNA double strand breaks then, inhibition of this damage should have increased the bystander MF. Having obtained these results and trying to explain them led to further readings on DNA repair literature with regards to bystander signaling and it was found that although DNA PK is the major double strand break repair enzyme but, if inhibited, other repair enzymes like ATM and ATR can take over the repair process. Since this experiment needed more insight and to demonstrate the effect of repair inhibition (due to ATM/ATR and DNA PK) on DSB-ABE a more detailed experiment was set up.

When all three DNA damage repair enzymes were inhibited (Fig 3.17) there was no effect on the bystander mutation fraction, which indicated the fact that DSB-ABE and DNA repair capacity are independent processes. These results have to be replicated under stringent conditions therefore further analysis and experimentation is required to find support for these claims.

Investigation of the possible role of reactive oxygen species (ROS) and cytokines as bystander signals by degrading either the ROS with super oxide dismutase or blocking the MAPK pathway in naïve cells to which the conditioned medium was applied (Figure

3.18) indicated an involvement of MAPK pathway. However to understand the role of one possible sub pathway of MAPK, further testing and western analysis is required.

To conclude the DSB-ABE phenomenon, the ability of E18 cells to generate bystander signal due to I-Sce1 was compared to TK6 for DNA damage associated bystander signaling capacity. Results (figure 3.19) indicated that when bystander MF of E18 was compared with that of TK6 significant result was obtained at a p-value of 0.019.

Future considerations:

After having optimized the techniques for E18 cell model, it was pertinent to confirm the presence of I-Sce1 site within intron 2 of *TK1* gene and to cut it with the I-Sce1 restriction enzyme. These experiments were carried out and the I-Sce1 site sequenced to confirm the findings and to be sure about the results of future planned experiments. Some of the experiments planned at this point are to transfect varying units (5, 10, 15, 20 units) of restriction enzymes and keeping the mixture cold to minimize protein structural loss due to heat during electroporation. An absolute background of electroporation can also be established to find out what additive effect electroporation has on up regulating the MF besides using a cell model that does not have I-Sce1 insert.

The experimental data from mutation assays has indicated that electroporation is indeed mutagenic since it upregulates the direct and bystander MF therefore the next step will be to change the delivery system for transfecting the pAdTrackCMV I-Sce1 plasmid into

host E18 cells to lipofection. One option is to develop a TET on/off system for the purpose, based on the fact that this system is not leaky.

The actual direct effects of electroporation on model cell systems have been reported to be mutagenic in the past but the bystander aspect has never been examined. The results reported here show that electroporated cells can produce a bystander signal which can cause DNA damage in naïve cells. It will be of interest to examine the overall ability of other delivery systems like ethyleneamine and chariot and to evaluate an inducible system like TET on/off to generate a bystander signal.

These future experiments will help me in answering the following questions:

1. How much does bystander effect (BSE) contribute to direct mutagenesis?
2. In the bystander kinetics, is there a second wave of bystander signal that was noticed at 15 hour time point?
3. Is there a feedback for the production of bystander signal and if yes, is it positive or negative?

In a modified alkaline comet assay, fluorescently labeled probes can be used to identify DNA damage caused by the transfection of respective restriction enzymes including I-Sce1, which is believed to cut only once in the genome. This increased resolution of detecting the number of DNA strand breaks will help me determine if DNA breaks can indeed generate a bystander signal. Comet assays using rare cutting restriction enzymes will also be beneficial in determining the minimum number of DNA double strand breaks required to establish a threshold value for DNA break associated bystander effect (DSB-ABE).

Enforced/exogenous expression of c-Myc in MAPK inhibited cells, which is predicted to restore the normal bystander response of increased bystander MF will hopefully substantiate the claims that bystander signal is indeed a TGF based cytokine that activates the MAPK pathway in naïve cells and induces p-53 mediated apoptosis to cause cells to pre-maturely apoptose instead of accumulating mutations and increasing the bystander MF.

Proposed model of DSB-ABE:

Based on the findings of electroporation versus lipofection of restriction enzymes into E18 cells, it can be argued that since Sfi1 has a higher molecular weight than Not1 or I-Sce1 therefore it has a lower probability of entering the voltage based and electroporation induced pores created in the plasma membrane, while lipofection could deliver the restriction enzymes directly into cells regardless of their size. This is the reason why Sfi1 produced a higher direct MF in figure S3 (appendix 2) compared to figure 3.10. However the overall design of these experiments and the choice of a delivery system depended on lower mutagenicity. For these reasons it was decided to use electroporation because it has a lower direct mutagenic effect on cells compared to lipofection.

Proposed model for DNA strand break associated bystander effect (DSB-ABE)

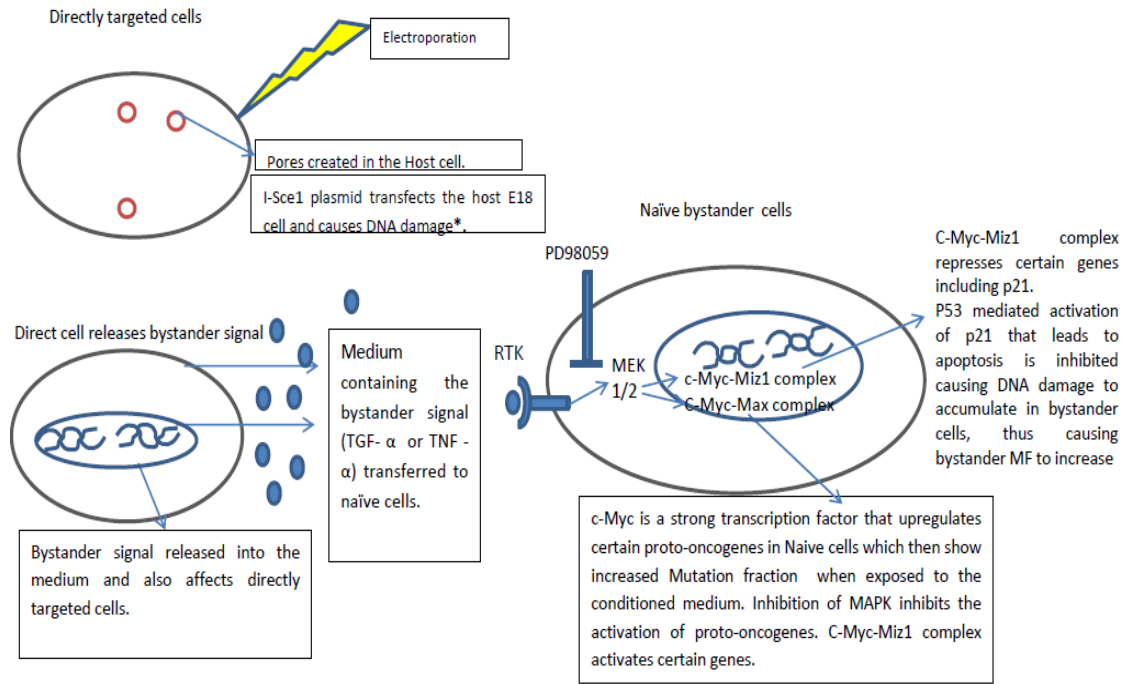


Figure 3.20: Transfection of E18 cells with pAdTrack CMV I-Sce1 causes I-Sce1 induced DNA strand breaks at the I-Sce1 site in intron 2 of the *thymidine kinase 1* gene. Induced DNA damage causes the production of cytokines or a soluble cell signal (through an unknown process) which is released into the surrounding medium. The bystander signal activates MAPK pathway in the naïve cells to affect a change in their mutation fraction. It is postulated that out of the many downstream signaling pathways that MAPK can activate, c-Myc activation is the most possible candidate for upregulation of mutation fraction. c-Myc heterodimerizes with protein Max (c-Myc/Max complex) to upregulate target genes or heterodimerizes with Miz1 (c-Myc-Miz1 complex) to repress certain genes, including p-21, which is p-53 dependent. Depending on the extent of p-53 mediated activation of p-21, there are two possible outcomes as reported by (Ceballos et al., 2005). A high p-53 mediated activation of p-21 can promote Apoptosis while lower p-53 activation can cause growth arrest. If apoptotic pathway is activated then proto-oncogene activated naïve bystander cells die, but if cells undergo growth arrest then they can re-enter the cell cycle and accumulate mutations, thus raising the bystander MF in naïve cells.

Based on the data generated, a model is proposed for DSB-ABE, in which the cell containing an I-Sce1 insert is targeted for DNA strand breaks by a plasmid expressing the I-Sce1 gene. The plasmid expression causes DNA strand breaks at the I-Sce1 site and causes the release a bystander signal into the medium. Upon transfer of this conditioned medium to naïve cells an increase in bystander mutation fraction is observed. Having observed no effect of degradation of ROS with super oxide dismutase, their involvement as possible bystander signal was ruled out. Based on a significant decrease in bystander MF due to MAPK inhibition (with PD98059), it can be postulated that the bystander signal is some kind of a cytokine, rather than reactive oxygen species, and that this cytokine activates the receptor tyrosine kinase on naïve cells, leading to a cascade of downstream signaling events that somehow cause the bystander MF to increase. For now nothing can be said about how an increase in MF is brought about but possible pathway could be the activation of c-Myc transcription factor which activates certain proto-oncogenes that can lead to an increase in bystander MF of naïve cells. Although the involvement of p-53 cannot be ignored, but experiments done by other investigators (Zhang et al., 2009) with TK6 cell lines have shown that radiation exposure of up to 4 Gy is required to cause any change in p53 levels. Since DSB-ABE cell model mimics a radiation dose exposure of less than 1 Gy (Figure 3.13 and table 3.04) the role of p53 as a downstream target of MAPK pathway is ruled out.

Chapter 4: Discussion and Conclusion

Purpose of study:

The purpose of this study was to test a new cell model system containing an I-Sce1 insert in the *TK1* gene and to target the extremely rare cutting restriction enzyme I-Sce1 to induce one DNA double strand and investigate any possible bystander signal generation. The study became very interesting with the measurement of a sufficient amount of bystander signal generated by targeted cells that could affect the naïve bystander cells.

Research questions answered:

This research project successfully answered the following questions.

- a. Is bystander signal produced by induced DNA double strand breaks?
- b. Is this kind of bystander effect time dependent?
- c. Could the DNA strand break associated bystander signal produced by directly targeted cells be sufficient to affect naïve cells?
- d. Is DNA damage repair capacity independent of DSB-ABE?
- e. What is the mechanism of action and nature of this unique cell signal?

Conclusion:

Honma et al. (2003) constructed a similar I-Sce1 system and reported that most of the I-Sce1 induced double strand breaks were repaired by non homologous end joining (NHEJ). Up to 70% of these breaks that were repaired by NHEJ showed 100-4000 bp

deletions with 0-6 bp homology, while 30% showed complex DNA rearrangements probably due to sister chromatid fusions/exchanges (SCEs). His team also showed that NHEJ repair pathway was used 270 times more frequently than homologous recombination (HR).

The extent and size of deletions (Honma et al., 2003) that are associated with NHEJ repair were shown to be classified into 4 groups and shown in table 4.01 below:

Table 4.01

Percentage contribution of I-Sce1 induced deletions in the cell model used by Honma et al. (2003)

<u>Deletion class</u>	<u>size</u>	<u>percent contribution</u>
Small deletions	80-7.8kb	25%
Medium deletions I	>876bp	52%
Medium deletions II	>7.8kb	6.8%
Large deletions	>4.5Mb	2.3%

Total Percentage		86.1%

Considering the I-Sce1 cell model constructed by Honma et al. (2003) in which the I-Sce1 site was 75 bp upstream of exon 5; their system was compared to E18 and their data used to explain mutation spectrum in the E18 cell model system.

Since the I-Sce1 site in E18 is located at position 1692-1710 (in intron 2) 640 bp upstream of exon 3 the contributing deletions that might cause loss of heterozygosity and hence mutations in E18 could be medium I, medium II and large deletions reported by Honma et al. (2003). The total percentage contribution of these three classes was 61.1% ($52+6.8+2.3=61.1$) towards a total MF of 274×10^{-6} .

An average of mutation fractions induced by pAdTrack CMV I-Sce1 in all 45 experiments (in which the plasmid was electroporated to get a direct MF) was calculated and was compared with Honma's data. The average direct MF calculated for transfecting E18 cells with the plasmid was 30×10^{-6} . Please see table 4.02 below for how this average of averages was calculated. Figure 3.15 and table 3.04 also provided additional information about the number of double strand breaks that can be induced in E18 cell system by electroporation of pAdTrackCMV I-Sce1. An average MF of 30×10^{-6} could be translated into 20-40 double strand breaks that are induced by radiation. If only one double strand break is caused by the plasmid pAdTrack CMV I-Sce1 then an additional 19-39 breaks are a result of electroporation.

The expected MF for E18 cells as calculated from Honma et al. (2003) was $61.1/100 \times 274 = 167 \times 10^{-6}$, while the observed MF for E18 cells was 30×10^{-6} . Hence the difference in expected and observed MF for E18 (as compared to Honma's cell model) could be attributed to the difference in the position of I-Sce1 site to the nearest exon (exon 3 which is 694 bp upstream of the I-Sce1 site) in the *TK1* gene and the difference in transfection efficiency, which was 54% in E18 while 64% in Honma's experiments. The vicinity of I-Sce1 site which was 75 base pairs upstream of exon 5 could be attributed to higher fraction of mutations.

Overall the direct MF data for E18 cells confirms the findings of Honma et al. (2003) and shows that E18 is similar to the cell model TSCE5 reported by Honma et al. (2003). Some later time course experiments showed and confirmed findings of Zhang et al. (2009) that radiation induced bystander signal could be produced immediately and plateaued at 12 hours. In DSB-ABE this time course phenomenon was in fact observed and it reached a maximum at 4-5 hours after transfection but it dissipated in 5-10 hours. It was concluded that E18 cells have an I-Sce1 in intron 2 at position 1692-1710 of the *TK1* active allele and that this site could be targeted for double strand break associated bystander effect with pAdTrackCMV I-Sce1 plasmid to cause the release of bystander signal from directly targeted cells into the surrounding medium. This conditioned medium could cause an increase in bystander mutation fraction when transferred to naïve E18 cells. Based on the mutation spectrum data generated by Honma et al. (2003) from a cell line that was very similar to E18 and also had an I-Sce1 insert, a comparison was done to validate the findings of DSB-ABE. A detailed analysis in tables 4.01 and 4.02 shows how this was done.

Table 4.02

Table shows how average of averages of direct MF induced by I-Sce1 was calculated from all experiments (carried out under identical conditions). Column 1 shows the reference figure in this thesis, while column 2 shows the average of direct induced MF from several experiments and column 3 shows the total of averages.

Figure # in this thesis	MF x10 ⁻⁶	Total of averages
3.7	8	8
3.8	39	39
3.9	17	17
3.12	48+47+23+60+62+47	287
3.16	11	11
3.17	30	30
3.18	8+15+11	34
Average of averages		426/14= 30 x10⁻⁶

Dose dependence and temporal dynamics of DSB-ABE:

The data has shown that radiation independent DNA damage can produce bystander signal almost immediately after plasmid pAdTrackCMV I-Sce1 was transfected into the host E18 cells. Significant increase in bystander MF was recorded between 4 and 5 hours hence temporal kinetics for DSB-ABE exist. A two fold increase in mutations at thymidine kinase locus was recorded immediately after transfection and application of conditioned medium to naïve bystander cells. Maximum number of bystander mutations was recorded at 5 hours where a 9 fold increase could be measured (Fig. 3.12). This trend was also seen in another experiment (Fig. 3.8) where the maximum mutations were recorded at 5 hours but decreased at 10 and 15 hours post transfection. The direct induced and bystander induced mutation fractions were also mathematically measured by subtracting the MF that may have been caused by electroporation (Fig. 3.13) and concluded that a temporal response existed for the direct and bystander mutation fractions.

While trying to investigate a bystander dose response, by using three rare cutting restriction enzymes that were transfected into E18 cells, the resulting mutation fraction suggested that a dose response does not exist. The number of breaks caused by an 8 base cutter (Not1) were not significantly different from a 13 base cutter (Sfi1 which is technically an 8 base cutter due to its non-specific restriction site) and also not significantly different from an 18 base cutter (I-Sce1). It was, hence concluded that no matter how many DNA breaks are induced, the same level of bystander activation resulted.

DNA repair capacity is independent of DSB-ABE:

When DNA PK was inhibited with 10nM of NU7026 it had a significant increase in the bystander MF when repair enzyme DNA PK was uninhibited. Since it has been argued in the literature review section that there are other repair enzymes that can take over the repair process, if one is inhibited and that bystander effect is independent of the repair capacity a more detailed experiment validated those earlier observations from experiments performed with RIBE. Results shown in figure 3.16, indicated that DNA strand break associated bystander effect (DSB-ABE) is independent of the DNA repair capacity. In order to confirm those findings all three known DNA repair enzymes were chemically inhibited evidence was found in support of the fact that DNA repair capacity is not linked to the bystander signal generation, since an increase in direct MF was not reflected in bystander MF upon conditioned medium transfer.

This finding correlates with pre-existing data generated by other investigators while working with radiation induced bystander effect. At this point it is hard to correlate the two effects since radiation causes a range of DNA lesions besides cellular damage while DNA double strand break associated bystander effect focuses on only one aspect of bystander signaling. However if logical explanation of DNA repair capacity affecting DSB-ABE is required then given my understanding of DSB-ABE, it can be explained with three possible theories:

- a. Evidence exists to support the idea that when one DNA repair enzyme (DNA PK in this case) is inhibited with NU7026 other repair enzymes like ATM and ATR can take over the function of repair (Zhang et al., 2009).

b. DNA repair capacity and DNA strand break associated bystander effect are not dependent on each other (Kashino et al., 2007).

c. A third possibility, with regards to the reception of bystander signal by naïve cells is that ATR inhibition is important while ATM and DNA PK do not have a role to play (Burdak-Rothkamm et al., 2007).

Considering the data presented here and literature available on the subject, theory (b) seems more logical, since DNA damage is immediate, while repair can take 6-10 hours. If DNA repair is at all involved then its effects could not have been detected by the immediate production of bystander signal that was separated (as conditioned medium) from directly targeted cells and applied to naïve cells at 5 hours after transfection of I-Sce1 plasmid into E18 cells. It is important to mention again that investigations into complete inhibition of DNA repair and its effect on DSB-ABE are required to understand the phenomenon better.

Signaling pathway indication for DSB-ABE (Fig 3.17):

Inhibition of MAPK pathway with 5nM of PD98059 or sequestration of reactive oxygen species (ROS) with 20 units of super oxide dismutase (SOD) showed amazing results (figure 3.17). It appeared that sequestration of reactive oxygen species with SOD did not inhibit the bystander signal since I-Sce1 induced bystander MF was not significantly reduced compared to the background level. On the other hand inhibition with PD98059 or PD98059 in tandem with SOD significantly reduced the bystander MF to background levels. This indicates that MAPK pathway may be involved in reception of the bystander signal by naïve cells. The experimental data also indicated that ROS could not be considered as the possible bystander signal produced during the transfection of I-Sce1

plasmid into E18 cells that caused the site-directed double strand break. This theory also finds support from radiation induced bystander effect data, which shows that ROS, generated during irradiation of target cells have a very short half-life and can travel only on a nano meter scale. The objective of investigating ROS in these experiment was to investigate if electroporation could have produced any reactive oxygen species that could be implicated in bystander effect. It is possible that electrical current, may have changed the membrane potential of mitochondria or the plasma membrane and resulted in the release of H^+ , Ca^{++} , K^+ ions or even the release of apoptotic signals from mitochondria. However these ions remain to be investigated and are currently beyond the scope of this investigation.

Contribution of this study:

At a point of divergence where the investigators of DNA damage repair consider that DNA damage is not essential for bystander signal generation and that irradiation of cytoplasm can also produce the same effect, it was important to investigate if DNA damage, regardless of the source of damage, can produce any signal at all.

Electroporation was used as the delivery system of choice due to its high transfection efficiency and low cell mortality. Electroporation was recently used for electrochemotherapy and gene delivery (Jaroszeski et al., 2000; Marty et al., 2006; Mir et al., 2005) but current investigations have revealed that electroporation not only causes additive DNA damage (Meaking et al., 1995; Goldberg and Rubinsky, 2010) but also results in the production of bystander signals that would increase mutations in the non-targeted cells *in-vivo*, thereby putting the patient at a risk of secondary tumors arising from electrochemotherapeutic practices. A long-term study using bleomycin as an anti-

tumor drug, using electroporation as delivery method, caused the death of one out of 189 patients treated between 1973 and 2007 (Linnert and Gehl 2009).

Since this study has successfully demonstrated that non-radiation induced DNA strand breaks can produce a bystander signal that would increase the mutation fraction in naïve cells, it is going to have an impact in the pharmaceutical industry to revise their IC_{50} for some anti-cancer drugs that target tumor cells by damaging their DNA. This study will also help to revise some radiation quality standards for radiotherapy since all ionizing radiations used for such purpose induce heavy DNA damage in tumor cells.

Future research implications

This thesis has implications for improving cancer therapy, especially radiotherapy that attempts to target a defined mass of tumor, yet the recurrence of cancer is high. This recurrence may depend on the in-vivo bystander signal generation from irradiated cells that affect the surrounding healthy cells to transform them into a cancerous mass. As already mentioned bystander effect is a highly complex cell signaling process, it is not known as to how many signaling pathways regulate this phenomenon.

Future research in this field could involve looking at the specific phosphorylated proteins of the MAPK pathway. Another possible direction is the effect of complete inhibition of DNA repair process in the directly targeted cells.

Limitations of this study and recommendations for further research:

The inability to physically observe or measure the double strand breaks in naïve cells had limited my investigations. A modified comet assay to look at double strand breaks was beyond the scope of this present study. However this could be the next project in this research to separate regular DNA replication breaks from induced strand breaks and assess by what extent the bystander MF could be increased. This study also could not address the following question that arose during the investigations:

- a. If induced DNA breaks could produce a bystander signal then a cell would logically produce bystander signals during each replication cycle when topoisomerase II cuts the DNA to relieve stress on supercoiled DNA. How does the cell counter bystander signal generation in the wake of naturally occurring DNA damage?
- b. If cells that are directly electroporated with pAdTrackCMVI-SceI plasmid can produce a bystander signal, the “Direct cells” could also be affected by this signal in a positive feedback loop. The extent to which the bystander signal produced by these “Direct cells” was affecting them could not be determined as well.

Hopefully these questions could be an interesting project to undertake in the coming years as it would involve setting up a purpose built apparatus that will continually remove the bystander signal containing medium from direct cells and transfer it to naïve cells.

References:

Alexandre, J., Y. Hu, W. Lu, H. Pelicano, P. Huang (2003) Novel action of paclitaxel against cancer cells: bystander effect mediated by reactive oxygen species. *Cancer Res.* 2007 Apr 15;67(8):3512-7. doi: 10.1158/0008-5472.CAN-06-3914.

Allen, R.G. and M. Tresini (2000) Oxidative stress and gene regulation. *Free Radic Biol Med.* 2000 Feb 1;28(3):463-99. doi.org/10.1016/S0891-5849(99)00242-7.

Angelika, G., B. Haubold, S. Pasquet and S. P. Watson (1998) Direct Inhibition of Cyclooxygenase-1 and -2 by the Kinase Inhibitors SB 203580 and PD 98059. *Journal of Biological Chemistry*, October 30, 1998 273, 28766-28772. doi: 10.1074/jbc.273.44.28766.

Asur, R., B. Mamtha, B. Marples, R.A. Thomas, and J.D. Tucker (2010) Bystander effects induced by chemicals and ionizing radiation: evaluation of changes in gene expression of downstream MAPK targets. *Mutagenesis* (2010) 25(3): 271-279 doi:10.1093/mutage/geq003.

Asur, R.S., R.A. Thomas, J.D. Tucker (2009) Chemical induction of the bystander effect in normal human lymphoblastoid cells. *Mutation Research/Genetic Toxicology and Environmental Mutagenesis* Volume 676, Issues 1-2, 31 May 2009, Pages 11-16. doi.org/10.1016/j.mrgentox.2009.02.012.

Azzam, E. I., S.M. de Toledo and J.B. Little (2003) Oxidative metabolism, gap junctions and the ionizing radiation-induced bystander effect. *Oncogene*, 22, 7050–7057. doi:10.1038/sj.onc.1206961.

Azzam, E. I., S.M. de Toledo, D.R. Spitz and J.B. Little (2002) Oxidative Metabolism Modulates Signal Transduction and Micronucleus Formation in Bystander Cells from α -Particle-irradiated Normal Human Fibroblast Cultures. *Cancer Res.* 2002 62; 5436.

Bellaiche, Y., V. Mogila and N. Perrimon (1999) I-SceI endonuclease, a new tool for studying DNA double-strand break repair mechanisms in *Drosophila*. *Genetics*. 1999 July; 152(3): 1037–1044.

Benov, L.C., P.A. Antonov and S.R. Ribarov (1994) Oxidative damage of the membrane lipids after electroporation. *Gen. Physiol. Biophys.* (1994). 13, 85—97.

Bertucci, A., R. D. J. Pocock, G. Randers-Pehrson and D. J. Brenner (2009) Microbeam Irradiation of the *C. elegans* Nematode. *Journal of Radiation Research*, Vol. 50, A49-A54. doi:10.1269/jrr.08132S.

Bishayee, A., H.Z. Hill, D. Stein, D.V. Rao and R.W. Howell (2001) Free radical-initiated and gap junction-mediated bystander effect due to nonuniform distribution of

incorporated radioactivity in a three-dimensional tissue culture model. *Radiat Res.* 2001 Feb; 155(2):335-44. <http://www.jstor.org/stable/3580647> .

Blyth, B.J., E. I. Azzam, R. W. Howell, R. J. Ormsby, A. H. Staudacher, P. J. Sykes (2010) Radiation Research (2010) An adoptive transfer method to detect low-dose radiation-induced bystander effects in vivo. *Rad. Res.* Volume: 173, Issue: 2, Pages: 125-137. PubMed: 0095844.

Blyth, B.J., P.J. Sykes (2011) Radiation-induced Bystander Effects: What are they, and how relevant are they to human radiation exposures? *Rad. Res.*, 176(2): 139-157. DOI: 10.1667/RR2548.1.

Bragg, W. H., R. Kleeman, (1905) *Phil. Mag.*, 10, 318.

Bray, R.C., S.A. Cockle, E.M. Fielden, P.B. Roberts, G. Rotilio and L. Calabrese (1974) Reduction and inactivation of superoxide dismutase by hydrogen peroxide. *Biochem J.* 139: 43-47, 1974.

Bruskov, V.I., Z. Masalimov and A.V. Chernikov (2002) Heat-induced generation of reactive oxygen species in water. *Dokl Biochem Biophys.* 2002 May-Jun; 384:181-4. DOI: 10.1023/A:1016036617585.

Burdak-Rothkamm, S., S.C. Short, M. Folkard, K. Rothkamm, K.M. Prise (2007) ATR-dependent radiation-induced gamma H₂AX foci in bystander primary human astrocytes and glioma cells. *Oncogene* 2007; 26:993-1002. doi:10.1038/sj.onc.1209863.

Ceballos, E., M.J. Munoz-Alonso, B. Berwanger, J.C. Acosta, R. Hernandez, M. Krause, O. Hartmann, M. Eilers, and J. Leon (2005) Inhibitory effect of c-Myc on p53-induced apoptosis in leukemia cells. Microarray analysis reveals defective induction of p53 target genes and upregulation of chaperone genes. *Oncogene* (2005) 24, 4559-4571. doi:10.1038/sj.onc.1208652.

Chang, H., S. Benchimol, M.D. Minden and H.A. Messner (1994). Alterations of p53 and c-myc in the clonal evolution of malignant lymphoma *Blood*, 83, 452-459.

Choulika A., A. Perrin, B. Dujon, J.F. Nicolas (1995) Induction of homologous recombination in mammalian chromosomes by using the I-SceI system of *Saccharomyces cerevisiae*. *Mol Cell Biol.* 1995 Apr;15(4):1968-73. PMID: PMC230423.

Christen, S., T.M. Hagen, M.K. Shigenaga, B.N. Ames (1999) Chronic inflammation, mutation, and cancer. In Parsonnet J, Hornig S eds. *Microbes and malignancy: infection as a cause of cancer.* New York: Oxford University Press, 1999: 35-88.

Cohen-Tannoudji, M., S. Robine, A. Choulika, D. Pinto, F. El Marjou, C. Babinet, D. Louvard and F. Jaisser (1998) I-SceI-Induced Gene Replacement at a Natural Locus in Embryonic Stem Cells. *Mol. Cell. Biol.* March 1998 vol. 18 no. 3, 1444-1448.

Colotta, F., P. Allavena, A. Sica, C. Garlanda, A. Mantovani (2009) Cancer-related inflammation, the seventh hallmark of cancer: links to genetic instability. *Carcinogenesis*, 30 (2009), pp. 1073–1081. doi: 10.1093/carcin/bgp127.

Crescenzi, E., G. Palumbo, J.D. Boer, et al. (2008) Ataxia Telangiectasia Mutated and p21CIP1 Modulate Cell Survival of Drug-Induced Senescent Tumor Cells: Implications for Chemotherapy. *Clin Cancer Res* 2008;14:1877-1887. doi: 10.1158/1078-0432.CCR-07-4298.

Dahle, J., E. Angell-Petersen, H.B. Steen, and J. Moan (2001) Bystander effects in cell death induced by photodynamic treatment UVA radiation and inhibitors of ATP synthesis. *Photochem Photobiol.* 2001 Apr;73(4):378-87. DOI: 10.1562/0031-8655.

Davis, C.A., A.S. Hearn, B. Fletcher, J. Bickford, J.E. Garcia, V. Leveque, J.A. Melendez, D.N. Silverman, J. Zucali, A. Agarwal, H.S. Nick (2004) Potent Anti-tumor Effects of an Active Site Mutant of Human Manganese-Superoxide Dismutase evolutionary conservation of product inhibition. *The Journal of Biological Chemistry*, March 26, 2004, 279, 12769-12776. doi: 10.1074/jbc.M310623200.

Demidem, A., D. Morvan, J.C. Madelmont (2006) Bystander effects are induced by CENU treatment and associated with altered protein secretory activity of treated tumor cells: a relay for chemotherapy? *Int. J. Cancer.* 2006 Sep 1;119(5):992-1004. DOI: 10.1002/ijc.21761.

Dent, P., A. Yacoub, J. Contessa, R. Caron, G. Amorino, K. Valerie, M.P. Hagan, S. Grant and R. Schmidt-Ullrich (2003) Stress and radiation-induced activation of multiple intracellular signaling pathways. *Radiat Res.* 2003 Mar;159(3):283-300. <http://www.jstor.org/stable/3580894>.

Efeyan, A. and M. Serrano (2007) p53: Guardian of the Genome and Policeman of the Oncogenes. *Cell Cycle* 6:9, 1006-1010, 1 May 2007. <http://dx.doi.org/10.4161/cc.6.9.4211>.

Essers, J., H. van Steeg, J. de Wit, S.M. Swagemakers, M. Vermeij, J.H. Hoeijmakers, R. Kanaar (2000) Homologous and non-homologous recombination differentially affect DNA damage repair in mice. *EMBO J.* 2000 Apr 3;19(7):1703-10. doi:10.1093/emboj/19.7.1703.

Fournier, C., P. Barberet, T. Pouthier, S. Ritter, B. Fischer, K.O. Voss, T. Funayama, N. Hamada, Y. Kobayashi and G. Taucher-Scholz, (2009) No Evidence for DNA and Early Cytogenetic Damage in Bystander Cells after Heavy-Ion Microirradiation at Two Facilities. *Radiat. Res.* 171, 530–540 (2009). Online ISSN: 1938-5404.

Gabbita, S. P., K.A. Robinson, C.A. Stewart, R.A. Floyd and K. Hensley (2000) Redox Regulatory Mechanisms of Cellular Signal Transduction. Archives of Biochemistry and Biophysics Volume 376, Issue 1, 1 April 2000, Pages 1-13. <http://dx.doi.org/10.1006/abbi.1999.1685>.

Goldberg, A. and B. Rubinsky (2010) The effect of electroporation type pulsed electric fields on DNA in aqueous solution. Technol Cancer Res Treat. 2010 Aug;9 (4):423-30. ISSN 1533-0338.

Grosovsky, A.J., B.N. Walter, C.R. Giver (1993) DNA-sequence specificity of mutations at the human thymidine kinase locus. Mutat Res 289:231-243. [http://dx.doi.org/10.1016/0027-5107\(93\)90074-P](http://dx.doi.org/10.1016/0027-5107(93)90074-P).

Gudkov S.V., S.A. Garmash, I.N. Shtarkman, A.V. Chernikov, O.E. Karp, V.I. Bruskov (2010) Long-lived protein radicals induced by X-ray irradiation are the source of reactive oxygen species in aqueous medium. Dokl Biochem Biophys. 2010 Jan-Feb;430:1-4. DOI: 10.1134/S0006350910040020.

Gutkind, J.S. (1998) The pathways connecting G protein-coupled receptors to the nucleus through divergent mitogen-activated protein kinase cascades. J Biol Chem. 1998 Jan 23;273(4):1839-42. 10.1074/jbc.273.4.1839.

Hagan M., A. Yacoub, P. Dent (2004) Ionizing radiation causes a dose-dependent release of transforming growth factor alpha in vitro from irradiated xenografts and during palliative treatment of hormone-refractory prostate carcinoma. Clin. Cancer Res. 2004 10(17):5724-31. doi: 10.1158/1078-0432.CCR-04-0420.

Halliwell, B., and J. M. C. Gutteridge. (2006) Free radicals in biology and medicine. Journal of Pharmaceutical Sciences Volume 75, Issue 1, pages 105–106, January 1986. DOI: 10.1002/jps.2600750133.

Hamada, N., H. Matsumoto, T. Hara, and Y. Kobayashi (2007) Intercellular and Intracellular Signaling Pathways Mediating Ionizing Radiation-Induced Bystander Effects. Journal of Radiation Research Vol. 48 (2007) , No. 2 87-95. DOI: 10.1269/jrr.06084.

Hartmann, A. and G. Speit (1995) Genotoxic effects of chemicals in the single cell gel test (SCG) with human blood cells in relation to the induction of sister chromatid exchanges (SCE). Mutat. Res. 346:49-56.

Hartmann, A., K. Herkommer, M. Glück, and G. Speit (1995) The DNA-damaging effect of cyclophosphamide on human blood cells in vivo and in vitro studied with the single cell gel test (SCG). Environ. Mol. Mutagen. 25, 180–187. DOI: 10.1002/em.2850250303.

He, T. C., S. Zhou, L.T. da Costa, J. Yu, K.W. Kinzler, B. Vogelstein (1998) A simplified system for generating recombinant adenoviruses. Proc Natl Acad Sci U S A. 1998 Mar 3;95(5):2509-14.

Hei, T. K. (2006) Cyclooxygenase-2 as a signaling molecule in radiation-induced bystander effect. *Mol. Carcinog.* 2006 Jun;45(6):455-60. DOI: 10.1002/mc.20219.

Hei, T. K., H. Zhou, V.N. Ivanov, M. Hong, H.B. Lieberman, D.J. Brenner, S.A. Amundson, C.R. Geard (2008) Mechanism of radiation-induced bystander effects: a unifying model. *Journal of pharmacy and pharmacology. Journal of Pharmacy and Pharmacology* Volume 60, Issue 8, pages 943–950, August 2008. DOI: 10.1211/jpp.60.8.0001.

Hoffman, B. and D.A. Liebermann (2008) Apoptosis signaling by c-Myc. *Oncogene* (2008) 27, 6462-6472. doi:10.1038/onc.2008.312.

Honma, M., M. Izumi, M. Sakuraba, S. Tadokoro, H. Sakamoto, W. Wang, F. Yatagai and M. Hayashi (2003) Deletion, rearrangement, and gene conversion; genetic consequences of chromosomal double-strand breaks in human cells. *Environ Mol Mutagen.* 2003;42(4):288-98. DOI: 10.1002/em.10201.

Honma, M., M. Sakuraba, T. Koizumi, Y. Takashima, H. Sakamoto, M. Hayashi (2007) Non-homologous end-joining for repairing I-SceI-induced DNA double strand breaks in human cells. *DNA Repair (Amst).* 2007 Jun 1;6(6):781-8. Epub 2007 Feb 12. <http://dx.doi.org/10.1016/j.dnarep.2007.01.004>.

Hu, B., L. Wu, W. Han, L. Zhang, C. Chen, A. Xu, T.K. Hei and Z. Yu (2006) The time and spatial effects of bystander response in mammalian cells induced by low dose radiation. *Carcinogenesis* (February 2006) 27(2): 245-251. doi: 10.1093/carcin/bgi224.

Iyer, R. and B.E. Lehnert (2000) Effects of ionizing radiation in targeted and nontargeted cells. *Arch. Biochem Biophys.* Apr 1;376(1):14-25. <http://dx.doi.org/10.1006/abbi.1999.1684>.

Jamali, M. and K.R. Trott (1996) Persistent increase in the rates of apoptosis and dicentric chromosomes in surviving V79 cells after X-irradiation. *International Journal of Radiation Biology.* 1996, Vol. 70, No. 6: 705-9.

Jarozeski, M., R. Heller and R. Gilbert (2000) Electrochemotherapy, electrogenetherapy, and transdermal drug delivery: Electrically mediated delivery of molecules to cells. Humana, Totowa, NJ. (Chapter in a book, published by Humana press). ISBN: 978-0-89603-606-2 .

Jordan, E.T., M. Collins, J. Terefe, L. Ugozzoli, and T. Rubio (2008) Optimizing electroporation conditions in primary and other difficult-to-transfect cells. *J Biomol Tech.* 2008 December; 19(5): 328–334. PMID: PMC2628074.

Kashino, G., K. Suzuki, N. Matsuda, S. Kodama, K. Ono, M. Watanabe, K.M. Prise (2007) Radiation induced bystander signals are independent of DNA damage and DNA repair capacity of the irradiated cells. *Mutation Research* 619 (2007) 134–138. <http://dx.doi.org/10.1016/j.mrfmmm.2007.02.005>.

Krisch, R.E., M.B. Flick and C.N. Trumbore (1991) Radiation chemical mechanisms of single and double strand break formation in irradiated SV40 DNA. *Rad Res* 1991 146: 251-259.

Kroll, R., E. Frears and A. Bayliss (1989) An Oxygen Electrode-Based Assay of Catalase Activity as a Rapid Method for Estimating the Bacterial Content of Foods, *J. Appl. Microbiol* 66, 209-217. DOI: 10.1111/j.1365-2672.1989.tb02471.x

Krug, U., A. Ganser, and H.P. Koeffler (2002). Tumor suppressor genes in normal and malignant hematopoiesis. *Oncogene*, 21, 3475–3495. DOI: 10.1038/sj/onc/1205322.

Kutsenko, A.S., R.Z. Gizatullin, A.N. Al-Amin, F. Wang, S.M. Kvasha, R.M. Podowski, Y.G. Matushkin, A. Gyanchandani, O.V. Muravenko, V.G. Levitsky, N.A. Kolchanov, A. Protopopov, V.I. Kashuba, L.L. Kisselev, W. Wasserman, C. Wahlestedt, E.R. Zabarovsky (2002) NotI flanking sequences: a tool for gene discovery and verification of the human genome. *Nucleic Acids Res.* 2002 Jul 15;30(14):3163-70. doi: 10.1093/nar/gkf428

Lehnert, B.E., (2002) Exposure to low-level chemicals and ionizing radiation: reactive oxygen species and cellular pathways. *Hum Exp Toxicol* February 2002 vol. 21 no. 2 65-69. doi: 10.1191/0960327102ht212oa.

Li, H., S.T. H. Chan, F. Tang (1997) Transfection of rat brain cells by electroporation. *J Neurosci Methods.* 1997 Jul 18;75(1):29-32. [http://dx.doi.org/10.1016/S0165-0270\(97\)02259-0](http://dx.doi.org/10.1016/S0165-0270(97)02259-0).

Liang, X., Y.H. So, J. Cui, K. Ma, X. Xu, Y. Zhao, L. Cai, and W. Li (2011) The Low-dose Ionizing Radiation Stimulates Cell Proliferation via Activation of the MAPK/ERK Pathway in Rat Cultured Mesenchymal Stem Cells. *J. Radiat. Res.*, 52, 380–386. doi:10.1269/jrr.10121.

Liber, H.L., and W.G. Thilly (1982) Mutation assay at the thymidine kinase locus in diploid human lymphoblasts. *Mutation Res.*, 94, 467-485. [http://dx.doi.org/10.1016/0027-5107\(82\)90308-6](http://dx.doi.org/10.1016/0027-5107(82)90308-6).

Lieberman, M.W., R. N. Baney, R. E. Lee, S. Sell and E. Farber (1971) Studies on DNA Repair in Human Lymphocytes Treated with Proximate Carcinogens and Alkylating Agents. *Cancer Res* September 1971 31; 1297.

Linnert, M. and J. Gehl (2009) Bleomycin treatment of brain tumors: an evaluation. *Anticancer Drugs.* 2009 Mar; 20(3):157-64. DOI:10.1097/CAD.0b013e328325465e.

Lippert, M.J., Q. Chen and H.L. Liber (1998) Increased transcription decreases the spontaneous mutation rate at the thymidine kinase locus in human cells. *Mutat Res.* 1998 Jun 5; 401(1-2):1-10. [http://dx.doi.org/10.1016/S0027-5107\(98\)00011-6](http://dx.doi.org/10.1016/S0027-5107(98)00011-6).

- Little, J.B., H. Nagasawa, P.C. Keng, Y. Yu and C.Y. Li (1995) Absence of radiation-induced G1 arrest in two closely related human lymphoblast cell lines that differ in p53 status. *J Biol Chem.* 12; 270(19):11033-6.
- Little, J.B., L. Gorgojo, H. Vetrovs (1990) Delayed appearance of lethal and specific gene mutations in irradiated mammalian cells. *Int. J. Rad. Onc. Biol. Phys.* Volume 19, Issue 6, December 1990, Pages 1425–1429. [http://dx.doi.org/10.1016/0360-3016\(90\)90354-M](http://dx.doi.org/10.1016/0360-3016(90)90354-M).
- Löbrich, M., S. Ikpeme and J. Kiefer (1994) Measurement of DNA Double-Strand Breaks in Mammalian Cells by Pulsed-Field Gel Electrophoresis: A New Approach Using Rarely Cutting Restriction Enzymes. *Radiation Research*, Vol. 138, No. 2 (May, 1994), pp. 186-192. Published by: Radiation Research Society. Article Stable URL: <http://www.jstor.org/stable/3578588>.
- Lyng, F.M., C.B. Seymour, C. Mothersill (2000) Production of a signal by irradiated cells which lead to a response in unirradiated cells characteristic of initiation of apoptosis. *Br. J Cancer.* 2000 Nov; 83(9):1223-30. doi:10.1054/bjoc.2000.1433.
- Lyng, F.M., C.B. Seymour, C. Mothersill (2006) The involvement of calcium and MAP kinase signaling pathways in the production of radiation-induced bystander effects. *Radiat. Res.* 2006 Apr; 165(4):400-9. doi: <http://dx.doi.org/10.1667/RR3527.1>.
- Maguire, P., C. Mothersill, B. McClean, C. B. Seymour and F. M. Lyng (2007) Modulation of Radiation Responses by Pre-exposure to Irradiated Cell Conditioned Medium. *RADIATION RESEARCH* 167, 485–492.
- Małgorzata, A. Ś, A.M. Sharon, J.M. Nigel and E.G.S. David (2009) Quantification of Radiation-Induced Single-Strand Breaks in Plasmid DNA using a TUNEL/ELISA-Based Assay. *Radiation Research: November 2009*, Vol. 172, No. 5, pp. 529-536. doi: <http://dx.doi.org/10.1667/RR1684.1>.
- Mansour S. J., W.T. Matten, A.S. Hermann, J. M. Candia, S. Rong, K. Fukasawa, G.F. Vande Woude, N.G. Ahn (1994) Transformation of mammalian cells by constitutively active MAP kinase kinase. *Science* 265:966–970. DOI: 10.1126/science.8052857.
- Marty, M., G. Sersa, J.R. Garbay, J. Gehl, C.G. Collins, M. Snoj, et al. (2006) Electrochemotherapy – An easy, highly effective and safe treatment of cutaneous and subcutaneous metastases: Results of ESOPE (European Standard Operating Procedures of Electrochemotherapy) study. *Ejc Supplements.* 4, 3–13. <http://dx.doi.org/10.1016/j.ejcsup.2006.08.002>.
- Matsumoto, H., S. Hayashi, M. Hatashita, K. Ohnishi, H. Shioura, T. Ohtsubo, R. Kitai, T. Ohnishi and E. Kano. (2001) Induction of Radioresistance by a Nitric Oxide-Mediated Bystander Effect. *Radiation Research*, Vol. 155, No. 3 (Mar., 2001), pp. 387-396. Article Stable URL: <http://www.jstor.org/stable/3580525>.

McCubrey, J. A., L.S. Steelman, W.H. Chappell, S.L. Abrams, E.E.T. Wong, F. Chang, B. Lehmann, D.M. Terrian, M. Milella, A. Tafuri, F. Stivala, M. Libra, J. Basecke, C. Evangelisti, A.M. Martelli, and R.A. Franklin (2007) Roles of the raf/mek/erk pathway in cell growth, malignant transformation and drug resistance. *Biochim Biophys Acta*. August 2007; 1773(8): 1263–1284. <http://dx.doi.org/10.1016/j.bbamcr.2006.10.001>.

McGlynn, A. P., G. Wasson, J. O'Connor, G. McKerr, V.J. McKelvey-Martin and S.C. Downes (2000) The bromodeoxyuridine comet assay: detection of maturation of recently replicated DNA in individual cells. *Cancer Res* 2000; 60:1472.

Meaking, W.S., J. Edgerton, C.W. Wharton, R.A. Meldrum (1995) Electroporation-induced damage in mammalian cell DNA. *Biochim Biophys Acta*. 1995 Dec 27;1264(3):357-62. PMID: 8547324.

Milligan, J.R., J.A. Aguilera, R.A. Paglinawan, J.F. Ward, C. L. Limoli (2001) DNA strand break yields after post-high LET irradiation incubation with endonuclease-III and evidence for hydroxyl radical clustering. *Int J Radiat Biol*. 2001 Feb;77(2):155-64. DOI: 10.1080/0955300001001344 5.

Milligan, J.R., J.A. Aguilera, T.T. Nguyen, R.A. Paglinawan, J.F. Ward (2000) DNA strand-break yields after post-irradiation incubation with base excision repair endonucleases implicate hydroxyl radical pairs in double-strand break formation. *Int J Radiat Biol*. 2000 Nov;76(11):1475-83. PubMed PMID: 11098850.

Mir, L.M., P.H. Moller, F. Andre and J. Gehl (2005) Electric pulse-mediated gene delivery to various animal tissues. *Adv. Genet.* 54, 83–114. [http://dx.doi.org/10.1016/S0065-2660\(05\)54005-7](http://dx.doi.org/10.1016/S0065-2660(05)54005-7).

Moscone, D., M. Miscini, (1988) Determination of superoxide dismutase activity with an electrochemical oxygen probe. *Analytica Chimica Acta* 211 (1988): 195-204. [http://dx.doi.org/10.1016/S0003-2670\(00\)83679-X](http://dx.doi.org/10.1016/S0003-2670(00)83679-X).

Mothersill, C., T.D. Stamato, M.L. Perez, R. Cummins, R. Mooney, C.B. Seymour (2000) Involvement of energy metabolism in the production of 'bystander effects' by radiation. *Br. J. Cancer*. 2000 May; 82(10):1740-6. doi:10.1054/bjoc.2000.1109.

Mothersill, C., M. A. Kadhim, S. O'Reilly, D. Papworth, S. J. Marsden, C. B. Seymour, E. G. Wright (2000) Dose- and time-response relationships for lethal mutations and chromosomal instability induced by ionizing radiation in an immortalized human keratinocyte cell line. *International Journal of Radiation Biology* (2000) Volume: 76, Issue: 6, Pages: 799-806. PubMed: 10902734.

Mothersill, C., C. B. Seymour (2002) Bystander and Delayed Effects after Fractionated Radiation Exposure. *Rad. Res.* 158, 626–633.

Myers, R.M., (1999) Mapping and sequencing the human genome. Grant # 3P50HG000206-09S2 National Human Genome Research Institute IRG: GRRC.<http://www.researchgrantdatabase.com/g/3P50HG000206-07S1/MAPPING-AND-SEQUENCING-THE-HUMAN-GENOME/>

Nagasawa, H., and J.B. Little (1992) Induction of sister chromatid exchanges by extremely low doses of α -particles. *Cancer Res.* 52: 6394-6396.

Nakagawa, K., N. Morishima and T. Shibata (1992) An endonuclease with multiple cutting sites, Endo.SceI, initiates genetic recombination at its cutting site in yeast mitochondria. *EMBO J.* 1992 July; 11(7): 2707-2715.

Neumann, E., S. Kakorin and K. Toensing (2000) Principles of Membrane Electroporation and Transport of Macromolecules. *Methods in Molecular Medicine.* Volume: 37: 1-35, DOI: 10.1385/1-59259-080-2:1.

Nolin, S.L., and C.S. Dobkin, (1991) Cloning the ends of size selected Sfi I fragments. *American Journal of Medical Genetics* 1991. Volume 38, Issue 2-3, pages 384-390. DOI: 10.1002/ajmg.1320380246.

Ohba K., K. Omagari, T. Nakamura, N. Ikuno, S. Saeki, I. Matsuo, H. Kinoshita, J. Masuda, H. Hazama, I. Sakamoto, S. Kohno (1998) Abscopal regression of hepatocellular carcinoma after radiotherapy for bone metastasis. *Gut.* 1998 Oct; 43(4):575-7. doi: 10.1136/gut.43.4.575.

Olive, P. L. and R.E. Durand (2005) Heterogeneity in DNA damage using the comet assay. *Cytometry* (2005), Part A, 66A: 1-8. doi: 10.1002/cyto.a.20154.

O'Reilly, S., C. Mothersill, C.B. Seymour (1994) Postirradiation Expression of Lethal Mutations in an Immortalized Human Keratinocyte Cell Line. *International Journal of Radiation Biology* Jan 1994, Vol. 66, No. 1, Pages 77-83: 77-83. PMID: 8027614.

Pardali, K. and A. Moustakas, A. (2007) Actions of TGF- β as tumor suppressor and pro-metastatic factor in human cancer. *Biochimica et Biophysica Acta* 1775 (2007) 21-62. <http://dx.doi.org/10.1016/j.bbcan.2006.06.004>.

Petek, L.M., D.W. Russell and D.G. Miller (2010) Frequent Endonuclease Cleavage at Off-target Locations In Vivo. *Mol Ther.* 2010 May; 18(5): 983-986. DOI: 10.1038/mt.2010.35

Ponnaiya, B., G.J. Baker, D.J. Brenner, E.J. Hall, G.R. Pehrson and C.R. Geard (2004) Biological Responses in Known Bystander Cells Relative to Known Microbeam-Irradiated Cells. *Radiation Research:* October 2004, Vol. 162, No. 4, pp. 426-432. doi: <http://dx.doi.org/10.1667/RR3236>.

Ponnaiya, B., M. Suzuki, C. Tsuruoka, Y. Uchihori, Y. Wei, T.K. Hei (2011) Detection of chromosomal instability in bystander cells after Si490-ion irradiation. *Radiat Res.* 2011 Sep;176(3):280-90. Epub 2011 Jun 30. doi: 10.1667/RR2428.1.

Ponnaiya, B., M.N. Cornforth and R.L. Ullrich (1997) Induction of Chromosomal Instability in Human Mammary Cells by Neutrons and Gamma Rays. *Radiation Research*: March 1997, Vol. 147, No. 3, pp. 288-294. <http://www.jstor.org/stable/3579335>.

Poon, R.C.C., N. Agnihotri, C. B. Seymour, C. Mothersill (2007) Bystander effects of ionizing radiation can be modulated by signaling amines. *Environmental Research*, Volume 105, Issue 2, October 2007, Pages 200-211, ISSN 0013-9351, 10.1016/j.envres.2006.12.003.

Powell, S.N., J.S. De Frank, P. Connell (1995) Differential Sensitivity of p53(-) and p53(+) Cells to Caffeine-induced Radiosensitization and Override of G 2 Delay. *Cancer Res* 1995;55:1643-1648.

Prise, K. M., M. Folkard, V. Kuosaitė, L. Tartier, N. Zyuzikov and C. Shao (2006) What role for DNA damage and repair in the bystander response? *Mutat Res.* 2006 May 11; 597(1-2):1-4. <http://dx.doi.org/10.1016/j.mrfmmm.2005.06.034>.

Prise, K.M., G. Schettino, M. Folkard, K.D. Held (2005) New insights on cell death from radiation exposure. *Lancet Oncol.* 2005 Jul;6(7):520-8. [http://dx.doi.org/10.1016/S1470-2045\(05\)70246-1](http://dx.doi.org/10.1016/S1470-2045(05)70246-1).

Prise, K.M., J. M. O'Sullivan (2009) Radiation-induced bystander signaling in cancer therapy. *Nat Rev Cancer.* 2009 May; 9(5): 351–360. 10.1038/nrc2603.

Prise, K.M., M. Folkard, B.D. Michael (2003) A review of the bystander effect and its implications for low-dose exposure. *Radiat Prot Dosimetry.* 2003;104(4):347-55. PMID: 14579891.

Prise, K.M., C.H.L Pullar, B.D. Michael (1999) A study of endonuclease III-sensitive sites in irradiated DNA: detection of α -particle-induced oxidative damage. *Carcinogenesis* (1999) 20 (5): 905-909. doi: 10.1093/carcin/20.5.905.

Redon, C.E., J.S. Dickey, A. J. Nakamura, I. G. Kareva, D. Naf, S. Nowsheen, T. B. Kryston, W. M. Bonner, A. G. Georgakilas, and O. A. Sedelnikova (2010) Tumors induce complex DNA damage in distant proliferative tissues in vivo. *PNAS early edition*, www.pnas.org/cgi/doi/10.1073/pnas.1008260107.

Riley, T., S. Eduardo, P. Chen, & A. Levine (2008) Transcriptional control of human p53-regulated genes. *Nature Reviews Molecular Cell Biology* 9, 402-412 (May 2008) | doi:10.1038/nrm2395.

Rubanyi, G.M., E.H. Ho, E.H. Cantor, W.C. Lumma, L.H. Botelho (1991) Cytoprotective function of nitric oxide: Inactivation of superoxide radicals produced by human leukocytes. *Biochemical and Biophysical Research Communications* Volume 181, Issue 3, 31 December 1991, Pages 1392-1397. [http://dx.doi.org/10.1016/0006-291X\(91\)92093-Y](http://dx.doi.org/10.1016/0006-291X(91)92093-Y).

Rugo, R.E., K.H. Almeida, C.A. Hendricks, V.S. Jonnalagadda, B.P. Engelward (2005) A single acute exposure to a chemotherapeutic agent induces hyper-recombination in distantly descendant cells and in their neighbors. *Oncogene*. 2005 Jul 28;24(32):5016-25. doi:10.1038/sj.onc.1208690.

Russell, K.J., L. W. Wiens, G. W. Demers, D. A. Galloway, S. E. Plon, and M. Groudine (1995) Abrogation of the G2 Checkpoint Results in Differential Radiosensitization of G1 Checkpoint-deficient and G1 Checkpoint-competent Cells. *Cancer Res* April 15, 1995 55; 1639.

Schettino, G., M. Folkard, K. M. Prise, B. Vojnovic, K. D. Heldb and B. D. Michaela. (2003) Low-Dose Studies of Bystander Cell Killing with Targeted Soft X Rays. *Radiation Research* 160, 505–511. doi: 10.1667/RR3060.

Sedelnikova, O.A., A. Nakamura, O. Kovalchuk, I. Koturbash, S. A. Mitchell, S. A. Marino, D. J. Brenner and W. M. Bonner (2007) DNA Double-Strand Breaks Form in Bystander Cells after Microbeam Irradiation of Three-dimensional Human Tissue Models. *Cancer Res* May 1, 2007 67; 4295. doi: 10.1158/0008-5472.CAN-06-4442.

Seymour C.B., C. Mothersill and T. Alper (1986) High yields of lethal mutations in somatic mammalian cells that survive ionizing radiation. *Int. J. Radiat. Biol. Relat. Stud. Phys. Chem. Med.* 1986 Jul;50(1):167-79. PMID: 3487520.

Seymour, C. B. and C. Mothersill (2004) Radiation-induced bystander effects — implications for cancer. *Nature Reviews Cancer* 4, 158-164 (February 2004) | doi:10.1038/nrc1277.

Shao, C., M. Folkard, B.D. Michael and K.M. Prise (2004) Targeted cytoplasmic irradiation induces bystander responses. *PNAS* September 14, 2004 vol. 101 no. 37 13495-13500. doi_10.1073_pnas.0404930101.

She, Q.B., N. Chen and Z. Dong (2000) ERKs and p38 Kinase Phosphorylate p53 Protein at Serine 15 in Response to UV Radiation. July 7, 2000 *The Journal of Biological Chemistry*, 275, 20444-20449. Doi: 10.1074/jbc.M001020200.

Shields, J.M., K. Pruitt, A. McFall, A. Shaub, C.J. Der (2000) Understanding Ras: ‘it ain’t over ’til it’s over’. *Trends in cell biology*, April 1, 2000; 10(4) 147-153. [http://dx.doi.org/10.1016/S0962-8924\(00\)01740-2](http://dx.doi.org/10.1016/S0962-8924(00)01740-2).

Shrivastava, M., L.P. Haro De, J.A. Nickoloff (2008) Regulation of DNA double-strand break repair pathway choice. *Cell Research* (2008) 18:134–147. doi: 10.1038/cr.2007.111.

Siikonen, T., H. Kettunen, K. Perajarvi, A. Javanainen, M. Rossi, W. H. Trzaska, J. Turunen and A. Virtanen (2011) Energy loss measurement of protons in liquid water. *Phys. Med. Biol.* 56 (2011) 2367–2374 doi:10.1088/0031-9155/56/8/003 .

Singh, N. P., M.T. McCoy, R.R. Tice and E.L. Schneider (1988) A simple technique for quantification of low levels of DNA damage in individual cells. *Exp. Cell Res.* 175, 184–191. [http://dx.doi.org/10.1016/0014-4827\(88\)90265-0](http://dx.doi.org/10.1016/0014-4827(88)90265-0).

Singh, N.P., R.E. Stephens, E.L. Schneider (1994) Modifications of alkaline microgel electrophoresis for sensitive detection of DNA damage. *Intl. J. Radiat. Biol* 66:23-28. <http://www.sciencedirect.com/science/article/pii/S0921877796000560>.

Sokolov, M.V., J. S. Dickey, W. M. Bonner, O. A. Sedelnikova (2007) γ -H₂AX in bystander cells. *Cell Cycle* 6:18, 2210-2212, 15 September 2007. <http://psychopharmaceuticals.com/journals/cc/SokolovCC6-18.pdf> .

Staudacher, A.H., B.J. Blyth, M.D. Lawrence, R.J. Ormsby, E. Bezak, P.J. Sykes (2010) If bystander effects for apoptosis occur in spleen after low-dose irradiation in vivo then the magnitude of the effect falls within the range of normal homeostatic apoptosis. *Radiat Res.* 2010 Dec;174(6):727-31. Epub 2010 Sep 17. doi: 10.1667/RR2300.1.

Taghian, D. G. and J.A. Nickoloff (1997) Chromosomal double-strand breaks induce gene conversion at high frequency in mammalian cells. *Mol. Cell. Biol.* November 1997 vol. 17 no. 11 6386-6393. PMID: PMC232490.

Takata, M., M.S. Sasaki, E. Sonoda, C. Morrison, M. Hashimoto, H. Utsumi, Y. Yamguchi-Iwai, A. Shinohara, S. Takeda (1998) Homologous recombination and non-homologous end-joining pathways of DNA double-strand break repair have overlapping roles in the maintenance of chromosomal integrity in vertebrate cells. *The EMBO Journal* (1998) 17, 5497 - 5508 doi:10.1093/emboj/17.18.5497.

Toledo, LI., M. Murga, R. Zur, R. Soria, A. Rodriguez, S. Martinez, J. Oyarzabal, J. Pastor, J.R. Bischoff, O. Fernandez-Capetillo (2011) A cell-based screen identifies ATR inhibitors with synthetic lethal properties for cancer-associated mutations. *Nature Structural & Molecular Biology* 2011 Volume: 18, Pages: 721–727. doi:10.1038/nsmb.2076.

Trikalinos T.A., T. Terasawa, S. Ip, G. Raman, J. Lau. (2009) Particle Beam Radiation Therapies for Cancer. Technical Brief No. 1. (Prepared by Tufts Medical Center Evidence-based Practice Center under Contract No. HHSA-290-07-10055.) Rockville, MD: Agency for Healthcare Research and Quality. Revised November 2009. Available at: www.effectivehealthcare.ahrq.gov/reports/final.cfm.

- Vogelstein B., K.W. Kinzler (1992) p53 function and dysfunction. *Cell*. 1992 Aug 21;70(4):523-6. [http://dx.doi.org/10.1016/0092-8674\(92\)90421-8](http://dx.doi.org/10.1016/0092-8674(92)90421-8).
- Vousden, K.H. & D.P. Lane (2007) p53 in health and disease. *Nature Reviews Molecular Cell Biology* 8, 275-283 (April 2007) | doi:10.1038/nrm2147.
- Ward, J.F., (1981) Some biochemical consequences of the spatial distribution of ionizing produced free radicals. *Rad. Res.* Vol. 86, No. 2, 185-195. May, 1981. <http://www.jstor.org/stable/3575500>.
- Ward, J.F., (2002) The radiation-induced lesions which trigger the bystander effect. *Mutat. Res. Mutation Research* 499 (2002) 151–154. [http://dx.doi.org/10.1016/S0027-5107\(01\)00286-X](http://dx.doi.org/10.1016/S0027-5107(01)00286-X).
- Wentzell, L.M., T.J. Nobbs, S.E. Halford (1995) The SfiI restriction endonuclease makes a four-strand DNA break at two copies of its recognition sequence. *J Mol Biol.* 1995 May 5;248(3):581-95. <http://dx.doi.org/10.1006/jmbi.1995.0244>.
- Wilkinson, M. G., J.B. Millar (2000) Control of the eukaryotic cell cycle by MAP kinase signaling pathways. *FASEB J.* 2000 Nov;14(14):2147-57. doi: 10.1096/fj.00-0102rev.
- Wiseman, H., B. Halliwell (1996) Damage to DNA by reactive oxygen and nitrogen species: role in inflammatory disease and progression to cancer. *Biochem J* 1996; 313: 17-29.
- Won, J., M. Kim, N. Kim, J.H. Ahn, W.G. Lee, S.S. Kim, K.Y. Chang, Y.W. Yi, T.K. Kim (2006) Small molecule-based reversible reprogramming of cellular lifespan. *NATURE CHEMICAL BIOLOGY* 2006 (2) 7: 369-374. doi:10.1038/nchembio800.
- Xia, F., X. Wang, Y.H. Wang, N.M. Tsang, D.W. Yandell, K.T. Kelsey, H.L. Liber (1995) Altered p53 status correlates with differences in sensitivity to radiation-induced mutation and apoptosis in two closely related human lymphoblast lines. *Cancer Res.* 1995 Jan 1;55(1):12-5.
- Zabarovsky, E.R., R. Allikmets, I. Kholodnyuk, V.I. Zabarovska, N. Paulsson, V.M. Bannikov, V.I. Kashuba, M. Dean, L.L. Kisselev, G. Klein (1994) Construction of Representative NotI Linking Libraries Specific for the Total Human Genome and for Human Chromosome 3. *Genomics* (1994) 20: 312-316.
- Zhang, J., M. Buonanno, G. Gonon, M. Li, M. Galdass, G. Shim, S. M. De Toledo and E. I. Azzam (2012) Bystander Effects and Adaptive Responses Modulate In Vitro and In Vivo Biological Responses to Low Dose Ionizing Radiation. *Radiobiology and Environmental Security NATO Science for Peace and Security Series C: Environmental Security*, 2012, 71-86, DOI: 10.1007/978-94-007-1939-2_8.
- Zhang, Y., J. Zhou, K.D. Held, R.W. Redmond, K.M. Prise, H.L. Liber, (2008) Deficiencies of double-strand break repair factors and effects on mutagenesis in directly

gamma-irradiated and medium-mediated bystander human lymphoblastoid cells. *Radiat Res.* 2008 Feb;169(2):197-206. Online ISSN: 1938-5404.

Zhang, Y., J. Zhou, J. Baldwin, K.D. Held, K.M. Prise, R.W. Redmond, H.L. Liber (2009) Ionizing radiation-induced bystander mutagenesis and adaptation: quantitative and temporal aspects. *Mutat Res.* 2009 Dec 1; 671(1-2):20-5. <http://dx.doi.org/10.1016/j.mrfmmm.2009.08.006>.

Zhou, L. and S.J. Elledge (2003) Sensing DNA Damage through ATRIP Recognition of RPA-ssDNA Complexes. *Science* 6 June 2003: Vol. 300 no. 5625 pp. 1542-1548. DOI: 10.1126/science.1083430.

Ziegler J. F., (2003) SRIM, Nuclear Instruments and Methods in Physics Research Section B: Beam Interactions with Materials and Atoms, Volumes 219–220, June 2004, Pages 1027-1036, ISSN 0168-583X, 10.1016/j.nimb.2004.01.208. <http://www.sciencedirect.com/science/article/pii/S0168583X04002587>.

Appendix 1:

Determining the transfection efficiency of experimental plasmid with Lipofection (Mirus TransIT 2020) as an alternative delivery system.

Note: (Mirus TransIT 2020 is a proprietary lipid-polymer mixture that forms lipopolyplexes with DNA and does not contain any components of animal origin.

The only difference in the lipofection experiment from electroporation based transfection was the use of Mirus® transfection reagent. An empty vector pAdTrack CMV was used as control. This vector has the same backbone as the experimental plasmid pAdTrack CMV I-Sce1 does not have the I-Sce1 insert. Green fluorescence was measured in cells that received the plasmid with the GFP marker in 5 random fields of view at 0, 5, 10 and 15 hours to establish the transfection efficiency (TE). TE was measured further at 24, 48 and 72 hours (results not shown in here, because of irrelevance), but green fluorescence started to increase again at 24 hours.

Since results shown in figure 3.8 had indicated that electroporation itself (C2B bar; electroporation of control plasmid) was possibly contributing to the overall bystander mutation fraction, it was important to find another suitable delivery system for transfection that could have lower mutagenicity or lower ability to induce additional release of bystander signal from the transfected cells. Both transfection efficiency and bystander mutagenesis were measured with lipofectamine based transfections. Although the transfection efficiency results proved promising, compared to the maximum transfection efficiency that was achieved with electroporation, but the impact of

lipofectamine mediated transfection on bystander mutagenesis showed this reagent to be more mutagenic than electroporation.

Figure S1 shows the transfection efficiency with a lipofectamine based delivery system (Mirus TransIT 2020 is a proprietary lipid-polymer mixture that forms lipopolyplexes with DNA). Lipofection proved to be a less efficient delivery system than electroporation; given the critical time period of 5 hours for bystander signal generation. Maximum transfection efficiency of 60% was recorded at 10 hours. It was further established that if the transfection efficiency experiment was continued for 72 hours, then the maximum efficiency of 74% could be recorded at a 24 hour time point. This suggests that Mirus transfection reagent would not be suitable for the bystander experiments since the maximum bystander signal was recorded at 5 hours with electroporation but with lipofectamine it takes almost 24 hours to get the same result. Also in separate studies it was determined that lipofection was accompanied by a high cell mortality in the medium (established by trypan blue viability assay). However within the frame of comparison between electroporation and lipofection (at 0, 5, 10 and 15 hours) the measured transfection efficiency was higher at 5 hour time point with electroporation rather than lipofection. Electroporation was also less toxic for the cells as the average cell viability loss after electroporation was 2-4% only (results not shown).

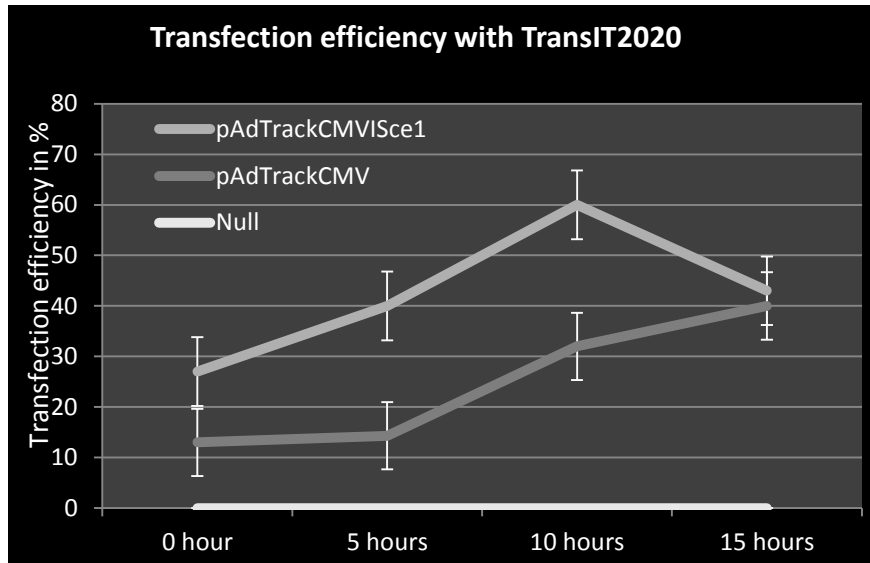


Fig. S1.1 Lipofectamine based transfection of (A) pAdTrack CMV I-Sce1

(B) pAdTrack CMV and (C) no plasmid and plotting for the number of positively transfected green fluorescent cells as a percentage on the Y-axis.

This lipofectamine reagent proved to be more toxic than electroporation and reduced the cell viability by almost 20 % following transfection. There was less than 4 % loss of viability following electroporation. This viability measure was taken by using trypan blue assay and counting the transfected and non-transfected cells with the Countess Cell counter.

Using lipofectamine as delivery system to study direct and bystander mutagenesis in E18 cells transfected with the I-Sce1 plasmid.

E18 cells that were transfected with the control and experimental plasmid were incubated for 5 hours (as this time point had already established by previous experiments to produce best results vis-à-vis bystander signal generation) to generate bystander signal, at which

point the medium was transferred from direct to bystander naïve cells. The medium in direct cells was replaced with fresh RPMI 1640 supplemented with horse serum and penicillin/streptomycin. Both direct and bystander cells were further incubated for 72 hours before finally plating for mutation assay.

A mutation assay was set up to compare the direct and bystander mutation fraction with the control plasmid pAdTrackCMV and experimental plasmid pAdTrackCMV I-Sce1.

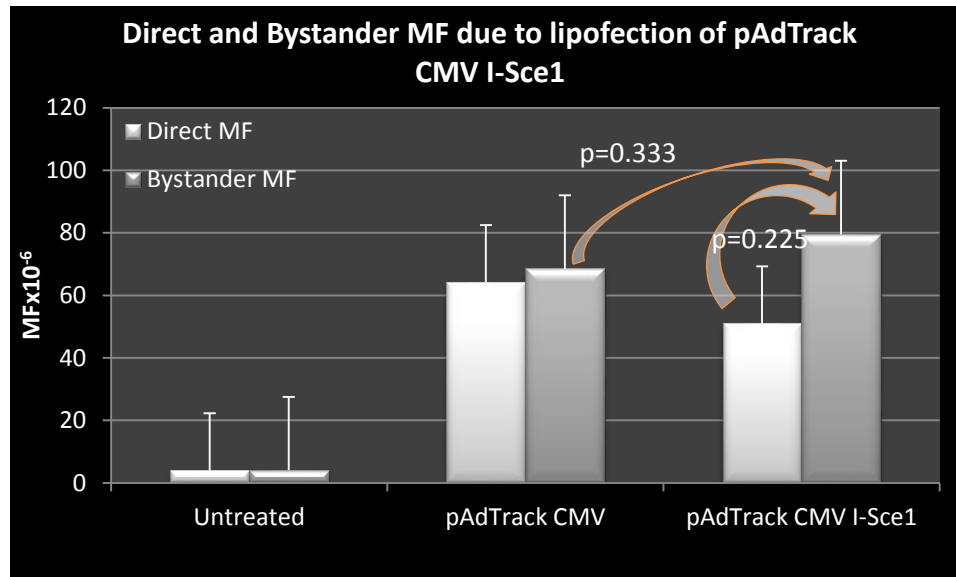


Fig. S 1.2 Lipofectamine based transfection of pAdTrack CMV I-Sce1 and plotting for Direct and Bystander MF.

Upon comparison of these results to the bystander mutation fraction due to electroporation of pAdTrackCMV I-Sce1 vector into E18 cells, it appeared that lipofection was more mutagenic and resulted in higher cell mortality than electroporation. The t-test comparison of two groups (directly induced MF due to I-Sce1 plasmid and

bystander induced MF due to I-Sce1 plasmid) gave a p-value of 0.225 which was not significant. Hence it was logical to conclude that lipofectamine based transfection system did not produce sufficient bystander signal in 5 hours to cause an increase in the naïve bystander cells, suggesting that the toxicity factor could be negatively affecting the total number of mutants being isolated from the lipofected population. Thus electroporation was chosen as the preferred delivery system for this project.

In an average of three replicate mutation assay experiments using lipofectamine as delivery system, a significant increase in the bystander mutation fraction could not be measured.

Appendix 2:

Mutation effects of lipofecting restriction enzymes into E18 cells using lipofectamine:

In order to compare the bystander effects due to the delivery system employed for transfecting plasmid into the cell model, the rare cutting restriction enzymes Not1, Sfi1 and I-Sce1 were lipofected into E18 cells. In the previous experiments these restriction enzymes were electroporated but here the same experiment was carried out using lipofectamine (Mirus® reagent) as the delivery system . Same conditions and same units of enzyme were used for this experiment as in electroporation, the only difference was replacing electroporation with the commercially available lipofection reagent Mirus TranIT2020®.

Since electrical current passed through the reaction mixture produces heat and literature has been cited (Meaking et al., 1995; Goldberg and Rubinsky, 2010) where DNA damaging effects of electroporation were investigated. There was a slight chance of enzyme denaturation due to conversion of electrical current into heat (+7°C) as per the cited reference. It was necessary to test lipofectamine as an alternative delivery system.

The direct and bystander mutation fractions obtained from electroporation were compared with those obtained from lipofection and a detailed analysis and comparison of results was used to answer the question if one delivery system was better than the other for my experiments. Earlier experimentation with lipofectamine showed that the delivery system was toxic for my cell model resulting in 20% average loss of viability. Despite those results it was important to find out how this delivery system would compare to electroporation vis-à-vis transfection of restriction enzymes into host cells to determine

the effect of any structural loss of enzyme proteins due to generation of heat associated with electroporation.

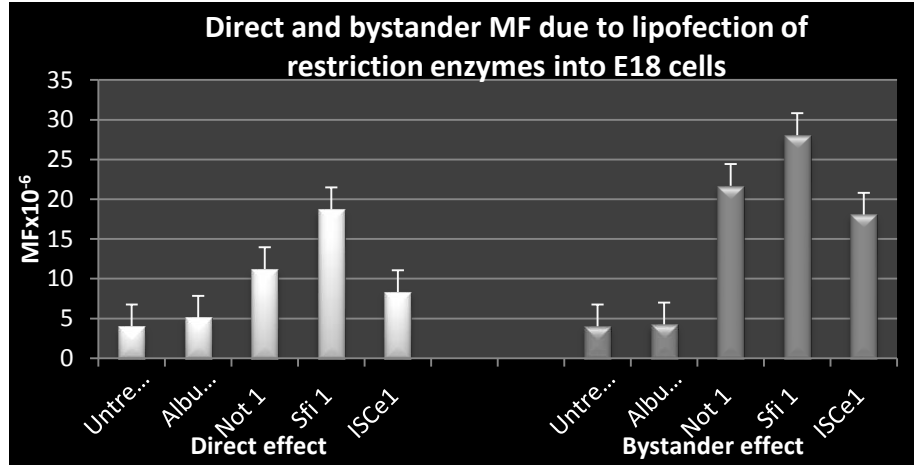


Fig. S 2.1. The direct and bystander mutation fraction measured in E18 cells, following transfection with rare cutting restriction enzymes (Not 1, Sfi 1 and I-Sce1) and using lipofectamine as the delivery system instead of electroporation.

The non-digesting protein albumin was used as control, (Compare with fig. 3.10).

Table ST 2.01: Statistical analysis of results shown in figure S3

	Direct MF	Remarks	Bystander MF	Remarks
Untreated vs Not1	0.005	Significant	<0.001	Significant
Untreated vs Sfi1	<0.001	Significant	0.085	Not significant
Untreated vs ISce1	<0.001	Significant	0.006	Significant

Discussion of results:

Lipofectamine based transfection figure. S3, showed very different results when compared with electroporation experiment (fig. 3.10). All of the direct and bystander mutation fraction increases were significant when compared with untreated background. The overall direct and bystander mutation fractions were also higher than in electroporation. Bystander MF due to lipofection produced the highest MF of 28×10^{-6} whereas the highest increase in electroporation was 12×10^{-6} (refer to figure 3.10). This observation verified the fact that lipofection is more mutagenic than electroporation and combined with earlier finding it is also more toxic for the cells, it was easy to conclude that lipofection is not a suitable delivery system for my cell model. Table ST.01 showed all relationships to be significant (except bystander MF for Sfi1). Due to the excessive toxicity and mutagenicity factor the actual relationships may have been masked and thus the results are hard to predict.

LIST OF ABBREVIATIONS

Ataxia telangiectasia mutated	ATM
ATM and RAD 3 related	ATR
Base excision repair	BER
Bromodeoxyuridine	BrdUrd
Bystander signal	BSS
Bystander effect	BSE
Chromosome healing	CH
Cytidine, hypoxanthine, aminopterin, thymidine	CHAT
DNA dependent protein kinase	DNA PK

DNA strand break
associated bystander
effect

DSB-ABE

DNA double strand
breaks

DSBs

DNA single strand breaks

SSBs

Extracellular signal-
regulated kinase

ERK

Galactic cosmic rays

GCRs

Green fluorescent protein

GFP

I-Sce1

I-SceI is an intron-encoded mitochondrial
endonuclease of *Saccharomyces cerevisiae*.

Loss of heterozygosity

LOH

Mitogen activated protein kinase

MAPK

Non- homologous end-joining	NHEJ
Penicillin, streptomycin	Pen/Strep
Phosphate buffered saline	PBS
Proliferating cell nuclear antigen	PCNA
Radiation induced bystander effect	RIBE or simply BE (unless otherwise specified)
Reactive Nitrogen species	RNS
Reactive Oxygen species	ROS
Replication protein A	RPA
RPMI 1640 culture medium	(Moore et al., Roswell Park Memorial Institute)
Sister chromatid exchanges	SCE
Solar particle events	SPEs

Telomere aberrations	TAs
Telomere double strand break fusion	TDSBF
Telomere position effect	TPE
Telomere sister chromatid exchange	TSCE
Thymidine, hypoxanthine, cytidine	THC
Tri fluoro thymidine	TFT